

SIGNIFICANCE OF CLEAN WATER FOR SUSTAINABLE GOOD HEALTH IN NIGERIA

¹Ayokunle O. FAMILUSI, ²Adebola A. ADEKUNLE, ³Adedayo A. BADEJO, ⁴Olayemi J. ADEOSUN,
⁵Kasali A. MUJEDU, ⁶Joel O. OLUSAMI, ⁷Babatunde E. ADEWUMI, ⁸Damilola A. OGUNDARE

^{1,2,3}Department of Civil Engineering: Federal University of Agriculture, Abeokuta, Nigeria,

⁴Department of Agricultural and Bio-Resources Engineering: Federal University of Agriculture, Abeokuta, Nigeria,

^{5,6,7,8}Department of Civil Engineering, Federal Polytechnic Ede, Nigeria

(Corresponding author's email: ayomacfamilson@gmail.com)

ABSTRACT

The significance of the impact of water-related diseases on human health has been recognized as a major threat to sustainable human development in some international forums. This study is an investigation into the correlation between unclean water and the outbreak of water-related diseases in Nigeria. It was established from the review of previous researches that the concept of clean water and sanitation is critical to the good health and well-being of all individuals. Nigeria still has a long way to go towards achieving the Sustainable Development Goal number 6 (SDG 6) of the United Nations, hence it is high time government at all levels and individuals embraced Water, Sanitation and Hygiene (WASH) agenda 2030.

Keywords: SDG, WASH, Water-Related Diseases, Well-Being

1. INTRODUCTION

Water is a foundational element of life and is vital to the wellbeing of families [1]. Water makes up more than two-thirds of the human body; in fact it is a vital component to every living organism in the world, especially the human species [2]. Unfortunately for many people in our world there is never enough water; especially clean water [1]. It is estimated that each person on earth requires 20 to 50 liters of clean safe water each and every day. This clean water is to be used for drinking, cooking, simple hygiene, etc. There are a number of different infectious agents detrimental to human health that grow in contaminated/unsanitary water which can cause a number of waterborne illnesses; such as cholera, hepatitis, typhoid, and diarrhea. Take for example, diarrheal diseases from cholera, this agent and illness is responsible for 1.8 million deaths worldwide. These deaths can be preventable with the proper knowledge, education, and infrastructure put in place. The importance of clean water is more often than not neglected in the developing world. Many people understand the importance of water; however these individuals tend to not completely understand the importance of that water being clean. The United Nations has labeled the access to clean water a basic human right [2]. In 2015, 750 million people lacked access to safe, clean drinking water and approximately 2,300 people die every day from diarrhoea. Water is not only an important factor of public health, but also of general livelihoods and development: crop production, livestock production, industry, commerce and daily life depend on access to water. Water-supply and sanitation conditions therefore directly affect health and food security and are key components in the fight against Hunger and Malnutrition (as cited in [3]). Having access to clean water is often neglected and not understood completely. It is crucial that attention is brought to this topic because of how many innocent people are dying every year. Initial goal needs to be implemented by government officials and policy makers to look out for those individuals that lack access to clean water [2]. Nigeria is a country in West Africa. It is the most populous country in Africa; geographically situated between the Sahel to the North, and the Gulf of Guinea to the South in the Atlantic Ocean; covering an area of 923,769 kilometres (574,003 mi), with a population of over 211 million. Nigeria borders Niger in the North, Chad in the North-East, Cameroon in the East, and Benin in the West. Nigeria is a federal republic comprising 36 states and the Federal Capital Territory, where the capital, Abuja, is located as shown in Figure 1. The largest city in Nigeria is Lagos, one of the largest metropolitan areas in the world and second largest in Africa [4]. The

aim of this study is to reiterate the significance of clean water for sustainable good health in the nation Nigeria.

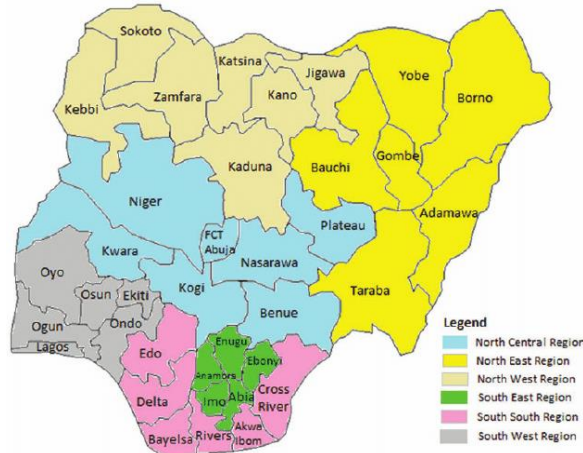


Figure 1: Map of Nigeria

2. METHODOLOGY

Several literatures were consulted and inferences were made from the works.

3. DISCUSSION

3.1. What Makes Water Unsafe?

Water is unsafe when it contains germs, worms, or toxic chemicals. Germs (tiny living things, too small to see, that cause many kinds of illness) and worms, such as whipworm, hookworm, and roundworm, cause many serious illnesses. Germs and worms live in human and animal waste (urine and faeces) and can cause serious and long-lasting illnesses when:

- there is no good way to get rid of human and animal wastes.
- water supplies are not protected and kept clean.
- there is no enough water to wash [5].

3.2 Water-Related Diseases

The Protocol on Water and Health defines “water-related disease” to mean “any significant adverse effects on human health, such as death, disability, illness or disorders, caused directly or indirectly by the condition, or changes in the quantity or quality, of any waters”. “Drinking-water” means “water which is used, or intended to be available for use, by humans for drinking, cooking, food preparation, personal hygiene or similar purposes”. Water-associated diseases are classified into five main groups:

- **Waterborne diseases** are caused by the ingestion of faecally contaminated water. Cholera and typhoid fever are classical examples of waterborne diseases, where only a few highly infectious pathogens are needed to cause severe diarrhoea. Shigellosis, hepatitis A, amoebic dysentery and other gastrointestinal diseases can also be waterborne. Examples include river blindness, guinea worm, and so on [6, 7].

- **Water-washed (water-hygiene) diseases** occur due to the lack of adequate water supply for washing, bathing and cleaning. Pathogens are transmitted from person to person or by contact with contaminated surfaces. Eye and skin infections as well as diarrhoeal illnesses occur under these circumstances. Waterborne pathogens include bacteria, viruses, protozoa and helminths [6, 7].
- **Water-scarce diseases** occur due to the lack of water available for washing, bathing and cleaning. Hence, pathogens are transmitted from person to person or from contaminated surfaces to a person and are spread by the faecal–oral route. In particular, eye (trachoma), yaw and skin infections (scabies), as well as diarrhoeal diseases occur under those conditions [6, 7].
- **Water-based diseases** are caused by organisms, in particular by different species of worms that spend parts of their life-cycle in different habitats. They have spent one development cycle in aquatic molluscs, and another as fully grown parasites in other animal or human hosts. Because stagnating surface waters, such as reservoirs, are the preferred habitat of parasitic worms, the occurrence of water-based diseases such as dracunculiasis and schistosomiasis can be heavily influenced by anthropogenic activities. Examples of water-based diseases also include kidney or liver diseases [6, 7].
- **Vector-borne diseases** are caused by bites from insects that breed in water. Insect vectors such as mosquitoes transmit diseases such as malaria, Chikungunya and other diseases [6].

3.3 Relationship between Unclean Water and Outbreak of Diseases in Nigeria

The findings from the work of [8] on the morbidity pattern of water-related diseases in some parts of Ibadan City point to the fact that Typhoid fever had the highest occurrence (39.3%) followed by bacillary dysentery and cholera. It was also found out that water sourced from rains and wells for domestic uses in different parts of the study area are not fit for drinking. Moreover, the application of potash alum for domestic water treatment especially, when visible contaminants are observed is quite inadequate as a method of treatment for water that has high coliform and bacteria load. It is therefore recommended, that potable water provision and water sanitation projects should be adopted as a veritable intervention option to solving health problems arising from water contamination rather than increased investment in drugs and building more hospitals. Again, effective and sustainable water treatment methods such as boiling, filtering, hygienic storing and handling, which can be managed at the household level, should be disseminated to households. On the other hand the ineffectiveness of alum application as a method of water treatment for drinking purposes should be discouraged. Agencies that oversee public hygiene and health issues in the urban centres should be empowered to provide and enforce management guidelines for private wells, while conducting routine assessment [8].

It was demonstrated in the survey by [9] with respect to the prevalence of water related diseases in all the local government areas (LGAs) of Benue State, Nigeria that malaria cases ranked the highest, followed by diarrhoea, dysentery, oncherciasis, filariasis, schistosomiasis, typhoid and cholera. The incidence of these water related diseases is reflection of the problems of water scarcity faced by the inhabitants living especially in rural areas. These people search for drinking water from all sorts of unprotected water sources. Consequently, they are exposed to all kinds of risks linked with drinking of polluted or unsafe water. Public education on personal hygiene, safe drinking water, and intervention by governments and non-governmental organization will go a long way in remedying the situation [9].

The work of [7] affirms that out of the top seven diseases that are most frequently reported in Ota Ogun State Nigeria, five were water related. These diseases include malaria, typhoid, vital organ failure, cholera and skin disease. Reasons for the high level of water related ailments were explained by poor level of supply of potable water to the municipality, as well as poor sanitation practices by the residents. While the poor supply of potable water to Nigerian communities has been identified as a primary factor in the prevalence of preventable diseases among citizens, it can also be seen that a lot of improvement has to be made with respect to personal hygiene and environmental sanitation by the citizens themselves [7].

The research work of [10] explored the incidence of water-related neglected tropical diseases (NTDs) in rural Nigeria, using data from the demographic and health survey of 2008 for Nigeria. The study found incidence of occurrence of four water-related NTDs (river blindness, elephantiasis, Guinea Worm, Schistosomiasis) in rural Nigeria. These NTDs were highly correlated with low educational status of head of households as well as poverty. Also, in light of the above, the study found that lack of access to potable water supply and sanitation was correlated with the incidences of occurrence of four water-related NTDs in rural Nigeria. Recognising the importance of wholesome water is very important in developing appropriate interventions towards eliminating the NTDs. The study concludes that water-related NTDs in rural Nigeria thrive in the presence of inadequate access to potable water for household use [10].

3.4 Goal Number 6 of United Nations' SDGs - Clean Water and Sanitation

In 2015, the world leaders adopted the 2030 Agenda for Sustainable Development. The results' framework of the 2030 Agenda comprises 17 Sustainable Development Goals (SDGs). The SDGs are described in the 2030 Agenda as indivisible and integrated, balancing the economic, social and environmental dimensions of sustainable development [11]. Water is key to sustainable development. It supports industry, agriculture and ecosystems, and is essential for human life and livelihoods. Therefore, water will serve as a foundation for the achievement of many of the SDGs, including SDG 6, the dedicated water goal: 'To ensure availability and sustainable management of water and sanitation for all' [12]. Should the global population reach 9.6 billion by 2050, better management of water and sanitation is needed to sustain human wellbeing, while preserving the resilience of the ecosystem. Significant progress has been attained between 1990 and 2015, as the proportion of global population with access to improved drinking water sources has increased from 76 to 91 percent. Nevertheless, over 2.5 billion people still do not have access to basic sanitation facilities globally, and the access to water supply is unevenly distributed across the world.

Poor sanitation, combined with irregular water supply, hinders development and claims the lives of countless of people, especially those living in informal settlements, often also referred to as "slums" in urban areas. These challenges are likely to magnify in the future due to an ever growing city population needing to share already inadequate and often badly managed resources. Being the primary factor that increases water, air, soil and food contamination, lack of proper access to water in dense urban areas exponentially increases local pollution problems. In most countries, local governments are providers of water and sanitation facilities. In some, they serve as the supervisor of private provision. However, their responsibilities go beyond simple provision of clean water and sanitation services and include:

- Maintaining existing and designing new water supply systems with a long-term perspective and dealing with cross-cutting regional problems, such as industrial development or resource scarcity impact urban water supply.
- Supervising water quality and implementing regulations regarding pollution, discharge of waste water and spread of hazardous substances.
- Monitoring and ensuring that water resources are accessible and shared fairly.
- Setting incentives to the private sector for collecting, recycling, reuse, as well as desalination technologies for water (where water provision is privately owned).
- Supporting horizontal cooperation in planning and environmental policy between municipalities and regions across borders.
- Adapting to new challenges, such as European cities adapting to the demands that heavy rains pose to sanitation systems and infrastructural planning [13].

3.5 Vision and Objectives of WASH (2016-2030)

According to [14], the vision of United Nations International Children Emergency Fund (UNICEF) for Water, Sanitation and Hygiene (WASH) is the realization of the human rights to water and sanitation for all.

The WASH Strategy's objectives are:

1. To achieve universal and equitable access to safe and affordable drinking water for all by 2030;
2. To achieve access to adequate and equitable sanitation and hygiene for all and end open defecation, paying special attention to the needs of women and girls and those in vulnerable situations by 2030.

These objectives align with the SDG 6 targets for drinking water, sanitation and hygiene and will contribute to the broader 2030 Agenda for Sustainable Development that is critical for children.

Why WASH

In 2010, the United Nations General Assembly explicitly recognized water and sanitation as human rights that are “essential for the full enjoyment of life and all human rights [14].

Water Pollution

Water pollution is a global challenge that has increased in both developed and developing countries, undermining economic growth as well as the physical and environmental health of billions of people [15]. The 2030 Agenda for Sustainable Development acknowledges the importance of water quality and includes a specific water quality target in Sustainable Development Goal (SDG) 6.2. The 2030 Agenda for Sustainable Development is expected to strongly influence future policies and strategies and to ensure that the control of water pollution is elevated in international and national priorities. Human settlements, industries and agriculture are the major sources of water pollution. Globally, 80 percent of municipal wastewater is discharged into water bodies untreated, and industry is responsible for dumping millions of tonnes of heavy metals, solvents, toxic sludge and other wastes into water bodies each year (as cited in [15]). Agriculture, which accounts for 70 percent of water abstractions worldwide, plays a major role in water pollution. Farms discharge large quantities of agrochemicals, organic matter, drug residues, sediments and saline drainage into water bodies. The resultant water pollution poses demonstrated risks to aquatic ecosystems, human health and productive activities (as cited in [15]). A typical source of water pollution in Nigeria is eutrophication, in which detergents, cow manure, agricultural fertiliser and other human wastes would be forced to go into the water bodies as shown in Figure 2. Eutrophication blocks sunlight from penetrating the water bodies, thus reducing oxygen and making them inhabitable.



Figure 2: Pollution of River Water Through Eutrophication

WASH and diarrhoea

Diarrhoea is simply referred to as the passage of three or more loose or liquid stools per day. However globally, diarrhoeal diseases are caused by infectious agents such as bacteria (e.g. *E. coli*, salmonella, shigella, campylobacter), viruses (e.g. rotaviruses, noroviruses and adenoviruses), and protozoa (e.g. cryptosporidium, amoeba and giardia). However, the aetiology of diarrhoeal diseases varies from region to region. Rotavirus is the main cause of severe and moderate diarrhoea. Only a small proportion of diarrhoea cases result from non-infectious conditions (such as intoxication or non-infectious inflammatory diseases). Diarrhoeal diseases are characteristically transmitted via the faecal-oral route. Poor WASH increases an individual's exposure to faecal pathogens through multiple pathways, as demonstrated in the 'F-diagram' shown below [16] in Figure 3. The figure outlines five major ways through which the susceptible can contract disease(s) from the host. The ways include flies, fields (soils), food, fluids (water) and fingers (hand).

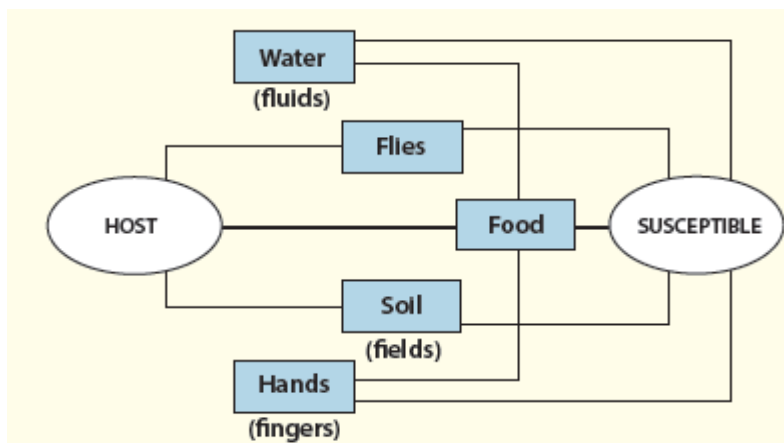


Figure 3: The F-diagram Detailing Individual's Exposure to Faecal Pathogens [16]

It has been estimated that in 2012, a total of 842,000 diarrhoea deaths were caused by inadequate WASH (502,000 from water, 280,000 from sanitation and 297,000 from hand hygiene). This represents over half of diarrhoeal diseases, or an estimated 1.5% of the total disease burden (as cited in [16]). There is little doubt, however, that improving access to adequate amounts of water from an adequately distanced source, hygienic sanitation facilities and promotion of handwashing with soap should be the cornerstones of integrated WASH campaigns (as cited in [16]). Sanitation and hygiene promotion are still the two most effective interventions for controlling endemic diarrhoea (as cited in [16]).

Cholera

With regard to cholera, although it is largely perceived to be a waterborne disease, person-to-person transmission, limited access to sanitation, an inadequate water supply and poor hygienic practices may contribute to the rapid progression of an epidemic. The WHO promotes safe drinking water, sanitation, personal hygiene, health education and food safety as specific control measures. Improved sources include piped water to the plot or household, public taps or standpipes, tube wells or boreholes, protected dug wells, protected springs, or rainwater. However, these provide varying degrees of safety, according to their differentiated ability to protect from outside contamination. For example, systematically managed piped water from an improved point source of water reduces diarrhoeal disease risk by an estimated 73%, while that same water source is likely only to provide a 28% reduction if treated at point of use and stored in the household [as cited in 16].

3.6 Achieving Clean Water, Sanitation and Hygiene for All in Nigeria

Access to water, sanitation and hygiene are human rights and crucial for good outcomes in health, nutrition, education, gender equality, livelihoods and for the socio-economic development of a country. A lack of access to these basic life-saving services impact virtually all aspects of human development, disproportionately affecting the life chances of women and girls. Goal 6 of the United Nations Sustainable Development Goals (SDGs) is focused on ensuring inclusive and equitable access to safe and affordable drinking water, sanitation and hygiene for all. However, in lower and middle-income countries like Nigeria, millions of people are without access to clean water and sanitation. According to the Water, Sanitation and Hygiene National Outcome Routine Mapping (WASHNorm) in 2018, about 55 million Nigerians still do not have access to clean water supply services, 110 million Nigerians lack decent toilets, and over 47 million practice open defecation [17].

Furthermore, some of the conflicts in the North-Central region have been attributed to poor access to water sources. Progress to address this water and sanitation crisis has been accelerated by the declaration of a State of Emergency by the Federal Government in November 2018 and the launch of a National Action Plan for the revitalisation of the sector. The Partnership for Expanded Water Supply, Sanitation and Hygiene (PEWASH), the Open Defecation Free Road Map and the Water Resources Bill all support this drive to ensure universal access for all by 2030 [17]. Delivering SDG 6 is a formidable challenge and can only be achieved by ensuring appropriate governance and coordination structures at all levels of government; improving access and finance data availability and transparency; addressing the problems relating to operations and maintenance (which currently undermine the sustainability of services); strengthening the enabling environment for the public and private sectors; and increasing civil society engagement to strengthen accountability for services and budgets. Additionally, flexible solutions need to be identified to tackle the problems within the sector in order to drive the needed reform [17].

4. CONCLUSION

Studies have shown that improving the microbiological quality of household water by on-site or point-of-use treatment and safe storage in improved vessels reduces diarrhoeal and other waterborne diseases in communities and households of developing and developed countries. Reductions in household diarrhoeal diseases of 6 – 90% have been observed, depending on the technology and the exposed population and local conditions [18]. It is also surprising that differences exist in some of the quality parameters of the water samples taken from the Clearwell of the waterworks and the ones taken from the public tap. These differences are attributable to inadequate sanitary measures in the vicinity of the Waterworks, Public tap and their appurtenances [19]. Over 30 million cases of water-related disease could be avoided globally each year through water and sanitation interventions (as cited in [20]). At current rates, Nigeria is off-track and still a long way from achieving the promise of SDG 6 and ensuring clean water and sanitation for all. The National Action Plan is an excellent opportunity to drive momentum towards universal access in Nigeria by 2030 [17]. With less than a decade to go before this crucial milestone, now is the time to mobilise the resources that are equal to the task. Prevention, they say is better than cure. Spending money on the treatment of water-related diseases is not as economical as putting in place adequate water infrastructure which will enable provision of clean water for all. Therefore, it is high time government at all levels and individuals embraced the WASH agenda.

REFERENCES

- [1] World Vision, *The Dangers of Dirty Water, the Power of a Safe, Clean Well*, A Publication of World Vision Australia, Retrieved from: <https://www.worldvision.com.au/global-issues/work-we-do/climate-change/dangers-of-dirty-water-power-of-a-safe-well> 2021.

- [2] M. Khalifa, S. Bidaisee, The Importance of Clean Water, *Scholar Journal of Applied Sciences and Research*, 1 (7), 2018, pp. 17-20.
- [3] S. Gomathi, P. L. Theresa, S. J. Debora, WASH (Water, Sanitation and Hygiene), *International Journal of Trend in Scientific Research and Development (IJTSRD)*, 2 (1), 2017, pp. 575 -579.
- [4] Wikipedia, *Nigeria*, A Publication of Wikimedia Foundation Inc., Retrieved from: <https://en.wikipedia.org/wiki/Nigeria> 2021.
- [5] Hesperian, What Makes Water Unsafe? Hesperian Health Guides, Retrieved from: [https://en.hesperian.org/hhg/A Community Guide to Environmental Health:What Makes Water Unsafe%3F](https://en.hesperian.org/hhg/A%20Community%20Guide%20to%20Environmental%20Health:What%20Makes%20Water%20Unsafe%3F) 2020.
- [6] F. Dangendorf, D. Schoenen, *Health Risks from Microbial Pathogens*, In: Technical guidance on water-related disease surveillance, Eds: E. Funari, T. Kistemann, S. Herbst and A. Rechenburg, A Publication of World Health Organisation, 2011.
- [7] D. O. Omole, C. P. Emenike, I. T. Tenebe, A. O. Akinde, A. A. Badejo, An Assessment of Water Related Diseases in a Nigerian Community, *Research Journal of Applied Sciences, Engineering and Technology* 10 (7), 2015, pp. 776-781.
- [8] O. Oguntoke, O. J. Aboderin, A. M. Bankole, Association of Water-Borne Diseases Morbidity Pattern and Water Quality in Parts of Ibadan City, Nigeria, *Tanzania Journal of Health Research*, 11 (4), 2009, pp. 189-194.
- [9] O. Maxwell, A. Oklo, A. Bernard, Profile of Water Related Diseases in Benue State, Nigeria, *American Journal of Human Ecology*, 1 (3), 2012, pp. 87-94.
- [10] T. A. Adeyemo, B. T. Omonona, Estimating the Incidence of Water Related Diseases: the case of Neglected Tropical Diseases in Rural Nigeria. *IOSR Journal of Agriculture and Veterinary Science (IOSR-JAVS)*, 10 (7), 2017, pp. 49-57, DOI: 10.9790/2380-1007014957.
- [11] United Nations, *Transforming our World: the 2030 Agenda for Sustainable Development*, NY, USA: <https://sustainabledevelopment.un.org/post2015/transformingourworld> 2015.
- [12] L. Guppy, P. Uytendaele, K. G. Villholth, V. Smakhtin, *Groundwater and Sustainable Development Goals: Analysis of Interlinkages*, UNU-INWEH Report Series, Issue 04, United Nations University Institute for Water, Environment and Health, Hamilton, Canada, 2018.
- [13] V. Freyling, *The Importance of All SDGs for Cities*, ICLEI BRIEFING SHEET - Urban Issues, No. 04. 2015.
- [14] UNICEF, *Strategy for Water, Sanitation and Hygiene 2016-2030*, A Publication of UNICEF, 2016.
- [15] J. Mateo-Sagasta, S. M. Zadeh, H. Turrall, *Water Pollution from Agriculture: A Global Review*, A Publication of Food and Agriculture Organization of the United Nations and International Water Management Institute, 2017
- [16] J. E. Mills, O. Cumming, *The Impact of Water, Sanitation and Hygiene on Key Health and Social Outcomes: Review of Evidence*, A Publication of London School of Hygiene and Tropical Medicine and UNICEF, 2016.
- [17] O. Oraka, *Achieving Clean Water, Sanitation and Hygiene for All in Nigeria*, A Publication of Wateraid. Retrieved from: <https://www.wateraid.org/ng/blog/achieving-clean-water-sanitation-and-hygiene-for-all-in-nigeria> 2020.
- [18] T. Thompson, M. Sobsey, J. Bartram, Providing Clean Water, Keeping Water Clean: An Integrated Approach. *International Journal of Environmental Health Research*, 13, 2003, pp. S89 – S94.
- [19] A. O. Familusi, B. E. Adewumi, *Quality-Comparison of Water Samples Collected at the Clearwell of the Waterworks with the Ones Running at the Tap*, A Paper Presented at the 6th National Conference on Sciences, Engineering and Environmental Technology Held at Ede Nigeria, 2011.
- [20] M. Exner, *Introduction on Water Related Diseases*, In: Technical Guidance on Water-Related Disease Surveillance, Eds: E. Funari, T. Kistemann, S. Herbst and A. Rechenburg, A Publication of World Health Organisation, 2011.

CORROSION RESISTANCE OF SURFACE-CONDITIONED 301 AND 304 STAINLESS STEELS BY SALT SPRAY TEST

Temitope Olumide Olugbade, Babatunde Olamide Omiyale

Department of Industrial and Production Engineering, Federal University of Technology, P.M.B. 704, Akure, Ondo State, Nigeria.
E-mail: boomiyale@futa.edu.ng

ABSTRACT

The corrosion rate of surface-conditioned 301 and 304 stainless steels (SS) was determined by salt spray test in a controlled accelerated corrosive medium (9.5 L of pure distilled water + 500 g NaCl). Surface conditioning via mechanical attrition treatment was firstly carried out before the salt spray test. The corrosion rate was determined by weight loss method before and after the salt spray test. Compared to the untreated 301 SS sample with a weight loss of 0.15 g, the surface-conditioned 301 SS samples treated for 300 s and 1200 s experienced a lower weight loss of 0.04 and 0.02 g, respectively. A similar reduction in weight loss was achieved for 304 SS sample when treated for 300, 600, and 1200 s.

Keywords: Salt spray test; 301 SS; 304 SS; corrosion rate; weight loss.

1. INTRODUCTION

AISI 304 and 301 stainless steels (SS) are widely used engineering materials in most manufacturing and production industries due to their good corrosion behaviour and excellent high hardness-strength combination. Despite their good corrosion properties, there is still a high tendency of material failure due to usage and exposure to corrosive environment over time [1-4]. Hence, there is a need to determine their actual corrosion rate in a monitored accelerated corrosive medium to predict their behaviour in a real-life application. Over the years, various corrosion testing methods have been adopted to determine the resistance of materials to corrosion which includes polarization tests and salt spray test [5-7].

As a form of corrosion testing method, salt spray test determines the rate of corrosion of engineering materials over a long period of time in a controlled corrosive environment. It is a promising method for identifying the time when the first sign of corrosion is evident after subjecting the material to a long corrosion test. In the past, salt spray test method has been successfully used to evaluate the corrosion behaviour of different material systems including stainless steel [5, 8-9], $\text{Al}_2\text{O}_3\text{-ZrO}_2$ [10], Al_2O_3 [11-12], ZrO_2 [12-13], alumina coating [14-15], Mg-Al alloy [16], and galvanized steel [17-18].

Stainless steel types 301 and 304 are presently attracting considerable attention due to their good mechanical and corrosion properties and they find applications in most manufacturing and production industries. However, further study is still needed on their corrosion resistance especially when they are subjected to surface treatment. Hence, the corrosion resistance of treated SS in a monitored accelerated corrosive medium will be a good subject of investigation.

In the present study, 301 and 304 SS samples were first subjected to surface conditioning through mechanical attrition treatment. Thereafter, the corrosion behaviour of the untreated and treated samples was investigated through salt spray test using 5% concentration salt solution. The weight of the samples before and after salt spray test were determined and the corrosion rate was therein determined through weight loss method.

2. EXPERIMENTAL DETAILS

2.1 Material preparation

A typical commercial 304 and 301 stainless steels (SS) samples of dimension 70 x 60 x 1 mm³ were used in this study, with a chemical composition in Table 1. All samples were cut using electrical discharge machining (Model: ALN400G, Thailand) and properly cleaned using acetone before the corrosion test. The

samples were then surface conditioned via mechanical attrition treatment for 300, 600, and 1200 s. The mechanical attrition procedure has been previously described in the literature [19-20].

Table 1. Elemental composition of untreated 304 and 301 stainless steels.

Elements	Conc. (wt. %)	
	304 SS	301
C	0.04	0.15
Si	0.52	1.00
Mn	1.18	2.00
Cr	17.59	18.00
Ni	8.03	10.00
S	0.03	0.03
P	0.04	0.05
Fe	Bal	Bal

2.2 Salt spray test

The corrosion rate of the untreated and treated samples was determined by subjecting the samples to salt spray test using a salt spray tester (Model: SH-90, China) with a chamber volume of 270 liters, salt solution tank size of 25 liters and spray rate of 1-2 ml/80 cm²/hour. The apparatus and the setup are shown in Figure 1.

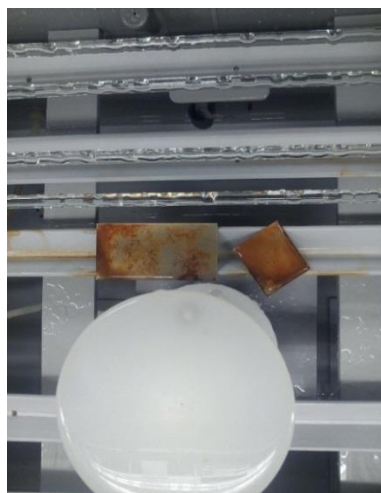


Figure 1. Salt spray tester and the specimens after the salt spray test.

The chamber and standard air tank temperatures are 35°C and 47°C, respectively. The tester operated at the air compressor of 0.32 MPa, pressure adjuster of 1 kg/cm² and the pressure reducer was in the range 2 – 3 kg/cm². The testing time was 240 h and the sample tilt angle is 10°. According to ASTM B117 standard (ASTM B117-16 2016) [21], the salt solution used for the test comprised the mixture of 9.5 liters of pure distilled water and 500 g NaCl salt (5 % concentration). The test determines the relative corrosion resistance of the untreated and treated samples for 300, 600, and 1200 s. To ensure uniform exposure to the salt spray mist, all the steel samples were frequently rotated in the test chamber. During the test, the rate of corrosion was determined by noting the time until the first sign of rust is evident on the samples. Weight loss was measured for each sample at every 24 h intervals and the mean weight loss was calculated.

The condensate collection was carried out twice a day and it was analyzed for both pH and concentration throughout the salt spray test. The pH and concentration of the collected condensate were within the range of 6.5 – 7.2 and 4 - 6 %, respectively. To replenish the salt solution inside the test chamber, fresh solution (5 % concentration) was prepared every 24 h of the test.

Before the test, the samples were arranged in the salt test chamber in such a way that they were not in contact with any metallic material or with each other and placed parallel to the direction of the fog flow. After the salt sprat testing, the treated samples were examined according to ASTM D1645-02 method, which provides a means of comparing and evaluating the common corrosion performance of the samples. To remove salt deposits from the treated sample surface after the salt spray test, the samples were carefully removed from the holder and gently washed in clean warm running water at about 38°C, and then immediately dried naturally in air. Thereafter, the weight of the treated samples after test were taken and the weight loss was subsequently determined.

3. RESULTS AND DISCUSSION

3.1 Corrosion rate for 304 steel samples

Figure 2 shows the cumulative weight losses of the untreated and treated 304 SS samples after the salt spray test for 240 h while the comparison of weights of untreated and treated 304 SS samples before and after salt spray test, at the end of 240 h is shown in Figure 3. A stain of red corrosion was evident after 24 h for the untreated sample whereas it first appeared after 240 h for the treated samples. It should be noted that the dimension of test samples obviously would affect the corrosion area and consequently change the weight loss results. The weight of the untreated sample before salt spray test was 43.06 g and the sample were kept inside the salt spray chamber. After the salt spray test, the weight of the sample was reduced to 40.91 g. The weight loss was 2.15 g, showing the effect of corrosion. For sample treated for 1200 s, the initial weight before salt spray test was 52.16 g and the final weight after salt spray test for 240 h was 51.92 g (Figure 3). As evident in Figure 2, the weight loss for the treated sample is 0.24 g. It is important to note that the corrosion resistance of a material is related to the weight loss. The lower the weight loss after salt spray test, the better the corrosion resistance. The treated 304 SS samples experienced lower weight loss after salt spray test. Table 2 shows the summary of the salt spray test for untreated and treated 304 SS samples after different times of exposure. After 240 h of treatment, compared with the treated samples with no change in colour and sign of red dust, a stain of red dust was observed along the edge of the untreated sample.

Table 2. Results of salt spray test for untreated and treated 304 SS samples after different times of exposure.

Treatment Time (min)	24	48	52	Time (h) 96	120	168	240
0	Stains	Stains	Stains	Stains	Stains	Stains	Stains
5	No change	No change	No change	No change	No change	No change	Stains
10	No change	No change	No change	No change	No change	No change	Stains
20	No change	No change	No change	No change	No change	No change	Stains

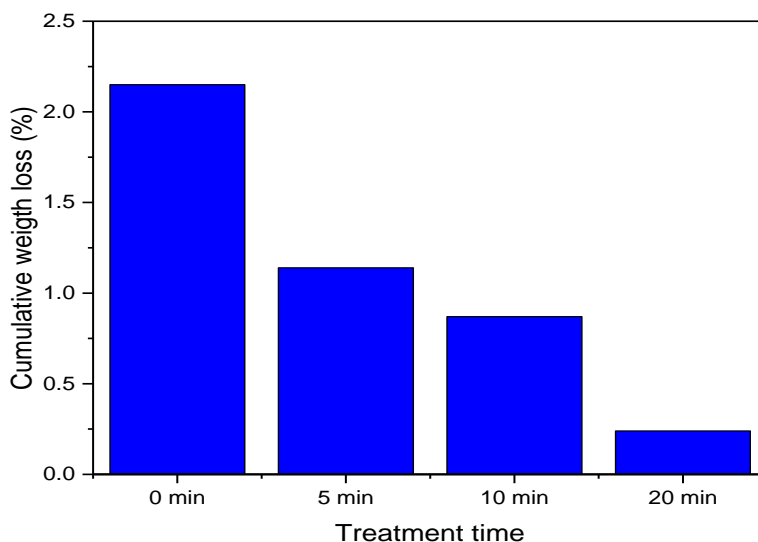


Figure 2. The cumulative weight losses for untreated and those 304 stainless steel samples treated for 5, 10, and 20 mins, after salt spray test for 240 h.

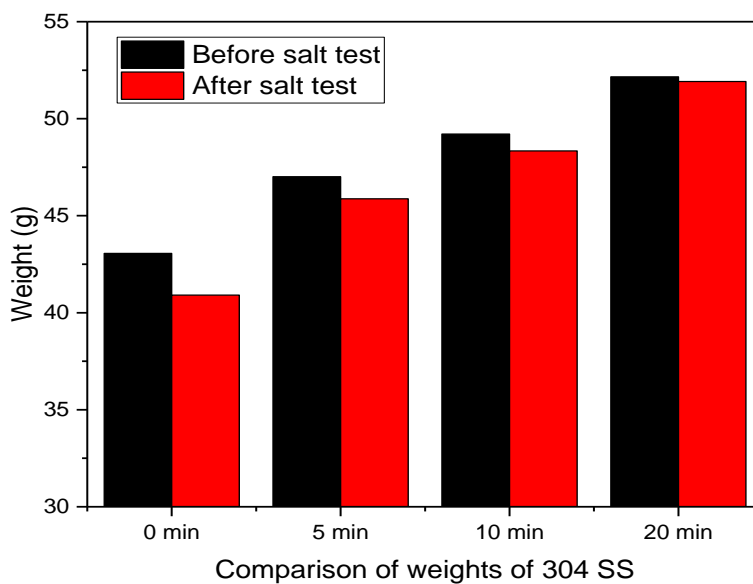


Figure 3. Comparison of weights of untreated and treated 304 SS samples, before and after salt spray test, at the end of 240 h.

3.2 Corrosion rate for 301 SS samples

Figure 4 shows the cumulative weight losses for untreated and treated 301 SS samples after salt spray test while Figure 5 shows the comparison of weights of untreated and treated 301 SS samples before and after the salt spray test at the end of 240 h. The first sign of red rust on the untreated sample was evident after 24 h.

The weight before salt spray test was 43.51 g and the sample were kept inside the salt spray chamber. After the salt spray test, the weight of the untreated sample has reduced to 43.32 g, indicating a weight loss of 0.19 g and shows the effect of corrosion. As shown in Figure 5, for 301 SS sample treated for 300 s, the initial weight before salt spray test was 43.23 g and the final weight after salt spray test for 240 h was 43.19 g, with a weight loss of 0.04 g while the weight loss for the treated 301 SS sample for 1200 s was 0.02 g (Figure 4)..

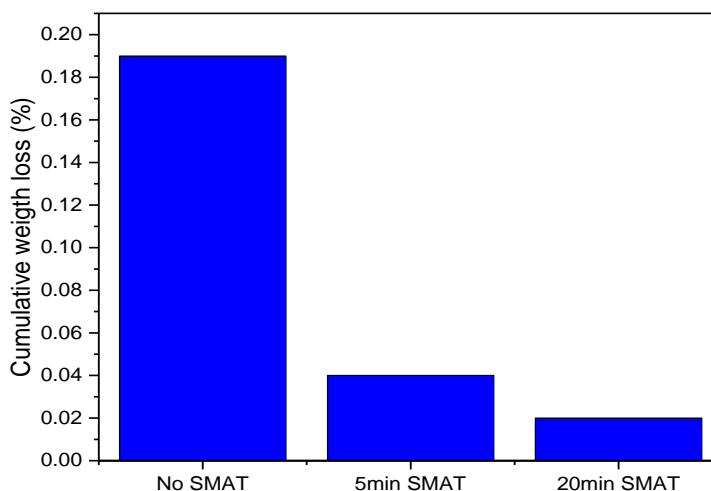


Figure 4. Salt spray test results showing the cumulative weight losses for untreated and treated 301 SS samples, at the end of 240 h.

The treated samples experienced a lower weight loss compared to the untreated one, denoting a lower corrosion rate.

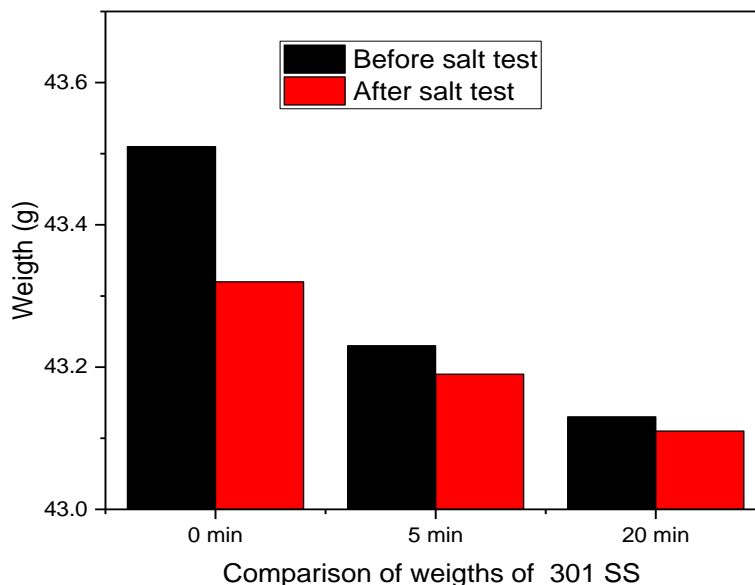


Figure 5. Comparison of weights of untreated and treated 301 SS samples before and after salt spray test, at the end of 240 h.

Table 3 summarizes the results of salt spray test results for untreated and treated 301 SS samples after different times of exposure. The salt spray test was performed for 240 h at 24 h interval. At 96 h, for the untreated sample, a point of red corrosion along the edge was spotted and abundant red corrosion was observed after 168 h up to 240 h of testing. For samples treated for 5 mins, points of red corrosion along the edge were observed after 96 h and red corrosion after 240 h of testing. Similar results were obtained when the samples are treated for 1200 s.

Table 3. Results of salt spray test for 301 SS after different times of exposure.

Treatment Time (min)	24	48	52	Time (h)	96	120	168	240
0	Subtle staining	Evident staining	No change	96	Point of red corrosion along the edge	Red corrosion	Abundant red corrosion	Abundant red corrosion
5	No change	Point of red corrosion along the edge	Points of red corrosion in the lower regions	96	Points of red corrosion along the edge	Red corrosion	Red corrosion	Red corrosion
20	No change	Point of red corrosion along the edge	Points of red corrosion in the lower regions	96	Points of red corrosion	Red corrosion	Red corrosion	Red corrosion

Figure 6 shows the surface condition of untreated and treated 304 SS samples before and after exposure to the salt spray test for 240 h. Compared to the untreated sample (Figure 6a), the treated samples (Figures 6b-d) experienced more corrosion attack.

The surface condition of untreated and treated 301 SS samples before and after exposure to the salt spray test for 240 h is shown in Figure 7. Compared to the treated samples, the untreated sample experienced more corrosion attack.

Several factors could influence the corrosion rate and consequently the weight loss after salt spray test including the extent of deformation, degree of exposure to heat treatment or corrosive environment [22-24].

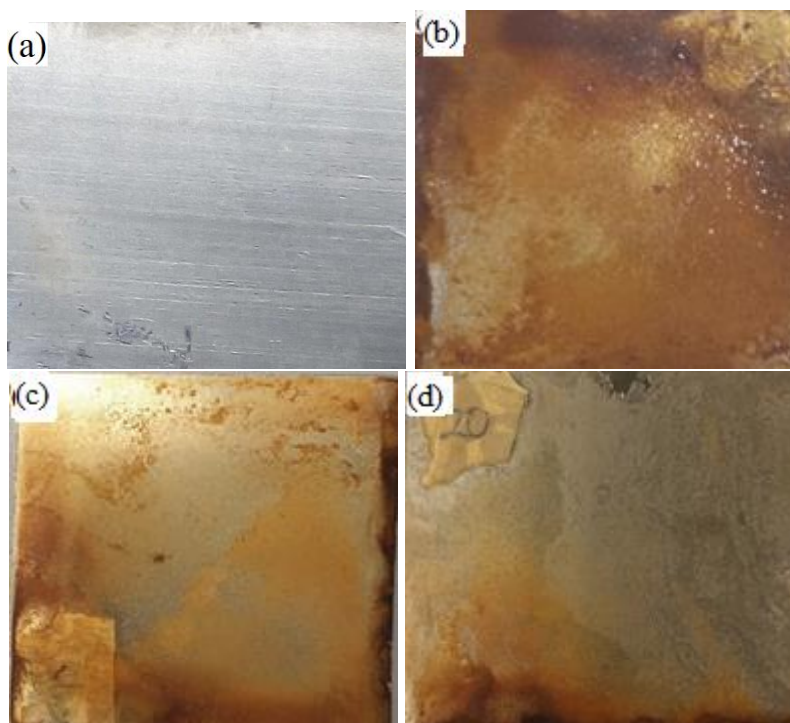


Figure 6. Surface condition of 301 stainless steel samples after exposure to the salt spray test for 240 h; (a) untreated sample without salt test, (b) untreated sample with salt test, (c) treated sample for 5min with salt test, (d) treated sample for 20min with salt test.

As obvious in Figure 7, the corrosion of test samples seems to be severer in the edges, which may indicate that the processing quality of sample edges has a significant effect on corrosion and might affect the weight loss result.

In addition, the dimension of test samples obviously would affect the corrosion area and consequently influence the weight loss results.

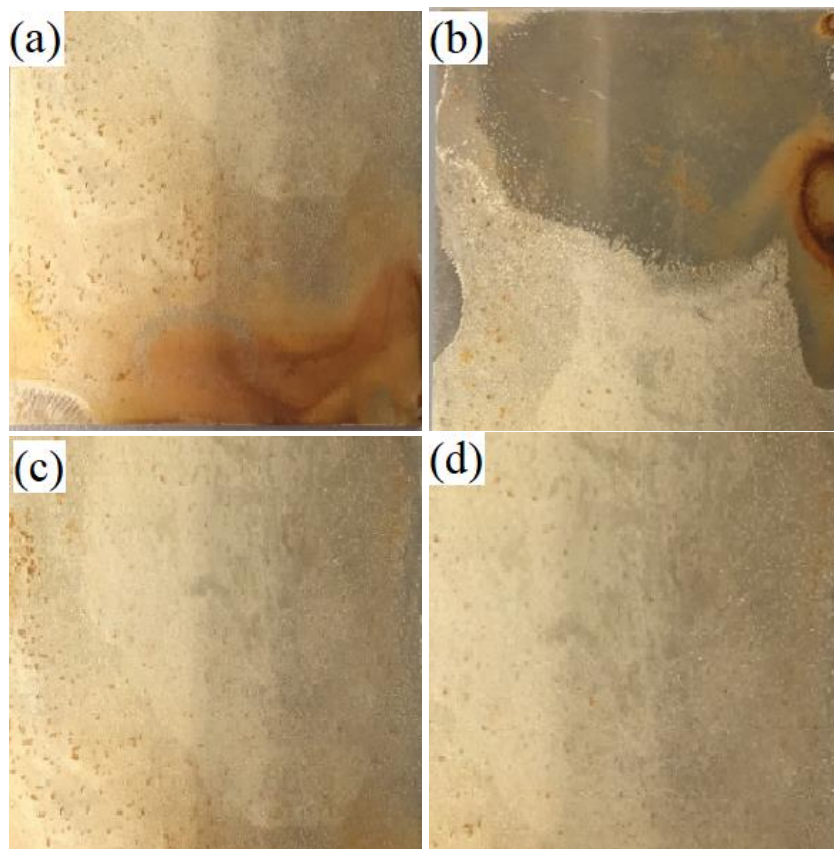


Figure 7. Surface condition of 304 stainless steel samples after exposure to the salt spray test for 240 h; (a) Untreated sample without salt test (b) Untreated sample with salt test (c) treated sample for 5min with salt test, (d) treated sample for 20min with salt test.

In the present study, an enhanced corrosion resistance of treated 301 and 304 stainless steels using salt spray corrosion test (5% concentration) was achieved (Figure 2, Figure 3, Figure 4, Figure 5, Table 2, Table 3). Similar improvement in the corrosion resistance was achieved when ceramic coatings (zirconia ceria powder and yttria-stabilized zirconia) were deposited on 304 steel. The samples with ceria powder coating exhibited more corrosion resistance than the yttria zirconia coating. If properly deposited in right proportions, coatings have the tendency of improving the fracture and corrosion resistance of materials [25-26]. In addition, Esfahani et al. [17] reported an increase in corrosion resistance of normal steel panel as compared with galvanized steel. In another study [16], the corrosion resistance of both AZ91D and AM50 alloys decreased with an increase in chloride concentration. After coatings/electrodeposition [27] and surface modifications by rolling [28], machining and moulding, mechanical treatment [29], an improvement in the electrochemical properties of 316 steel [30-33], 301 steel [4], 17-4PH steel [34], 304 steel [35], and mild steel was also reported. This was attributed to the passivation ability of the coating and nanostructured layers generated on the sample surfaces which protect the sample outer surface from corrosion especially in aggressive conditions. The surface-conditioned 301 and 304 SS with improved corrosion resistance will find applications in many manufacturing, aerospace and petroleum industries where excellent corrosion resistance over time is needed.

4. CONCLUSION

The effect of mechanical attrition treatment on corrosion resistance of 301 and 304 stainless steels (SS) was investigated in this work under salt spraying test in a controlled corrosive medium using 5 % concentration salt solution. The salt spray test and the corrosion rate of untreated and treated 301 and 304 stainless steel samples was determined by the weight loss after the salt spray test. The treatment method decreased the weight loss of 301 and 304 SS from 0.19 g to 0.02 g and from 0.15 g to 0.01 g after salt spraying test, respectively. In addition, the treated 304 SS samples showed the best result on exposure to salt spray, where the first spot of corrosion along the edge occurred at 240 h. Meanwhile, the untreated sample showed changes after 24 h of exposure. In addition, the first spot of red corrosion on the surface was noticed at 24 h and abundant red corrosion after 240 h for the untreated 301 SS sample.

Compared with the untreated 301 and 304 SS samples, the treated samples exhibited a lower weight loss, which denotes a low corrosion rate, hence an improved corrosion resistance.

DISCLOSURE STATEMENT

The authors declare no conflict of interest.

ACKNOWLEDGEMENTS

Many thanks to the members of Centre for Advanced Structural Materials (CASM), City University of Hong Kong, Hong Kong SAR as regards the surface treatment.

REFERENCES

- [1] Zhang, Y., C. Yang, L. Zhao, and J. Zhang. 2021. Study on the Electrochemical Corrosion Behavior of 304 Stainless Steel in Chloride Ion Solutions. *International Journal of Electrochemical Science* 16:210251.
- [2] Tian, W, Du, S. Li, S. Chen, and Q. Wu. 2014. Metastable pitting corrosion of 304 stainless steel in 3.5% NaCl solution. *Corrosion Science* 85:372–379.
- [3] Pan, C., L. Liu, Y. Li, and F. Wang. 2013. Pitting corrosion of 304SS nanocrystalline thin film. *Corros. Sci.* 73:2–43.
- [4] Olugbade, T., C. Liu, and J. Lu. 2019. Enhanced passivation layer by Cr diffusion of 301 Stainless Steel facilitated by SMAT. *Adv. Eng. Mater.* 21: 1900125.
- [5] Anderson, A. 2017. Corrosion resistance of ceramic coatings sprayed on stainless steel substrates. *International Journal of Ambient Energy.* 38(3):320-322.
- [6] Bao, Z.B., Q.M. Wang, W.Z. Li, J. Gong, T.Y. Xiong, and C. Sun. 2008. Corrosion Behaviour of AIP NiCoCrAlYSiB Coating in Salt Spray Tests. *Corrosion Science* 50: 847–855.
- [7] Rogerio, M.A., S.O. Rogero, M. Terada, E.F. Pieretti, and I. Costa. 2014. Localized Corrosion Resistance and Cytotoxicity Evaluation of Ferritic Stainless Steels for Use in Implantable Dental Devices with Magnetic Connections. *Int. J. Electrochem. Sci.* 9:1340 – 1354
- [8] Islak, S., S. Buytoz. 2011. Microstructure Properties of ZrO₂/Al₂O₃-% 13TiO₂ Composite Coating Produced with Plasma Spray Method on AISI 304 Stainless Steel. 6th International Advanced Technologies Symposium (IATS'11), Elazığ; May 16–18.
- [9] Zhang, J., A. Kobayashi. 2005. Corrosion Resistance of Al₂O₃ + ZrO₂ Composite Coatings Sprayed on Stainless Steel Substrates. *Transactions of JWRI.* 34 (2):17–22.

- [10] Mert, S, S. Mert, and S. Saridemir S. 2018. An investigation of $\text{Al}_2\text{O}_3\text{-ZrO}_2$ ceramic composite-coated engine parts using plasma spray method on a diesel engine. *International Journal of Ambient Energy*. DOI: 10.1080/01430750.2018.1501748.2014; 9: 1340–1354.
- [11] Liu, Z.Z., Y. Chu, Y. Dong, X. Yang, X. Chen, Y.D. Kong. 2013. The Effect of Metallic Bonding Layer on the Corrosion Behavior of Plasma Sprayed Al_2O_3 Ceramic Coatings in Simulated Seawater. *Vacuum* 101:6–9.
- [12] Sathish, S., M. Geetha. 2015. Comparative Study on Corrosion Behavior of Plasma Sprayed Al_2O_3 , ZrO_2 , $\text{Al}_2\text{O}_3/\text{ZrO}_2$ and $\text{ZrO}_2/\text{Al}_2\text{O}_3$ Coatings. *Transactions of Nonferrous Metals Society of China* 26:1336–1344.
- [13] Limarga, A.M., W. Sujanto, H.Y. Tick. 2005. Mechanical Properties and Oxidation Resistance of Plasma-Sprayed Multilayered $\text{Al}_2\text{O}_3/\text{ZrO}_2$ Thermal Barrier Coatings. *Surface and Coatings Technology*. 197:93–102.
- [14] Singh, V.P., A. Sil, and R. Jayaganthan. 2011. A Study on Sliding and Erosive Wear Behaviour of Atmospheric Plasma Sprayed Conventional and Nanostructured Alumina Coatings. *Materials and Design* 32:584–591.
- [15] Wang, Y., S. Jiang, M. Wang, S. Wang, T.D. Xiao, P.R. Strutt. 1999. Abrasive Wear Characteristics of Plasma Sprayed Nanostructured Alumina/Titania Coatings. *Wear*. 237: 176–185.
- [16] Mohedano, M., R. Arrabal, A. Pardo, M.C. Merino, K. Paucar, P. Casajús, E. Matykina. 2014. Salt spray corrosion behaviour of new Mg–Al alloys containing Nd or Gd. *Corrosion Engineering, Science and Technology*. 48(3):183-193.
- [17] Esfahani, S.L., Z. Ranjbar, and S. Rastegar. 2016. Comparison of corrosion protection of normal and galvanized steel coated by cathodic electrocoatings using EIS and salt spray tests. *Corrosion Engineering, Science and Technology* 51(2): 82-89.
- [18] Loveridge, M.J., H.N. McMurray, and D.A. 2006. Worsley. Chrome free pigments for corrosion protection in coil coated galvanized steels. *Corrosion Engineering, Science and Technology* 41(3):240-248.
- [19] Lu, K., and J. Lu. 1999. Surface Nanocrystallization (SNC) of Metallic Materials-Presentation of the Concept behind a New Approach. *Journal of Material Science Technology*. 15:193–197.
- [20] Lu, K., and J. Lu. 2004. Nanostructured surface layer on metallic materials induced by surface mechanical attrition treatment. *Mater. Sci. Eng., A*. 375–377: 38–45.
- [21] ASTM B117-16. 2016. Standard Practice for Operating Salt Spray (Fog) Apparatus. ASTM International. West Conshohocken, PA.
- [22] Abioye, T. E., T. O. Olugbade, and T. I. Ogedengbe. 2017. Welding of dissimilar metals using gas metal arc and laser welding techniques: a review. *Journal of Emerging Trends in Engineering and Applied Sciences (JETEAS)* 8: 225-228.
- [23] Abioye, T. E., I. S. Omotehinse, I.O. Oladele, T. O. Olugbade, and T. I. Ogedengbe. 2020. Effects of post-weld heat treatments on the microstructure, mechanical and corrosion properties of gas metal arc welded 304 stainless steel. *World Journal of Engineering* 17(1): 87–96.
- [24] Mohammed, T., T.O. Olugbade, and I Nwankwo. 2016. Determination of the effect of oil exploration on galvanized steel in Niger Delta, Nigeria, *Journal of Scientific Research and Reports* 10:1-9.
- [25] Olugbade, T.O., Ojo, O.T., Omiyale, B.O., Olutomilola, E.O., and Olorunfemi, B.J. (2021). A review on the corrosion fatigue strength of surface-modified stainless steels. *Journal of the Brazilian Society of Mechanical Sciences and Engineering* 43:421.
- [26] Olugbade, T.O. 2020. Stress corrosion cracking and precipitation strengthening mechanism in TWIP steels: progress and prospects. *Corrosion Reviews* 38: 473-488.
- [27] Olugbade, T.O., T.E. Abioye, P.K. Farayibi, N.G. Olaiya, B.O. Omiyale, T.I. Ogedengbe. 2021. Electrochemical properties of MgZnCa-based thin film metallic glasses fabricated via magnetron sputtering deposition coated on a stainless steel substrate. *Anal. Lett.* 54(10): 1588-1602

- [28] Olugbade, T.O. 2020. Electrochemical characterization of the corrosion of mild steel in saline following mechanical deformation. *Anal. Lett.* 54: 1055 - 1067.
- [29] Olugbade, T., and J. Lu. 2020. Improving the passivity and corrosion behaviour of mechanically surface-treated 301 stainless steel. *International Conference on Nanostructured Materials (NANO 2020)*, 117, Australia.
- [30]] Olugbade, T., and J. Lu. 2019. Enhanced corrosion properties of nanostructured 316 stainless steel in 0.6 M NaCl solution. *J Bio Tribo Corros.* 5: 38.
- [31] Olugbade, T., and J Lu. 2018. Effects of materials modification on the mechanical and corrosion properties of AISI 316 stainless steel. *Twelfth international conference on fatigue damage of structural materials*, Cape Cod, Hyannis, USA.
- [32] Olugbade, T. 2019. Datasets on the corrosion behaviour of nanostructured AISI 316 stainless steel treated by SMAT. *Data-in-brief* 25: 104033.
- [33] Hao, Y., B. Deng, C. Zhong, Y. Jiang, and J. Li. 2009. Effect of surface mechanical attrition treatment on corrosion behavior of 316 Stainless Steel. *Journal of Iron and Steel Research Intl.* 16:68-72.
- [34] Olugbade, T.O., and J. Lu. 2019. Characterization of the corrosion of nanostructured 17-4 PH stainless steel by surface mechanical attrition treatment (SMAT). *Anal. Lett.* 52: 2454-2471.
- [35] Lu, J.Z., H. Qi, K.Y. Luo, M. Luo, X.N. Cheng. 2014. Corrosion behaviour of AISI 304 stainless steel subjected to massive laser shock peening impacts with different pulse energies. *Corrosion Science* 80: 53-59.

A SHORT REVIEW ON PASSIVE STRATEGIES APPLIED TO MINIMISE THE BUILDING COOLING LOADS IN HOT LOCATIONS

¹*Qudama Al-Yasiri*, ²*Márta Szabó*

¹Doctoral School of Mechanical Engineering, Hungarian University of Agriculture and Life Sciences, Páter K. u. 1, Gödöllő, H-2100, Hungary

²Institute of Technology, Hungarian University of Agriculture and Life Sciences, Páter K. u. 1, Gödöllő, H-2100, Hungary
Corresponding author e-mail: qudamaalyasiri@uomislan.edu.iq

ABSTRACT

Cooling and air-conditioning systems are responsible for the highest energy consumption in buildings located in hot areas. This high share does not only increase the building energy demand cost but also increases the environmental impact, the topmost awareness of the modern era. The development of traditional systems and reliance on renewable technologies have increased drastically in the last century but still lacks economic concerns. Passive cooling strategies have been introduced as a successful option to mitigate the energy demand and improve energy conservation in buildings. This paper shed light on some passive strategies that could be applied to minimise building cooling loads to encourage the movement towards healthier and more energy-efficient buildings. For this purpose, seven popular passive technologies have been discussed shortly: multi-panned windows, shading devices, insulations, green roofing, phase change materials, reflective coatings, and natural ventilation using the windcatcher technique. The analysis of each strategy has shown that the building energy could be improved remarkably. Furthermore, adopting more passive strategies can significantly enhance the building thermal comfort even under severe weather conditions.

Keywords: Passive strategies, energy saving, cooling load reduction, insulations, thermal mass

1. INTRODUCTION

Buildings in hot locations require efficient cooling systems to overcome the high temperature and reach occupants' thermal comfort [1]. This is mainly due to the high thermal conductivity construction materials used, which causes high cooling loads [2]. These cooling and air-conditioning systems consume more than 50% of the total electric power provided by local electric networks. The researchers and experts resort to modern strategies that reduce thermal loads in buildings, which lead to environmental and economic benefits [3].

Recently, many methods have been used to reduce the cooling loads in buildings, actively and passively [4,5]. Passive strategies represent the intelligent use of renewable energy sources like the sun and wind to cool, ventilate, and light the building without using any equipment. This leads to a reduction of electrical energy, making buildings more energy-efficient. There is interest in such techniques as part of the evolution in architecture, and the world tends towards zero energy buildings [6]. The use of passive cooling strategies in modern buildings aims to eliminate the need for mechanical cooling equipment or reduce the size and cost of equipment, thus reducing maintenance operations [7]. Many types of passive cooling techniques could be used in hot locations that could be adopted for a better, healthier and efficient built environment.

In this paper, some popular passive strategies that can be applied to improve the building energy in hot locations have been presented and discussed briefly. These strategies are mainly applied for openings (windows and transparent building envelopes), building thermal mass (roofs and walls), minimising the incident solar radiation or improving air quality. Therefore, the heat response and energy performance of the building will be improved. Despite the brief description of these techniques, the information presented in this paper is believed to provide a sound vision of what and how passive strategies can be used to improve the building energy in hot locations.

2. STRATEGIES APPLIED ON THE WINDOWS

The primary role of these techniques is to control the solar radiation incident on building windows, taking into account the importance of sunlight for natural lighting. These strategies are popularly used worldwide despite the prevailing weather conditions. The main two types discussed in this regard are the multi-paned windows and shading devices.

2.1. Multi-paned windows

Huge heat gain of buildings comes through the open spaces such as windows. Controlling such elements and making them more efficient is one of the essential passive methods to reduce cooling loads. Multi-paned windows (MPWs) have developed a lot during the last century, and they could be double-pane, triple-pane and quadruple-pane windows [8]. For instant, the MPW is two glass panes placed away from each other by a 12-16 mm, discharged from the air or filled with argon gas. Triple-pane windows have the same construction as double-pane windows with an extra pane layer. Fig. 1 shows the typical illustration of single, double and triple-pane windows. The primary objective of MPWs is to increase the insulating of windows, wherein these panes and gas are used to reduce the amount of heat transfer that moves from outside to inside the buildings.

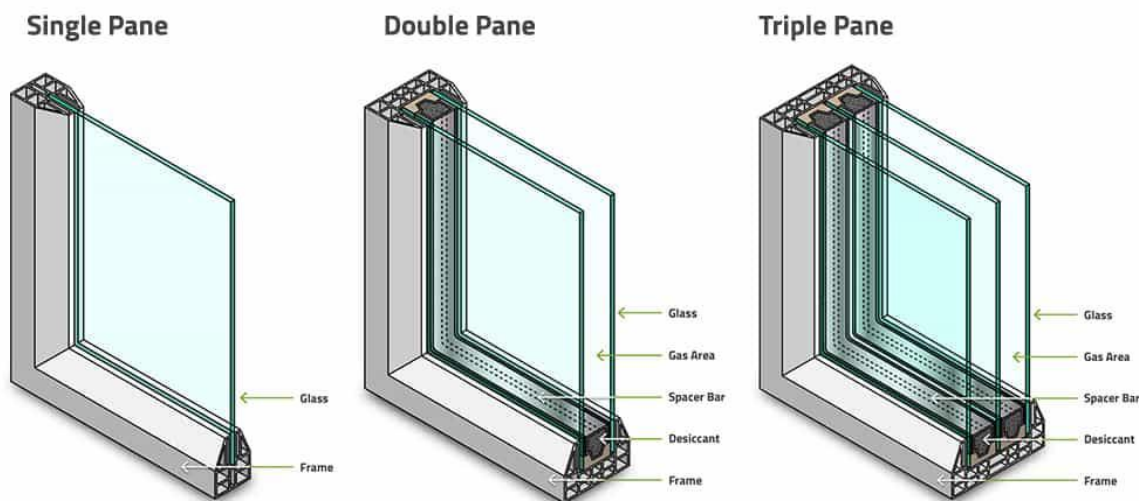


Figure 1. Typical single, double and triple-pane windows [9].

The number of panes can significantly influence the performance of MPWs, meaning that increasing pane number results in more energy saving. In this regard, Julián et al. [10] claimed that replacing clear single-pane windows with double-pane windows was reduced the heat flux by 72.6% under Mexican weather conditions. Furthermore, Arıcı et al. [11] revealed that replacing double-pane windows with triple or quadruple pane windows can save energy by about 50% or 67%, respectively.

The pane's U-value (U is the heat transmission coefficient) affects the MPWs in which low U-value panes performed better. Baek and Kim [12] reported that changing commercial panes of U-value ranging from 1.2-3.3 W/m².K to 0.7 W/m².K can reduce the greenhouse gas emissions and related heat flux by 45%-79% while using panes of 0.2 W/m².K can improve the window by up to 82%-93%.

Filling gaps between panes with gases denser than air is another modification strategy in MPWs. These gases can decrease the conductive heat coming from outside and reach better thermal comfort [13]. Filling panes' gaps with gas decrease the radiative heat transfer by absorbing, emitting, and scattering, reducing

heat flux [14]. This can contribute to up to 20% energy saving in buildings. Other strategies have been studied in the literature and showed remarkable contributions, such as pane coating with low thermal emissivity materials [15], a vacuum of panes gaps [16] and using of solar control coatings [17].

2.2. Shading devices

Shading devices are used to shade the sun radiation fallen on the building windows. The use of such devices can improve the internal environment of buildings [18]. Windows should well control the sun to reduce the radiation in the summer and get maximum radiation in the winter. These shading devices could be inside the building through blinds, rollers, curtains, or outside, such as fins, louvres, and overhangs. Venetian blinds are the most studied literature among other shading devices, particularly office buildings [19]. Fig. 2 shows some popular practical types of shaded devices.

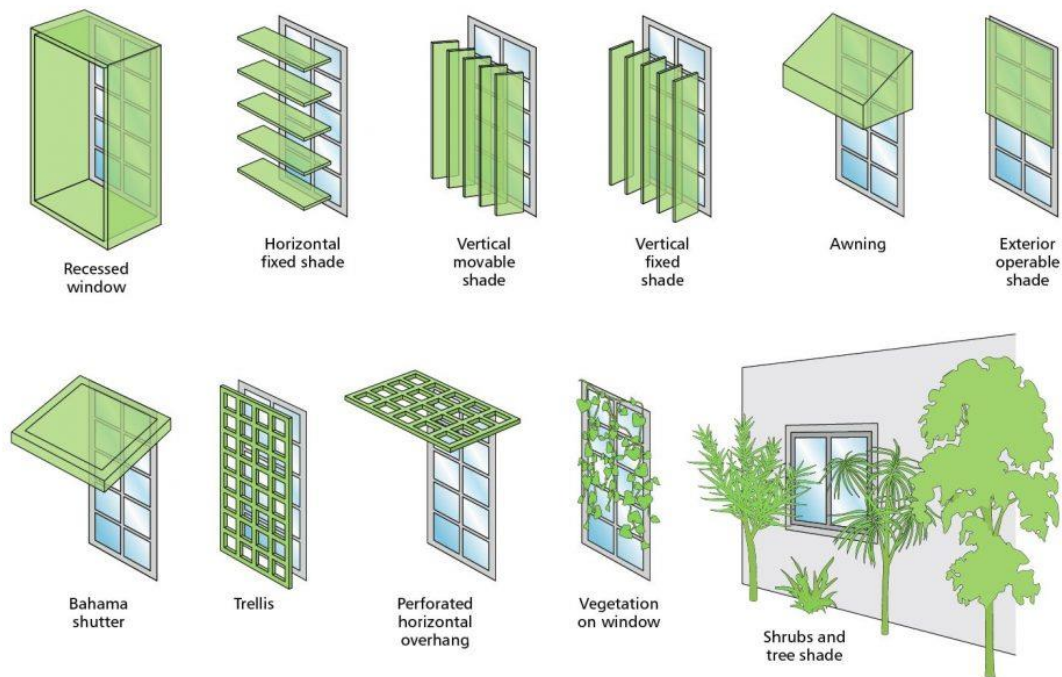


Figure 2. Types of external shading devices [20].

Shading devices can be placed horizontally or vertically in front of the window in various ways, and their effectiveness depends highly on the building geographical location [21]. Their shape, type, depth, and height differ depending on the building location, inclination angle, and window area [22]. The shading device is designed to block the sun in summer yet allows it to enter in winter. Typically, the inside shading device places behind the glass and can only reflect part of the radiation, while the rest is absorbed, convected and re-radiated into the room. External shading devices shade the window from direct radiation and prevent a large part of heat to get in. Hence, the location of these devices is very important. Glazed areas that are fully shaded from the outside can reduce the solar heat gain by up to 80% compared to those located behind the glazing surface [23].

3. THERMAL MASS STRATEGIES

Different successful passive strategies have been applied to enhance the building's thermal mass, especially for heavy and thermally-poor construction materials. Such techniques significantly impact future building sustainability by constructing thin buildings with minimal cost and raw construction materials. The main strategies discussed in this section include green roofing, insulations, and the incorporation of phase change materials.

3.1. Green roofing

Studies indicate that a massive amount of heat comes from the sun passes through the building roof. Therefore, using insulating techniques on the roof surface to reduce thermal loads is essential and gives promising results. Covering the roof with a layer of grass or plants situated over the waterproof membrane is one of the modern methods used and called green roofing (see Fig. 3). Studies have shown that green roofing decreases the indoor air temperature in the closed buildings by about 2 °C and reduces annual energy demand by 6% [24]. Other benefits of green roofing are the production of oxygen, which improves air quality around the building and rainwater absorption.



Figure 3. Green roofing technique [25].

Green roofing technique consists of sewage and barriers that prevent roots in addition to water channels composition. Spaces without panels allow air to move and create heat in the roots and thus provide better ventilation without membranes locked together to create a platform and stay stable. It will also include some of the sewage water runoff. The materials used for such purposes are mostly recycled plastics. There are two types of green roofing; intensive and extensive green roofs. The first type is thick with a minimum depth of 12.8 cm and allows a variety of plants to be planted. This type is heavy and requires more maintenance. The extensive roofs are shallow, ranging from 2-12.7 cm depth, lighter than intensive green roofs, and require minimal maintenance [26].

3.2. Insulation

Literature studies indicate that highly effective insulating materials are used to maintain acceptable comfort levels in buildings, significantly reduce heat gain, and reduce energy demand [27]. Many materials used as insulators, and mainly classified into three categories according to their origin and chemical composition: conventional (organic and inorganic insulation such as polystyrene, formaldehyde insulators, polyurethane and polyisocyanurate, cellulose, cork, mineral wool, calcium silicate, foam glass, perlite, and vermiculite),

state-of-the-art (closed-cell foam, aerogel, Transparent Insulation Materials, vacuum insulation panels, reflective multi-foiled insulation materials, and Nano Insulation materials) and sustainable insulators (natural insulation materials derived from agro and forest residues, and sheep wools Recycled insulation materials) [28].

As shown in Fig. 4, the insulation could be installed for walls, ceilings, and roofs in the internal or external building elements.



Figure 4. Insulations applied to the interior and exterior building envelope.

Insulations are working to reduce the heat gain through the building envelope by trapping large amounts of air (or other gases) in a way that results in a material that employs low thermal conductivity of small pockets of gas instead of the much higher than conventional solids conductivity. The effectiveness of insulation is commonly evaluated by its R-value (the temperature difference ratio across an insulator that measures the thermal resistance) [29]. The importance of insulations revealed more for multi-story buildings due to large building surfaces exposed to the incident solar radiation. For instance, a study conducted for a four-story building in Thailand indicated that mean overheating days can be reduced by 21.43% using insulation [30].

The type and quantity of insulations depend on the design of buildings, climate, energy costs, budget and personal preference [31]. Building insulation needs careful consideration of how (and where) the energy and heat transfer direction change during the day and season [32,33]. It is crucial to choose the right design, insulation materials and construction techniques fitted with the building [34].

3.3. Phase change materials

Phase change materials (PCMs) are materials that can store and release a considerable amount of heat in a latent form (in addition to the sensible form) within a relatively stable temperature called phase change/transition temperature [35][36]. PCMs have proved to control the heat through the building envelope by acting as a heat barrier under hot locations, resulting in an essential building thermal comfort and energy saving [37,38]. The working principle of PCMs is that the heat accumulated during the day is restricted and stored in a latent form (which is huge in these materials) and then released during the nighttime [39]. This mechanism is the same as insulations, except PCMs are more dynamic against heat transfer than insulators. PCMs have been integrated in different forms and techniques with the building

elements, such as roofs [40,41], walls [42], floors [43], mortars and concrete [44-46], insulation [47], bricks [48,49], windows [50], shading devices [51], etc. Considering the building thermal mass (i.e. roofs and external walls), studies have shown that PCMs can effectively shave and shift the peak indoor temperature, which maintains an acceptable thermal comfort even in severe hot locations [52,53]. Rathore and Shukla [54] experimentally showed that incorporation PCM with cubicles can reduce the maximum and total peak heat flux by 41.31% and 27.32%, respectively, compared with a cubicle without PCM under Indian weather conditions. At the same location, Saxena et al. [55] reported that the PCM can decrease 4.5 °C-7 °C of bricks inner surface temperature and the heat flux can be reduced by 40%-60%.

Several influential parameters need to be studied to use PCMs as efficient as possible for a longer time and minimal operational cost. These are mainly the optimal phase change temperature, the optimal position within the building element, and the optimal quantity to be involved [56-58]. Arıcı et al. [59] found that PCM temperature varied between 6 °C to 34 °C and a PCM layer thickness varied between 1–20 mm can improve the building thermal performance and time lag by 10.3 h in three different Turkish cities. Zhang et al. [60] indicated that PCMs of melting temperature varied between 22 °C-28 °C, placed to the interior position with 5mm thickness could reduce the indoor building surface temperature and the heat transfer by 6.6 °C and 52.9% under China weather conditions. All in all, these parameters need to be studied in parallel to obtain the best thermal performance of PCMs [61].

4. OTHER STRATEGIES

Many other passive strategies, other than those discussed above, have been used in hot location buildings. Some of them are used to minimise the incident solar radiation, such as coatings, and others adopt the night cooling effect and low-temperature air for ventilation. The main two strategies discussed in this section are the light colour reflective coatings and wind catchers.

4.1. Light colour reflective coatings

The indoor environment is affected by thermal loads that come through the building envelope exposed to the sun, wherein a large amount of heat is transferred into buildings of large envelopes. Painting exterior building envelopes with light-coloured coatings reduce the transferred heat remarkably thanks to the high reflectivity of these coatings against solar rays, as shown in Fig.5.

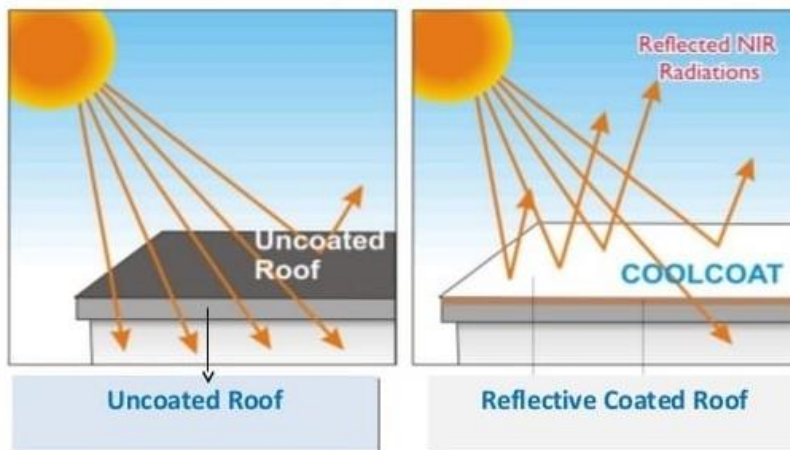


Figure 5. Principle of using light colour coatings to minimise solar radiation [62].

An experimental study reported that using light reflective paints has reduced the interior building temperature by up to 4.7 °C compared with painting with grey or dark colours [63]. This remarkably reduced the power consumption and cooling loads. The coating of the light colours depends on both the climate and the type of material used [64]. Pal et al. [65] investigated indoor temperature reduction through building envelope by applying exterior coloured coatings, namely white, yellow, pearl, straw, and sand. Findings showed that light colours (white and yellow) reduced the indoor temperature more than the others. The sand colour showed the worst performance in which the maximum difference of indoor temperature for sand/white and sand/yellow colour was 0.9 °C and 0.7 °C, respectively.

Thermochromic coatings (TCCs) are an advanced class of coatings that work dynamically to control the thermal load entering buildings [66]. TCCs change their optical properties according to the surface temperature; the colour becomes light at high temperatures, reflecting more sunlight and dark at lower surface temperatures and absorbing heat [67,68]. This property has a significant influence on the building energy in the summer and winter seasons. It has been reported that using TCCs can reduce the annual energy consumption and CO₂ emissions by 4.28–5.02 kWh/m² and 3.40–3.98 kg/m², respectively, compared with the common coatings [69].

4.2. Natural ventilation: windcatcher

Natural ventilation (sometimes called passive ventilation) is a knowledgeable method used to reduce thermal loads and improve occupants comfort in buildings. One of the oldest methods of natural ventilation systems is the windcatcher [70]. In windcatchers, the temperature and pressure directing the air inside buildings in which the airspeed and its direction are essential elements to control the airflow [71]. Windcatcher does not need any mechanical devices (fans) to provide buildings with fresh and healthy air with minimal pollution and dust.

Originally, the windcatcher was one of the traditional Persian architectural elements used to ventilate buildings with cool air during the summer period. It was built as a tall tower containing slots facing wind direction to catch the air and direct it down to cool the building. In the sandy places that carry dust and sand, windcatchers place away from the wind direction. Windcatchers were often used in combination with courtyards and domes (as shown in Fig. 6-a), and they do not necessarily cool the air itself but instead rely on the airflow rate to provide a cooling effect [72].

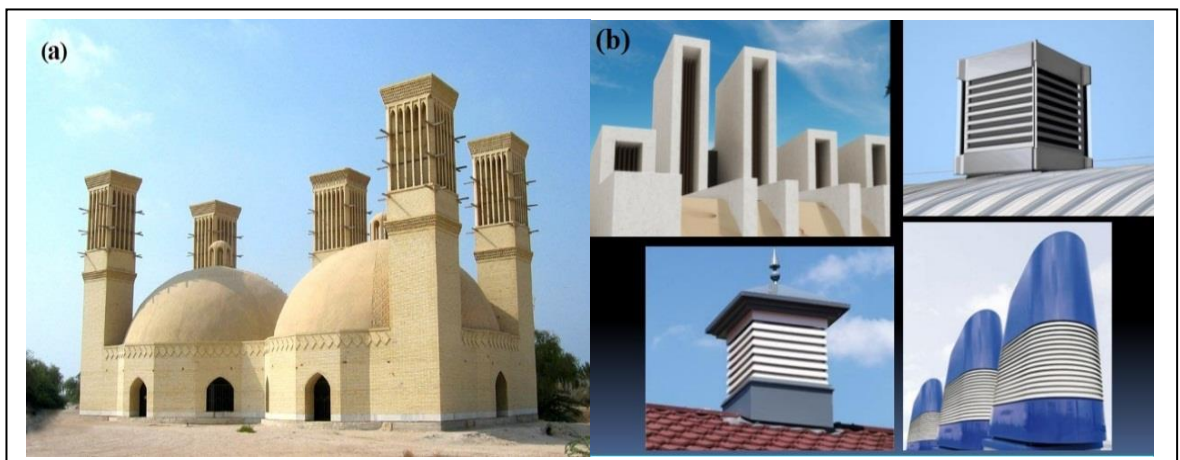


Figure 6. (a) Persian domes with wind catchers, (b) Modern wind catchers.

New advancements have recently been adopted to improve wind catchers with more control options (see Fig. 6-b). For instance, a newborn type of windcatcher has dampers, various types of sensors and an adjustable ceiling ventilator known as Monodraught, which is usually automatic and allows the temperature, humidity, airflow, noise level, and CO₂ to be adjusted depending on the need of the space [73].

5. CONCLUSIONS

The current paper presents and discusses the main passive strategies that could reduce the cooling loads in hot location buildings and maintain acceptable thermal comfort. These strategies are essential to improving building energy by decreasing the reliance on mechanical systems to cool buildings. All strategies have proven remarkable enhancements in the building energy by decreasing the indoor temperature. Most of them can be used in any building, and others can be only used for specific building types such as windcatchers. Matching some of these strategies can significantly improve the building energy performance and air quality, which results in further economic benefits. Modern life requirements required some control of these passive strategies to be more beneficial and competitive to the high-cost mechanical and electrical cooling devices.

REFERENCES

- [1] Internal Energy Agency (IEA), The future of cooling: opportunities for energy-efficient air conditioning, 2018.
- [2] Q. Al-Yasiri, M.A. Al-Furaiji, A.K. Alshara, Comparative study of building envelope cooling loads in Al-Amarah city, Iraq, *J. Eng. Technol. Sci.*, 51 (2019) 632–648.
- [3] I. Yüksek, T.T. Karadayi, Energy-efficient building design in the context of building life cycle, IntechOpen London, 2017.
- [4] R. Zhang, Y. Nie, K.P. Lam, L.T. Biegler, Dynamic optimization based integrated operation strategy design for passive cooling ventilation and active building air conditioning, *Energy Build.*, 85 (2014) 126–135.
- [5] T. Konstantinou, A.P. Hoces, Environmental design principles for the building envelope and more _: passive and active measures, in: *Energy-Resources Build. Perform.*, TU Delft Open, 2018: pp. 147–180.
- [6] International Energy Agency, UN Environment Programme, 2019 global status report for buildings and construction: Towards a zero-emission, efficient and resilient buildings and construction sector, 2019.
- [7] R. Yao, V. Costanzo, X. Li, Q. Zhang, B. Li, The effect of passive measures on thermal comfort and energy conservation A case study of the hot summer and cold winter climate in the Yangtze River region, *J. Build. Eng.*, 15 (2018) 298–310.
- [8] H. Karabay, M. Arıcı, Multiple pane window applications in various climatic regions of Turkey, *Energy Build.*, 45 (2012) 67–71.
- [9] Single Vs Double Pane Windows: What's The Difference?, (n.d.).
- [10] E. González-Julián, J. Xamán, N.O. Moraga, Y. Chávez, I. Zavala-Guillén, E. Simá, Annual thermal evaluation of a double pane window using glazing available in the Mexican market, *Appl. Therm. Eng.*, 143 (2018) 100–111.
- [11] M. Arıcı, H. Karabay, M. Kan, Flow and heat transfer in double, triple and quadruple pane windows, *Energy Build.*, 86 (2015) 394–402.
- [12] S. Baek, S. Kim, Potential Effects of Vacuum Insulating Glazing Application for Reducing Greenhouse Gas Emission (GHGE) from Apartment Buildings in the Korean Capital Region, *Energies*, 13 (2020) 2828.

- [13] M. Arıcı, M. Kan, An investigation of flow and conjugate heat transfer in multiple pane windows with respect to gap width, emissivity and gas filling, *Renew. Energy*, 75 (2015) 249–256.
- [14] M. Foruzan Nia, S.A. Gandjalikhan Nassab, A.B. Ansari, Transient numerical simulation of multiple pane windows filling with radiating gas, *Int. Commun. Heat Mass Transf.*, 108 (2019) 104291.
- [15] P. Mahtani, K.R. Leong, I. Xiao, A. Chutinan, N.P. Kherani, S. Zukotynski, Diamond-like carbon based low-emissive coatings, *Sol. Energy Mater. Sol. Cells*, 95 (2011) 1630–1637.
- [16] P.C. Eames, Vacuum glazing: Current performance and future prospects, *Vacuum*, 82 (2008) 717–722.
- [17] J. Xamán, C. Jiménez-Xamán, G. Álvarez, I. Zavala-Guillén, I. Hernández-Pérez, J.O. Aguilar, Thermal performance of a double pane window with a solar control coating for warm climate of Mexico, *Appl. Therm. Eng.*, 106 (2016) 257–265.
- [18] H. Radhi, A. Eltrapolsi, S. Sharples, Will energy regulations in the Gulf States make buildings more comfortable – A scoping study of residential buildings, *Appl. Energy*, 86 (2009) 2531–2539.
- [19] A. Kiritat, B.K. Koyunbaba, I. Chatzikonstantinou, S. Sariyildiz, Review of simulation modeling for shading devices in buildings, *Renew. Sustain. Energy Rev.*, 53 (2016) 23–49.
- [20] NEW CIBSE GUIDE FOR BUILDING IN TROPICAL ENVIRONMENTS, (n.d.).
- [21] S. Subhashini, K. Thirumaran, A passive design solution to enhance thermal comfort in an educational building in the warm humid climatic zone of Madurai, *J. Build. Eng.*, 18 (2018) 395–407.
- [22] A.I. Palmero-Marrero, A.C. Oliveira, Effect of louver shading devices on building energy requirements, *Appl. Energy*, 87 (2010) 2040–2049.
- [23] F. ASHRAE Hand Book, American Society of Heating, Refrigerating, and Air Conditioning Engineers, Inc., Atlanta, GA, 30329 (1997).
- [24] I. Jaffal, S.-E. Ouldboukhitine, R. Belarbi, A comprehensive study of the impact of green roofs on building energy performance, *Renew. Energy*, 43 (2012) 157–164.
- [25] DO YOU REALLY KNOW ALL THE BENEFITS OF GREEN ROOFS?, (n.d.).
- [26] A. Volder, B. Dvorak, Event size, substrate water content and vegetation affect storm water retention efficiency of an un-irrigated extensive green roof system in Central Texas, *Sustain. Cities Soc.*, 10 (2014) 59–64.
- [27] K.A.R. Ismail, J.N.C. Castro, PCM thermal insulation in buildings, *Int. J. Energy Res.*, 21 (1997) 1281–1296.
- [28] D. Kumar, M. Alam, P.X.W. Zou, J.G. Sanjayan, R.A. Memon, Comparative analysis of building insulation material properties and performance, *Renew. Sustain. Energy Rev.*, 131 (2020) 110038.
- [29] A.O. Desjarlais, Which Kind Of Insulation Is Best?, Oak Ridge Natl. Lab., (2013).
- [30] N. Bhikhoo, A. Hashemi, H. Cruickshank, Improving Thermal Comfort of Low-Income Housing in Thailand through Passive Design Strategies, *Sustainability*, 9 (2017) 1440.
- [31] A.M. Raimundo, N.B. Saraiva, A.V.M. Oliveira, Thermal insulation cost optimality of opaque constructive solutions of buildings under Portuguese temperate climate, *Build. Environ.*, 182 (2020) 107107.
- [32] M.S. Al-Homoud, Performance characteristics and practical applications of common building thermal insulation materials, *Build. Environ.*, 40 (2005) 353–366.
- [33] Z. Fang, N. Li, B. Li, G. Luo, Y. Huang, The effect of building envelope insulation on cooling energy consumption in summer, *Energy Build.*, 77 (2014) 197–205.
- [34] S. Schiavoni, F. Bianchi, F. Asdrubali, Insulation materials for the building sector: A review and comparative analysis, *Renew. Sustain. Energy Rev.*, 62 (2016) 988–1011.
- [35] A. Marani, M.L. Nehdi, Integrating phase change materials in construction materials: Critical review, *Constr. Build. Mater.*, 217 (2019) 36–49.
- [36] E. Tunçbilek, M. Arıcı, S. Bouadila, S. Wonorahardjo, Seasonal and annual performance analysis of PCM-integrated building brick under the climatic conditions of Marmara region, *J. Therm. Anal. Calorim.*, 141 (2020) 613–624.

- [37] M.T. Plytaria, C. Tzivanidis, E. Bellos, I. Alexopoulos, K.A. Antonopoulos, Thermal behavior of a building with incorporated phase change materials in the South and the North Wall, *Computation*, 7 (2019).
- [38] M. Sovetova, S.A. Memon, J. Kim, Thermal performance and energy efficiency of building integrated with PCMs in hot desert climate region, *Sol. Energy*, 189 (2019) 357–371.
- [39] Q. Al-Yasiri, M. Szabó, Incorporation of phase change materials into building envelope for thermal comfort and energy saving: A comprehensive analysis, *J. Build. Eng.*, 36 (2021) 102122.
- [40] Q. Al-Yasiri, M. Szabó, Experimental evaluation of the optimal position of a macroencapsulated phase change material incorporated composite roof under hot climate conditions, *Sustain. Energy Technol. Assessments*, 45 (2021) 101121.
- [41] D. Li, Y. Zheng, C. Liu, G. Wu, Numerical analysis on thermal performance of roof contained PCM of a single residential building, *Energy Convers. Manag.*, 100 (2015).
- [42] R.A. Kishore, M.V.A.A. Bianchi, C. Booten, J. Vidal, R. Jackson, Optimizing PCM-Integrated Walls for Potential Energy Savings in US Buildings, *Energy Build.*, 226 (2020) 110355.
- [43] S. Lu, B. Xu, X. Tang, Experimental study on double pipe PCM floor heating system under different operation strategies, *Renew. Energy*, 145 (2020) 1280–1291.
- [44] V.V. Rao, R. Parameshwaran, V.V. Ram, PCM-mortar based construction materials for energy efficient buildings: A review on research trends, *Energy Build.*, 158 (2018) 95–122.
- [45] N. Essid, A. Eddhahak-Ouni, J. Neji, Experimental and Numerical Thermal Properties Investigation of Cement-Based Materials Modified with PCM for Building Construction Use, *J. Archit. Eng.*, 26 (2020) 1–9.
- [46] L.F. Cabeza, L. Navarro, A.L. Pisello, L. Olivieri, C. Bartolomé, J. Sánchez, S. Álvarez, J.A. Tenorio, Behaviour of a concrete wall containing micro-encapsulated PCM after a decade of its construction, *Sol. Energy*, 200 (2020) 108–113.
- [47] A. Fateh, F. Klinker, M. Brütting, H. Weinläder, F. Devia, Numerical and experimental investigation of an insulation layer with phase change materials (PCMs), *Energy Build.*, 153 (2017) 231–240.
- [48] Q. Al-Yasiri, M. Szabó, Thermal performance of concrete bricks based phase change material encapsulated by various aluminium containers: An experimental study under Iraqi hot climate conditions, *J. Energy Storage*, 40 (2021) 102710.
- [49] E.M. Alawadhi, Thermal analysis of a building brick containing phase change material, *Energy Build.*, 40 (2008) 351–357.
- [50] D. Li, Y. Wu, C. Liu, G. Zhang, M. Arıcı, Energy investigation of glazed windows containing Nano-PCM in different seasons, *Energy Convers. Manag.*, 172 (2018) 119–128.
- [51] J.H. Park, B.Y. Yun, S.J. Chang, S. Wi, J. Jeon, S. Kim, Impact of a passive retrofit shading system on educational building to improve thermal comfort and energy consumption, *Energy Build.*, 216 (2020) 109930.
- [52] H.J. Akeiber, M.A. Wahid, H.M. Hussien, A.T. Mohammad, A newly composed paraffin encapsulated prototype roof structure for efficient thermal management in hot climate, *Energy*, 104 (2016) 99–106.
- [53] Z. Younsi, H. Najji, Numerical simulation and thermal performance of hybrid brick walls embedding a phase change material for passive building applications, *J. Therm. Anal. Calorim.*, 140 (2020) 965–978.
- [54] P.K.S. Rathore, S.K. Shukla, An experimental evaluation of thermal behavior of the building envelope using macroencapsulated PCM for energy savings, *Renew. Energy*, 149 (2020) 1300–1313.
- [55] R. Saxena, D. Rakshit, S.C. Kaushik, Experimental assessment of Phase Change Material (PCM) embedded bricks for passive conditioning in buildings, *Renew. Energy*, 149 (2020) 587–599.
- [56] S. Kenzhekhanov, S.A. Memon, I. Adilkhanova, Quantitative evaluation of thermal performance and energy saving potential of the building integrated with PCM in a subarctic climate, *Energy*, 192 (2020) 116607.

- [57] A. de Gracia, Dynamic building envelope with PCM for cooling purposes – Proof of concept, *Appl. Energy*, 235 (2019) 1245–1253.
- [58] Q. Al-Yasiri, M. Szabó, Case study on the optimal thickness of phase change material incorporated composite roof under hot climate conditions, *Case Stud. Constr. Mater.*, 14 (2021) e00522.
- [59] M. Arıcı, F. Bilgin, S. Nižetić, H. Karabay, PCM integrated to external building walls: An optimization study on maximum activation of latent heat, *Appl. Therm. Eng.*, 165 (2020) 114560.
- [60] Y. Zhang, J. Huang, X. Fang, Z. Ling, Z. Zhang, Optimal roof structure with multilayer cooling function materials for building energy saving, *Int. J. Energy Res.*, 44 (2020) 1594–1606.
- [61] M. Auzeby, S. Wei, C. Underwood, J. Tindall, C. Chen, H. Ling, R. Buswell, Effectiveness of using phase change materials on reducing summer overheating issues in UK residential buildings with identification of influential factors, *Energies*, 9 (2016) 605.
- [62] N. Zheng, J. Lei, S. Wang, Z. Li, X. Chen, Influence of heat reflective coating on the cooling and pavement performance of large void asphalt pavement, *Coatings*, 10 (2020) 1065.
- [63] H. Shen, H. Tan, A. Tzempelikos, The effect of reflective coatings on building surface temperatures, indoor environment and energy consumption—An experimental study, *Energy Build.*, 43 (2011) 573–580.
- [64] H.M. Taleb, Using passive cooling strategies to improve thermal performance and reduce energy consumption of residential buildings in UAE buildings, *Front. Archit. Res.*, 3 (2014) 154–165.
- [65] R.K. Pal, P. Goyal, S. Sehgal, Thermal performance of buildings with light colored exterior materials, *Mater. Today Proc.*, 28 (2020) 1307–1313.
- [66] Y. Zhang, X. Zhai, Preparation and testing of thermochromic coatings for buildings, *Sol. Energy*, 191 (2019) 540–548.
- [67] C.G. Granqvist, Recent progress in thermochromics and electrochromics: A brief survey, *Thin Solid Films*, 614 (2016) 90–96.
- [68] S.S. Kanu, R. Binions, Thin films for solar control applications, *Proc. R. Soc. A Math. Phys. Eng. Sci.*, 466 (2010) 19–44.
- [69] Z. Yuxuan, Z. Yunyun, Y. Jianrong, Z. Xiaoqiang, Energy saving performance of thermochromic coatings with different colors for buildings, *Energy Build.*, 215 (2020) 109920.
- [70] B.R. Hughes, J.K. Calautit, S.A. Ghani, The development of commercial wind towers for natural ventilation: A review, *Appl. Energy*, 92 (2012) 606–627.
- [71] F. Jomehzadeh, P. Nejat, J.K. Calautit, M.B.M. Yusof, S.A. Zaki, B.R. Hughes, M.N.A.W.M. Yazid, A review on windcatcher for passive cooling and natural ventilation in buildings, Part 1: Indoor air quality and thermal comfort assessment, *Renew. Sustain. Energy Rev.*, 70 (2017) 736–756.
- [72] M. Saeli, E. Saeli, Analytical studies of the Sirocco room of Villa Naselli-Ambleri: A XVI century passive cooling structure in Palermo (Sicily), *J. Cult. Herit.*, 16 (2015) 344–351.
- [73] O. Saadatian, L.C. Haw, K. Sopian, M.Y. Sulaiman, Review of windcatcher technologies, *Renew. Sustain. Energy Rev.*, 16 (2012) 1477–1495.

SIMULATION OF FAULT DETECTION IN PHOTOVOLTAIC ARRAYS

Róbert Lipták, István Bodnár

Institute of Physics and Electrical Engineering, Egyetemi út 1, 3515 Miskolc-Egyetemváros, Hungary
e-mail: elkrobi@uni-miskolc.hu

ABSTRACT

In solar systems, faults in the module and inverter occur in proportion to increased operating time. The identification of fault types and their effects is important information not only for manufacturers but also for investors, solar operators and researchers. Monitoring and diagnosing the condition of photovoltaic (PV) systems is becoming essential to maximize electric power generation, increase the reliability and lifetime of PV power plants. Any faults in the PV modules cause negative economic and safety impacts, reducing the performance of the system and making unwanted electric connections that can be dangerous for the user. In this paper have been classified all possible faults that happen in the PV system, and is presented to detect common PV array faults, such as open-circuit fault, line-to-line fault, ground fault, shading condition, degradation fault and bypass diode fault. In this studies examines the equivalent circuits of PV arrays with different topological configurations and fault conditions to evaluate the effects of these faults on the performance of a solar system, taking into account the influence of temperature and solar radiation. This work presents the validation of a simulated solar network by measuring the output curves of a low-power photovoltaic array system under real outdoor conditions. This method can be useful in future solar systems.

Keywords: photovoltaic (PV) arrays, electric faults, common PV array faults, fault detection, partial shading,

1. INTRODUCTION

Every situation of modern life depends on electricity. Solar-generated electricity is a very clean and desirable way to compensate our reliance on fossil fuels produced electricity [1]. PV systems operate quietly and have low maintenance requirements. It can offer extremely high reliability, and with the modularity features, the PV systems have very flexible system sizing for integration into buildings and for decentralized applications down to minimal load demands.

However, electric faults in PV arrays generate significant power losses, therefore it is necessary for effective ways to detect and classify these faults in order to improve system efficiency and reliability [2, 4]. Operational faults of the photovoltaic system is one of the important factor affecting the power-generation efficiency. But besides this, the performance of a photovoltaic system depends on the temperature of operation of the solar panels, solar radiation. Overall, the problems related to solar systems thus fall into three main categories: environmental effects, panel specific problems, electrical fails. Many cases can lead to failure. A possible way to identify to abnormal heat caused by faults, to measure the surface temperature of the PV modules by thermal camera. But the process is time consuming and we cannot provide testing of solar panels at all times [3].

2. PHOTOVOLTAIC (PV) MODULE MODELLING

To simulate the operation of a solar cell, the first step is to establish its electronic model. Solar panels are composed of multiple solar cells connected in series. A photovoltaic array can be made by connecting multiple solar panels. In this section, a one diode solar cell model is described in order to simulate photovoltaic arrays of dimensions $N_s \times N_p$, which means the array is composed of N_p strings connected in parallel, and each string is composed of N_s solar panels connected in series. Both internal and wire resistance is represented by an ohmic resistance in this case. A capacitor can also be connected in parallel to the diode, representing the parasitic capacitance between the two poles of the diode, but because of its value, it is negligible. Fig. 1. shows this model [5].

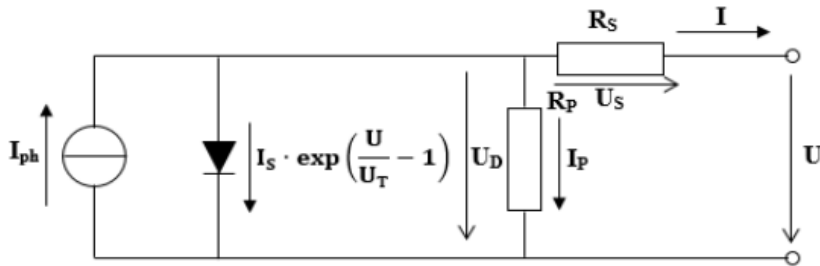


Figure 1. The circuit model of the solar cell

The produced current of the current generator depends on the intensity of illumination. The output current can be described with the following equation [3, 4, 5]:

$$I = I_{ph} - I_D - I_P. \tag{1}$$

The photocurrent I_{ph} can be described with the following equation [4, 5]:

$$I_{ph} = \frac{\beta(I_{sc} + K_i(T - T_r))}{1000} \tag{2}$$

The ID diode current can be defined by the help of the I_s diode saturation current, depending on the voltage and constants. [4, 5]:

$$I_D = I_s \left[\exp\left(\frac{e \cdot U_D}{n \cdot k \cdot T \cdot N_s}\right) - 1 \right] \tag{3}$$

The shunt current in the solar cell model I_P can be described with the following equation[4, 5]:

$$I_P = \frac{U_D}{R_p} = \frac{U + I \cdot R_s}{R_p} \tag{4}$$

The voltage is the following[5]:

$$U = U_D - U_s \tag{5}$$

Ideally $R_p \approx \infty$ and by shorting the circuit means: $R_D \gg R_s (R_{cp} \gg R_s)$

3. DEFINITION OF TYPICAL FAULTS ON DC SIDE OF IN PV SYSTEM

Because some electrical faults, such as discrepancies, always occur in each array, they result in the available DC power of the array being significantly less than the predicted level. Table 1. shows the typical electrical faults of PV system [3,6].

Table 1. Typical electrical faults of PV system [3, 4, 6]

Type of fault	Description of fault	Part
Upper ground fault	An unintentional path to ground with zero fault impedance occurs between the last two modules at PV string	DC
Lower ground fault	An unintentional path to ground with zero fault impedance occurs between the 2nd and the 3rd two modules at PV string with large backfeed current	
Series arc fault	An arc fault due to discontinuity in any of the current carrying conductors resulting from solder disjoint, cell damage, corrosion of connectors, rodent damage, abrasion from different sources	
Parallel arc fault	Insulation breakdown in current carrying conductors	
Line-to-line faults	An accidental short-circuit between two points in a string with different potentials	
Bypass diode faults	Short-circuit in case of incorrect connection	
Bridging fault	Low- resistance connection between two points of different potential in string of module or cabling	
Open-circuit fault	Physical breakdown of panel-panel cables or joints, objects falling on PV panels, and loose termination of cables, plugging and unplugging connectors at junction boxes	
MPPT faults	Problem in MPPT charge controllers	
Cabling faults	Disconnected cables	AC/DC
Inverter faults	Failure of each component of inverter such as IGBTs, capacitors, and drive circuitry can result in inverter failure	AC
Sudden natural disasters	Total blackout due to Lightning, storm, and so forth	AC/DC

In addition to electrical faults, in many cases there may be environmental problems in PV systems which can lead to performance degradation. The Hot spots is the most common issues with PV systems. Hot spots caused by the accumulation of dirt on the panels, shadow on the panels, badly soldered connections (it can happens during the production process). Besides many panel-specific problems can occur during operation, which can also lead to performance degradation.

Table 2. Typical environmental problems and panel-specific fails of PV system [3, 4, 6]

Type of fault	Description of fault
Environmental effects	Soiling The bird droppings and dirt on the surface of a PV module
	Snow covering Hot spots The worst temperatures depending on the geographical location and different weather conditions
	Irradiance distribution Various irradiance intensity during the day
Panel specific problems	Degradation faults Yellowing and browning, delamination, internal corrosion, micro-cracks, increasing of the internal series resistance

Fig. 2 shows a circuit diagram of the main faults that are analysed in this work.

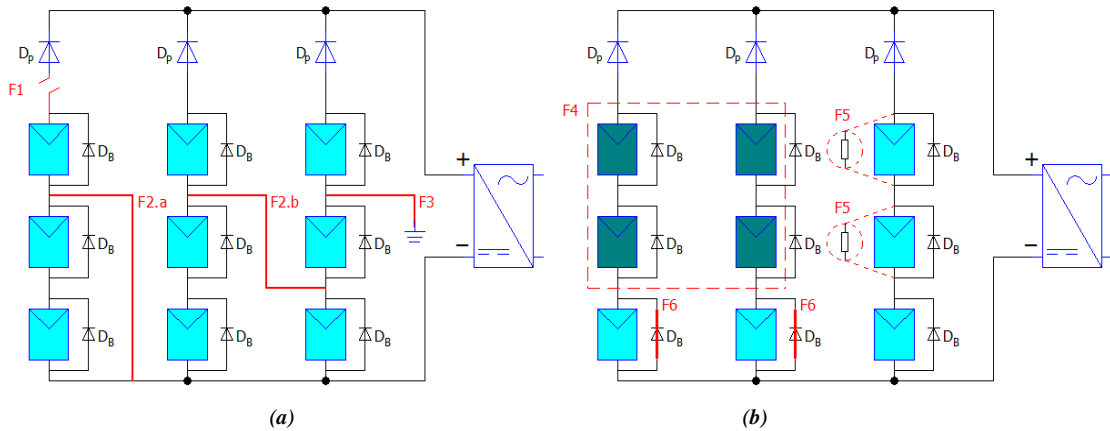


Figure 2. Circuit diagram of the main faults in PV array systems. (a) open-circuit and short-circuit fault and grounding fault (b) partial shading degradation fault and bypass diode fault

3.1. Open Circuit Fault

An open-circuit fault (shown as F1 in Figure 2.) is an accidental disconnection at a normal conductor during operation. Open circuit faults are symmetrical between strings. If the solar panels of the PV system have the same technical specifications and that all of them are under the same solar radiation and temperature conditions, in an open circuit fault, the voltage at the output of each string is the same. This means that if a string has an open circuit fault, the voltage at the output of the remaining strings will still be the same.

The voltage at the maximum power point will be the same even if the array changes its number of strings – because. Adding or removing strings, the equivalent circuit is only changing the output current of the full array [3,4,6].

3.2. Line-to-Line Fault

Line-to-line faults (shown as F2.a and F2.b in Figure 2.) in PV array systems are symmetrical between strings. This type of faults causing low impedance between two different strings in the PV array. It could happen inside PV arrays and potentially may involve large fault current or dc arcs. This paper examines line-to-line faults which are defined as an accidental short-circuiting between two points in the array with different potentials. A line-to-line fault can reverse the current flow through the faulty string. The amplitude of the fault current depends on the voltage difference between the points of the strings that are causing the fault [4,7]. Over Current Protection Devices (OCPD) are used to detect line-to-line faults, but these devices have some limitations if the current is lower than a threshold. If the line-to-line fault occurs under low illumination

(e.g., during the night, night-to-day transition, during the morning, day-to-night transition), the current through the affected string/strings is not large enough to melt the OCPD, and the fault may remain undetected until sufficient illumination is present to clear the OCPD [4,7].

3.3. Ground Fault

A ground fault (shown as F3 in Figure 2.) establishes an unintentional low impedance path between one of the current carrying conductors (CCCs) and the ground/earth, and a large fire in a PV array often destroys the origin of the fault. Several potential reasons for ground faults:

1. cable insulation damage during the installation, due to aging, impact damage, water leakage, and corrosion;
2. ground fault within the PV modules (e.g., degraded sealant and water ingress);
3. insulation damage of cables due to chewing done by rodents;
4. accidental short circuit inside the PV combiner box, often at the time of maintenance.

If a ground fault remains undetected, it may generate a dc arc within the fault and cause a fire hazard [4,7].

3.4. Partial Shading Fault

Partial shading is the phenomenon that a PV array receives uneven irradiation and temperature caused by passing clouds, adjacent buildings and towering trees and so on [8,9]. In the case of partial shading faults (shown as F4 in Figure 2), one part of the PV array is shaded while the other part is fully irradiated according to the current irradiation value resulting output power reduction. As the irradiation value is constantly changing, the actual irradiation value must also be taken into account when examining faults. When the PV array is partially shaded, the MPP current of the PV array declines obviously, but the short-circuit current and the open-circuit voltage of the PV array are basically invariant [3].

3.5. Degradation Fault

A degradation fault (shown as F5 in Figure 2) occurs attributed to the failure of the bond between different layers of the panel leading to delamination, some tiny cracks on the solar cell and frequent changes in temperature of the module with increasing internal series resistance. The decrease in output power could be the increase in the series resistance between the modules due to decreased adherence of contacts or corrosion caused by water vapor. When a degradation fault appears, the MPP current and voltage of the PV array are reduced. The short-circuit current and the open-circuit voltage of the PV array remain unchanged

3.6. Bypass Diode Fault

A bypass diode is usually connected in parallel across multiple cells to improve the operation of the solar system under the nonuniform condition. Bypass diode can fail due to lightning strikes or thermal runaway from frequent operation [10,12]. The recent study showed simulation results that damaged bypass diodes by lightning strikes to lead reverse current flowed from normal string to the failed string, which generates heat and burns out. [11,12]. Furthermore, bypass diodes can deteriorate due to the high temperature of thermal runaway by rapid transitioning from forwarding bias state to reverse bias [12,13,14]. In this regard, there is a study that released which changes in the electrical property at PV module caused by a failure of the bypass diode (shown as F6 in Figure 2). The failure bypass diodes lose their properties of forward and reverse bias to become a micro-resistance, and are in a short circuit state with solar cells that are connected to a fault bypass diode [12,15,16]. Furthermore, recent research reported, when the bypass diode is shorted failure while the PV system is stopped, the temperature of a junction box increases [12]. These mismatch factors change Maximum Power Point (MPP) of PV modules or strings bringing about the system output loss on the PV system. Even if only one full module is shorted by bypass diode, the maximum power and U_{oc} of the PV array drops significantly and short-circuit current remains the same as other normal strings.

4. PV ARRAY CONFIGURATION FOR VALIDATION

The first step of this research was to experimentally validate the electric model of a PV array. The configuration structure of the PV array and fault types set in Figure 3. P-U curve of the array was measured under different fault conditions in order to validate the model.

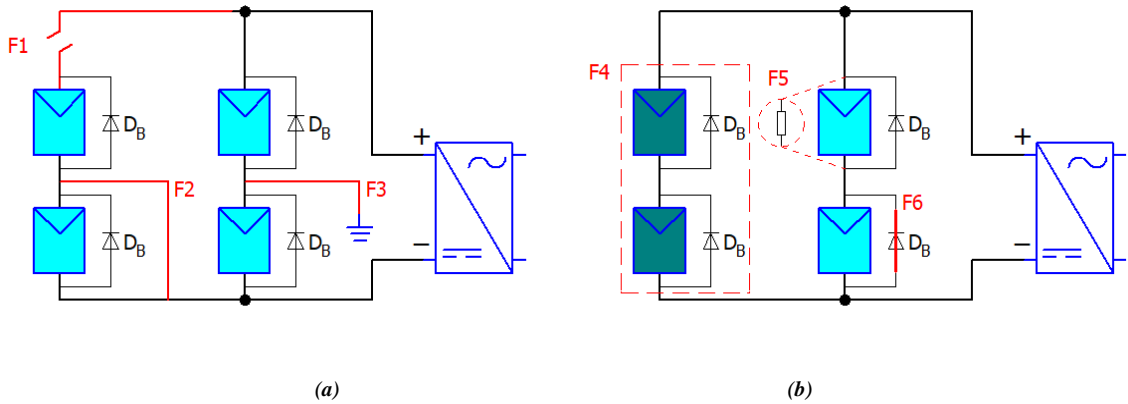


Figure 3. Circuit diagram of the PV system for validation. (a) open-circuit and short-circuit fault and grounding fault (b) partial shading degradation fault and bypass diode fault

The 20W solar panels were connected two in series in one string and two strings in parallel. The output of the PV array with $U_{oc} = 42.6$ V and $I_{sc} = 2.41$ A was measured. The array was connected to a variable load to obtain the U-I values measuring the voltage and current with a digital multimeter, MAXWELL MX-25 328. Eight 500 W R-500WFEH Halogen Floodlight lamps were used to simulate solar radiation, and radiation was measured 800 W/m² with a PCE-SPM 1 Solar Power Meter. The related parameters of each PV panel under STC ($G = 800$ W/m² and $T = 25$ °C) are $P_{mpp} = 20$ W, $U_{mpp} = 17.49$ V, $I_{mpp} = 1.14$ A, $N_s = 36$, $V_{oc} = 21.67$ V, and $I_{sc} = 1.22$ A and $CT = -0.33\%$ / °C.

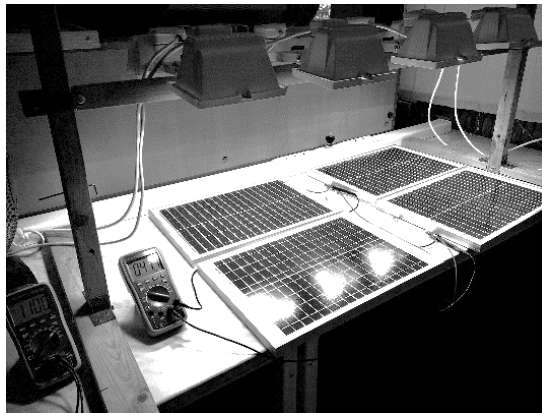


Figure 4. Measured PV array for validation

Figure 4. shows a photo of the PV array used in the lab to measure the U-I curve in order to validate the electric model. The electric model was validated using Matlab and Simulink, comparing the U-I curve obtained experimentally to the output characteristic curves generated by the model. The output characteristic curves of the PV array under fault types set are shown in Figure 5.

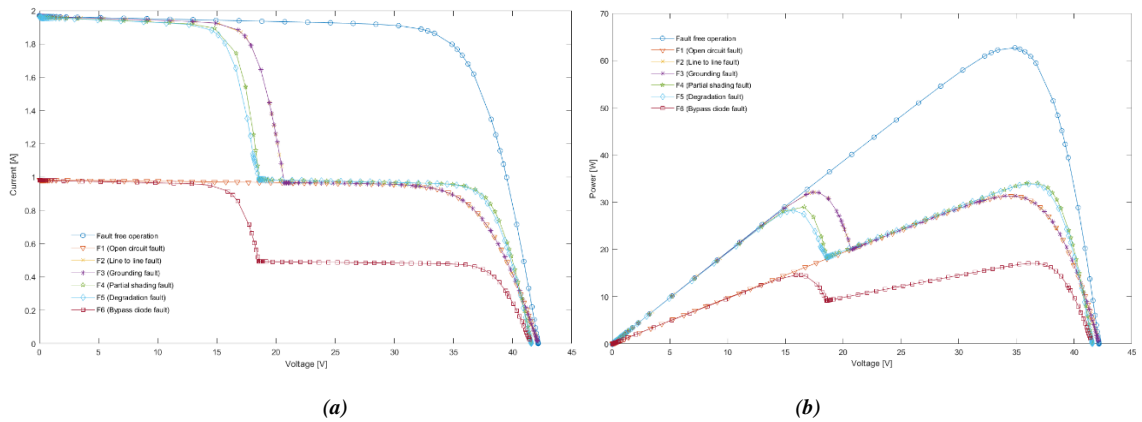


Figure 5. The output characteristic curves of the PV array under common fault conditions. (a) power-voltage curves (b) current-voltage curves.

5. INTERPRETATION AND SIMULATION OF THE MOST COMMON FAULTS

After the validating, a typical solar PV array with 6×5 PV modules is simulated. Figure 6 show the model for PV modules in MATLAB/Simulink. 6 modules in series per string and 5 strings in parallel. Using the widely used one-diode model for each individual solar panel, this paper builds simulation PV array (2.4 kW) in MATLAB/Simulink consisting of 6×5 PV panels that is capable of studying faults among panels. The related parameters of each PV panel under STC ($G = 1000 \text{ W/m}^2$ and $T = 25 \text{ }^\circ\text{C}$) are $P_{mpp} = 80 \text{ W}$, $V_{mpp} = 17.7 \text{ V}$, $I_{mpp} = 4.52 \text{ A}$, $N_s = 36$, $V_{oc} = 21.9 \text{ V}$, and $I_{sc} = 5 \text{ A}$ and $CT = -0.32\% / ^\circ\text{C}$. MATLAB/Simulink models of PV array (Figure 6) under electrical faults are developed to study the performance of the faulted PV array.

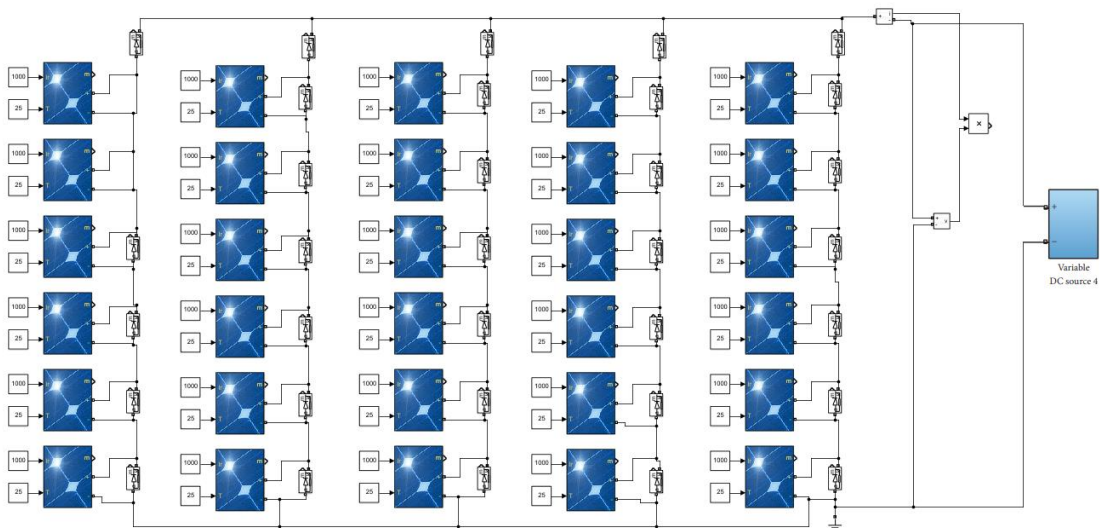


Figure 6. Schematic diagram of a PV farm system with 6×5 modules

This research studies six common fault types in 12 cases and compared the results with the normal condition. The characteristics of the PV panel with different types of faults are shown in Figures 7–12.

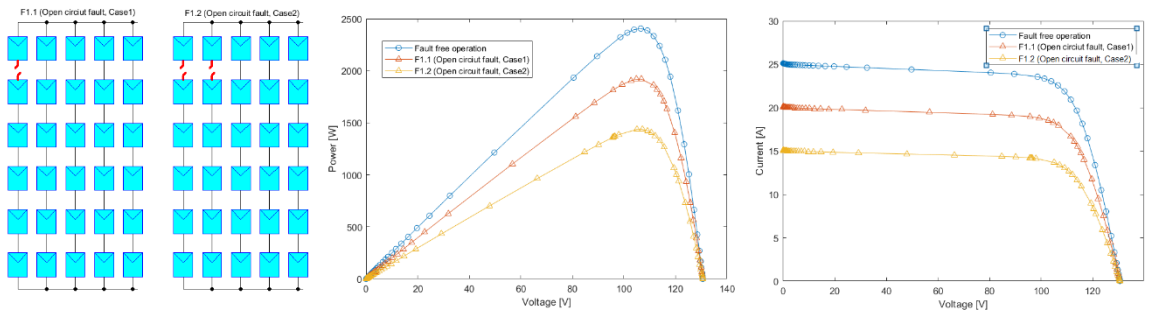


Figure 7. The PV array configuration for Open circuit fault

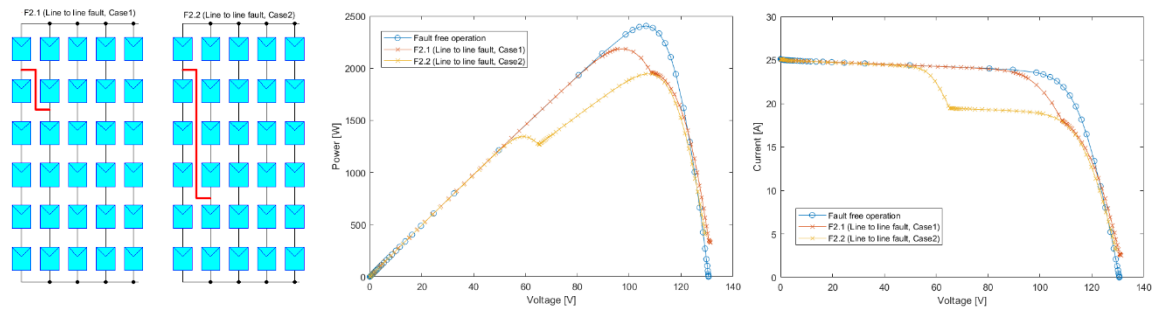


Figure 8. The PV array configuration for Line to line fault

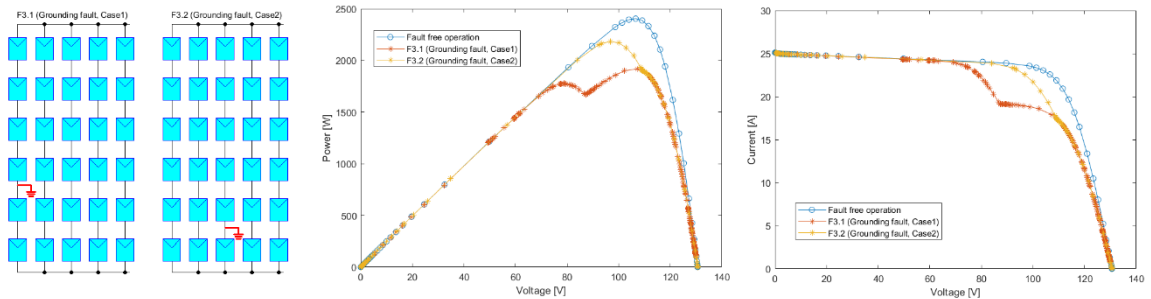


Figure 9. The PV array configuration for Grounding fault

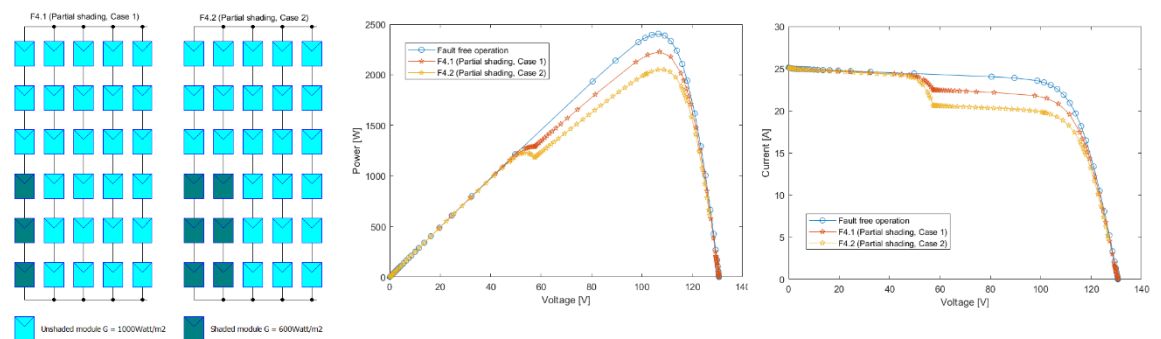


Figure 10. The PV array configuration for Partial shading

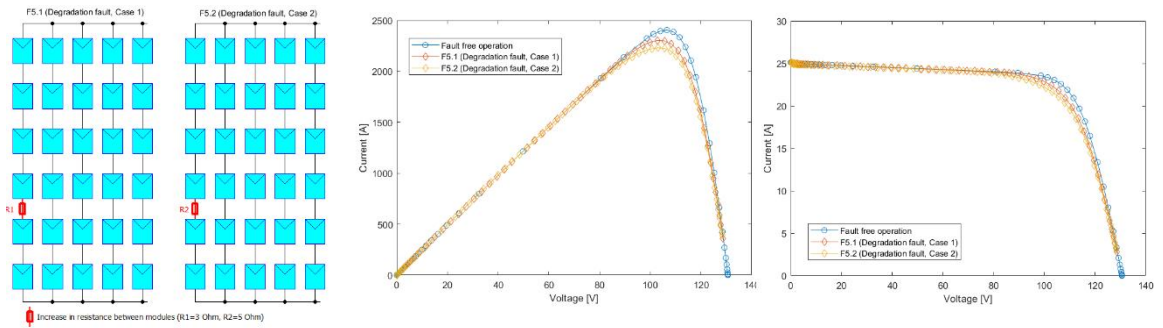


Figure 11. The PV array configuration for Degradation fault

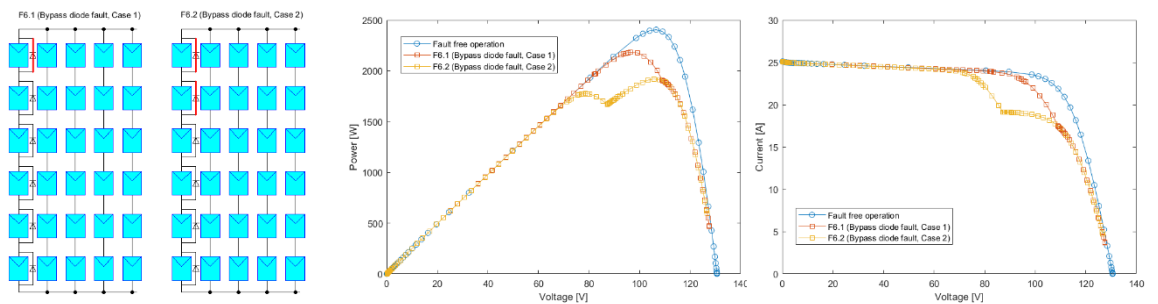


Figure 12. The PV array configuration for Bypass diode fault

7. RESULTS AND DISCUSSION

When different faults appear in a PV array, the output characteristic of PV array are very different in many cases. Electric faults in PV arrays can generate a local and global maximum point in the P-U curve at the output of the array. In this paper, a comprehensive definition of faults in DC side of PV system based on location and structure is presented. The performance of a typical PV array has been examined under typical fault conditions such as open-circuit fault, line-to-line fault, grounding fault, shading condition, degradation fault, bypass diode fault. To better visualize the P-U data under normal and fault conditions, the U-I and P-U characteristics of the array have been evaluated. Simulation experimental results show both normal operational curves and fault curves.

8. CONCLUSIONS

The off-line method used in this research can make difference many types of faults but cannot detect the location of the fault within the PV array. It would be useful to develop special MPPT schemes to track the maximum peak under these conditions and further methods capable of determining these locations. In a future work, the characterization method can be implemented inside an algorithm to detect and classify these common faults in a photovoltaic array system by only measuring the voltage and the current at the output of a photovoltaic array to obtain the P-U curve.

But a more accurate result can be obtained by measuring the current and voltage of each string, because this gives a more accurate picture of the exact location of the faults. In order to design an algorithm based on the characterization method, it is important to measure the temperature of the PV modules, solar radiation and the VP curve at the output of an array fast enough (<1s) to prevent significant solar radiation variations.

REFERENCES

- [1] F. Jackson, Grid-connected Solar Electric Systems, The Earthscan Expert Handbook for Planning, Design and Installation 711 Third Avenue, New York, NY 10017, ISBN: 978-1-84971-344-3
- [2] Guerriero, P., Di Napoli, F., Vallone, G., d'Alessandro V. and Daliento, S., Monitoring and diagnostics of PV plants by a wireless self powered sensor for individual panels, IEEE Journal of Photovoltaics, 6(1), pp. 286-294, 2016. DOI: 10.1109/JPHOTOV.2015.2484961
- [3] T. Pei, X. Hao, A Fault Detection Method for Photovoltaic Systems Based on Voltage and Current Observation and Evaluation, *Energies* 2019, 12(9),1712, <https://doi.org/10.3390/en12091712>
- [4] A. E. Nieto, F. Ruiz, D. Patiño, Characterization of electric faults in photovoltaic array systems, October 2019 Dyna (Medellin, Colombia) 86(211):54-63, DOI:10.15446/dyna.v86n211.79085
- [5] I. Bodnar, Electric Parameters Determination of Solar Panel by Numeric Simulations and Laboratory Measurements during Temperature Transient, *Acta Polytechnica Hungarica*, Vol. 15, No. 4, 2018
- [6] M. S. Arani, M. A. Hejazi, The Comprehensive Study of Electrical Faults in PV Arrays, Hindawi Publishing Corporation, Journal of Electrical and Computer Engineering, Volume 2016, Article ID 8712960, 10 pages, <https://doi.org/10.1155/2016/8712960>
- [7] Alam, M.K., Khan, F., Johnson, J. and Flicker, J., A Comprehensive Review of Catastrophic Faults in PV arrays: types, detection, and mitigation techniques, IEEE Journal of Photovoltaics, 5(3), pp. 982-997, 2015. DOI: 10.1109/JPHOTOV.2015.2397599
- [8] Ishaque, K.; Salam, Z. A review of maximum power point tracking techniques of PV system for uniform insolation and partial shading condition. *Renew. Sustain. Energy Rev.* 2013, 19, 475–488.
- [9] Li, G.; Jin, Y.; Akram, M.W.; Chen, X.; Ji, J. Application of bio-inspired algorithms in maximum power point tracking for PV systems under partial shading conditions—A review. *Renew. Sustain. Energy Rev.* 2018, 81, 840–873, <https://doi.org/10.1016/j.jclepro.2021.127279>.
- [10] Fahrenbruch SA. Solar bypass diodes: Then and now. *A PV Management Magazine* 2010.
- [11] Ishikura N, Okamoto T, Nanno I, Hamada T, Oke S, Fujii M. Simulation analysis of really occurred accident caused by short circuit failure of blocking diode and bypass circuit in the photovoltaics system. In: 7th Int. IEEE Conf. Renew. Energy Res. Appl. ICRERA 2018, vol. 5. IEEE; 2018. p. 533e6. <https://doi.org/10.1109/ICRERA.2018.8566896>.
- [12] Chung G. L., Woo G. S., Jong R. L., Gi H. K., Young C. J., Hye M. H., Hyo S. C., Suk W. K., Analysis of electrical and thermal characteristics of PV array under mismatching conditions caused by partial shading and short circuit failure of bypass diodes, *Energies* 218. 2021, <https://doi.org/10.1016/j.energy.2020.119480>
- [13] Posbic J, Rhee E, Amin D. High temperature reverse by-pass diodes bias and failures. 2013. 2013, https://www.energy.gov/sites/prod/files/2014/01/f7/pvmrw13_ps3_memc_posbic.pdf.
- [14] Shiradkar NS, Schneller E, Dhare NG, Gade V. Predicting thermal runaway in bypass diodes in photovoltaic modules. In: 2014 IEEE 40th Photovolt. Spec. Conf. PVSC. Institute of Electrical and Electronics Engineers Inc.; 2014. p. 3585e8. <https://doi.org/10.1109/PVSC.2014.6924881>. 2014
- [15] Shin W-G, Jung T-H, Go S-H, Ju Y-C, Chang H-S, Kang G-H. Analysis on thermal & electrical characteristics variation of PV module with damaged bypass diodes. *J Korean Sol Energy Soc* 2015;35:67e75. <https://doi.org/10.7836/kses.2015.35.4.067>.
- [16] Shin WG, Ko SW, Song HJ, Ju YC, Hwang HM, Kang GH. Origin of bypass diode fault in c-Si photovoltaic modules: leakage current under high surrounding temperature. *Energies* 2018;11. <https://doi.org/10.3390/en11092416>.

CHANGES IN THE ENERGY PRODUCTION TO REDUCE THE ENVIRONMENTAL IMPACT

Gábor Hornyák, Péter Bencs

University of Miskolc, Department of Fluid and Heat Engineering, Miskolc-Egyetemváros, HU-3515,
Miskolc, Hungary
e-mail: hornyakgabi97@gmail.com

ABSTRACT

One of the most debated topics of our time is climate change. For this reason, the European Union and the countries of the world are taking several steps to reduce and reverse the effect. When we talk about climate change or sustainable development, it is very important to also talk about the energy sector. The European Union aims to achieve climate neutrality by 2050, which will require significant changes in our lives, it will be a major challenge for mankind. In 2019, fossil fuels accounted for 80% of the world's energy production. The production of energy from fossil fuels has several negative effects aside from climate change. When fossil fuels are burned, gases and particles harmful to human health are released into the air and some of the fossil fuels are raw materials to produce plastics, for example. If we use it for energy production, we waste our raw materials. What are the options for reducing the environmental impact? How can coal-based energy production be replaced? What are other ways to reduce the environmental impact? These topics are discussed in the article.

Keywords: climate, energy, sustainability, emissions, waste

1. INTRODUCTION

Climate change means lasting and significant change locally or globally in average temperature, average rainfall, or wind [1]. We have been talking about climate change since the 19th century, the first calculation was made in 1896 by Samuel Pierpoint Langely and his partner Frank W. Very, who tried to determine the surface temperature. In the late 19th century, scientists first debate those large-scale emissions of greenhouse gases from human activities could change the climate. In the 1960s, there was more and more convincing evidence of warming caused by carbon emissions a fact that is already proven today [2]. Climate change is caused by the appearance of higher than natural concentrations of greenhouse gases, the percentage of which is shown in Fig. 1. Natural greenhouse gases play a role in the Earth's heat economy. Greenhouse gases: water vapor, carbon dioxide, methane, nitrogen oxides, and halogenated hydrocarbons (CFCs) [3-4].

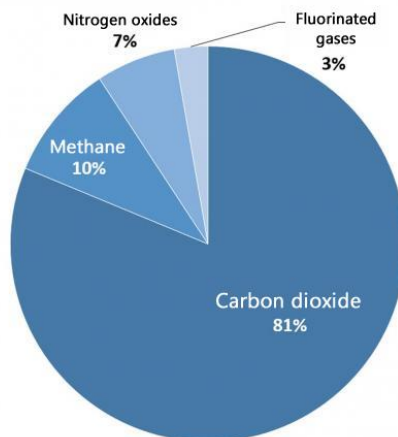


Figure 1. Greenhouse gas emission [5]

The most significant greenhouse gas in the atmosphere is water vapor. The presence of carbon dioxide is a small part of the atmosphere, however, according to NASA’s research, its presence contributes more to the warming trend. Furthermore, the situation is further aggravated by deforestation, which allows carbon dioxide to be present in higher concentrations.

Phenomena according to NASA’s researchers that could cause global warming [3]:

- Variations in the Intensity of the Sun
- Industrial Activity
- Agricultural Activity
- Deforestation
- Earth on a Feedback Loop

2. CURRENT ENERGY PRODUCTION’S IMPACT ON THE ENVIRONMENT

As mentioned earlier, the largest source of greenhouse gas emissions from energy production is carbon dioxide.

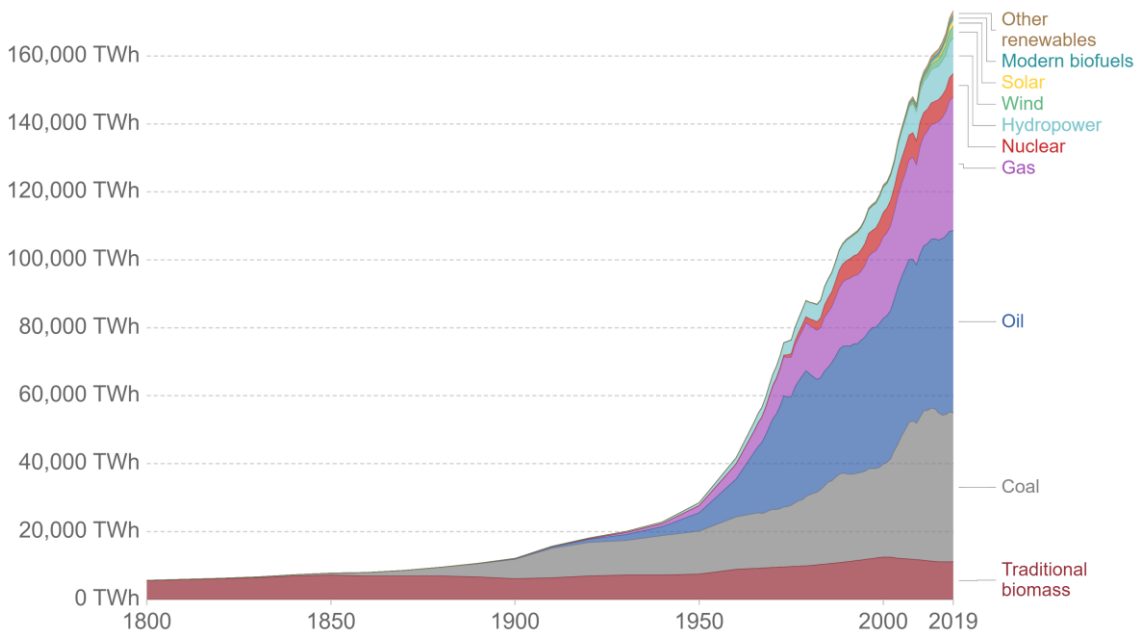


Figure 2. Change in the composition of energy production over the years [6]

It can be seen in Fig. 2 that currently energy production is primarily from fossil fuels (coal, oil, gas) accounting for almost 80% of the world’s energy demand in 2019. In 2019, 10% of energy demand was covered by renewable energy and about 4% by nuclear energy. The proportion of nuclear energy has not changed significantly over the years while renewables (Solar, Wind, Hydro, Other renewables) have grown by 70% in the last ten years, most significantly the solar power which has over 3000% increase. In addition, a steady increase in energy demand can be observed, the growing demands must be produced from environmentally friendly sources [6].

The production of energy from fossil fuels has several negative effects such as global warming, air pollution, declining amounts of fossil fuels, which are also raw materials to produce plastics, for example. If we use it for energy production, we waste our raw materials. Global warming (or climate change) is one of the problems; the other is air pollution which caused health problems to the people. One of the goals of

the European Union and the world is to achieve a circular economy and sustainable development for which the production of energy in a sustainable way is essential. According to a study by Martins [7], a significant proportion of European countries still produce 60% of their energy from fossil fuels, but in some countries, the proportion is even higher, at almost 80%.

2.1. Health effects of fossil fuels

During the combustion of coal, carbon oxides, sulphur oxides, nitrogen oxides, particulate matter and in some cases, heavy metals are released into the atmosphere.

In addition to greenhouse gases, there are also significant emissions of sulphur dioxide, amounting to about 88 Mt per year, from the combustion of sulphur-containing fuels, the smelting of ores and the industrial processing of elemental sulphur. The danger of sulphur dioxide lies not only in its toxic effects but also in its reaction with atmospheric water vapor since it is highly soluble in water and forms sulphuric acid [8].

Carbon oxides from the combustion of carbonaceous fuels may include carbon monoxide (CO), carbon dioxide (CO₂), carbon suboxide (C₃O₂) and metal anhydride (C₁₂O₉). Of the above oxide compounds, only carbon monoxide can be considered an air pollutant that is toxic to humans and animals. The harmful effects of carbon dioxide on naturally occurring processes are one of the main environmental problems today.

The pollutants in the ambient air are largely nitrogen oxides, which can come from households, industrial combustion plants and power plants, as well as from transport. Exposure to nitrogen oxides can cause respiratory illness. Nitrogen oxides also contribute significantly to the formation of acid rain [8].

In industrial and power plant applications, increased attention is paid to the number of compounds emitted in the air. The legislation currently in force in Hungary is (4/2011 (I. 14.) VM) which contains the emission limit values [9].

2.2. Another important factor

In addition to fossil fuel-fired power plants, it should also be emphasized that, in addition to power plants and transport, the household also plays a significant role in greenhouse gas emissions. According to EUROSTAT, 20% of total CO₂ emissions (which is 3.5 million tonnes CO₂ equivalent) come from households, 21% from industrial applications, 22% from power plants and 12% from transport [10-11].

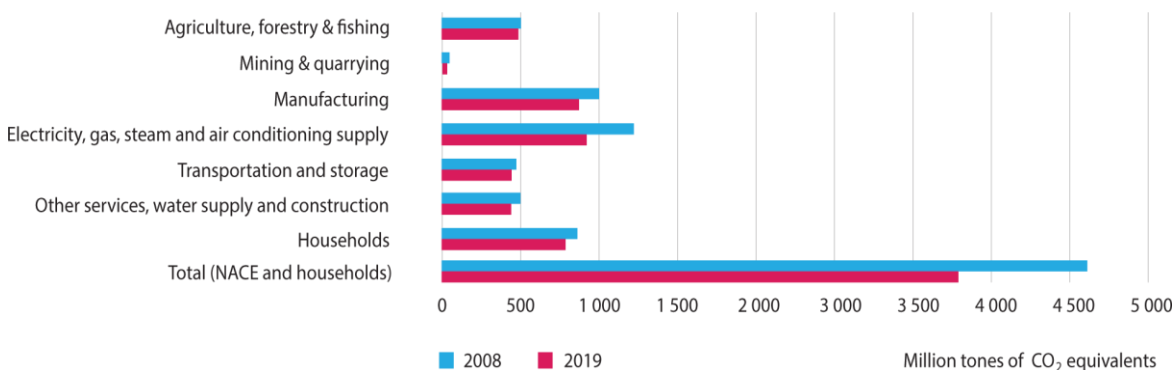


Figure 3. Greenhouse gas emissions by economic activity, EU-27 2008 and 2019 [10]

Fig. 3 shows that the number of emissions from households rivals the amounts emitted by power plants and industrial activities. It also shows that emissions from transport are only 60% of emissions from households, so households' emissions are not a negligible factor.

3. CLIMATE PROTECTION MEASURES

Global warming is now an everyday topic for scientists, politicians, and the public. Several energy and climate plans have been developed over time, some of which are briefly reviewed in this section. The common goal is to keep the global average temperature rise below 1.5 Celsius. In International and domestic climate plans, the priority is to decarbonise energy production and everyday life. The largest energy and climate plan currently underway in Europe is the European Green Deal.

3.1. European Green Deal

The European Union has been fighting against climate change from the beginning. The current policy on climate change is the European Green Deal. According to Green Deal the European Union's expectation of member states is to have an overall climate-neutral economy by 2050. The short-term goal of the Green Deal is to reduce emissions by 55% until 2030 compared to the 1990 emissions. The long-term goal is climate neutrality or sometimes also called zero carbon. This also means that the use of natural gas must be completely replaced, and transport must be placed entirely on an electric basis [12-13].

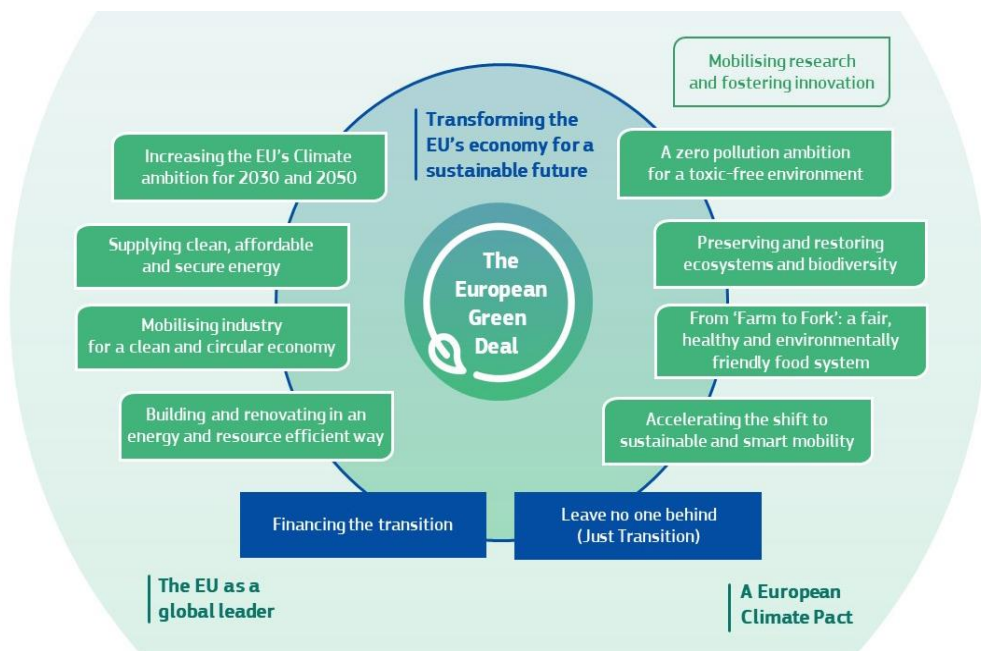


Figure 4. European Green Deal [14]

The European Climate Law assists in the implementation of the Green Deal by setting up a monitoring system with continuous monitoring and necessary intervention to ensure climate neutrality [14].

Targets set for 2020 (which have been achieved) [15]:

- 20% reduction in greenhouse gas emissions (compared to 1990)
- 20% of EU energy production from renewable sources
- 20% improvement in energy efficiency

3.2. EU's Emissions Trading System

The Emissions Trading System limits the number of greenhouse gases that can be emitted by energy-intensive industries, power plants and airlines. The quantity of allowances is subject to a cap set by the EU. Based on this, companies will receive units or buy more. Over time, the cap is reduced, so the number of emissions also gradually decreases. The ETS aims to stimulate innovation and the use of low-carbon technologies [16].

- It operates in all EU countries, including Iceland, Liechtenstein and Norway
- Emission limitation of about 10,000 installations in the energy sector, industry, and aviation
- Covers about 40% of the EU's greenhouse gas emissions

ETS gases:

- Carbon dioxide (CO₂) from electricity and heat production, energy-intensive industries, oil refineries, steel mills, iron smelters, aluminium production, paper production, chemical plants and commercial flights.
- Nitrogen oxides (NO_x)

4. POSSIBLE STRATEGIES FOR REDUCING EMISSIONS

Table 1. Possible strategies for reducing CO₂ emissions [19]

Strategy	Application	Advantages	Limits
Energy efficiency and energy conservation	Applied mainly in commercial and industrial buildings	Energy-saving from 10% to 20% is easily achievable	May need a larger investment
Use of clean fuels	Replacing coal-fired power plants with natural gas	Natural gas operates with 40-50% fewer emissions, higher combustion efficiency and cleaner flue gas	Higher costs, more expensive natural gas
Clean coal technologies	Integrated gasification combined cycle (IGCC)	Lower emissions can be achieved with coal	More investment is needed to the technology
Renewable energy	Construction of hydro, solar, wind and biopower plants	The use of local resources does not emit harmful substances or greenhouse gases	Highly dependent on local resources, may be more expensive than conventional energy production
Nuclear power plants	Nuclear power plants, fusion power plants (currently under research)	It does not emit harmful substances or greenhouse gases	Negative social repercussions especially since the Fukushima disaster
Afforestation and reforestation	Accepted in all countries	Natural and sustainable CO ₂ sinks	Limits future land use
Carbon capture and storage	Applicable for point sources	Efficiencies of up to 80% can be achieved	The industrial application of the technology has not yet been proven

4.1. Carbon Capture and Storage (CCS)

Carbon capture and storage (CCS) is a way to reduce CO₂ emissions from fossil fuel power plants. During the CCS process, the carbon dioxide is separated from the flue gas generated in the power plants and then transferred to geological storage. With this method, power plants can reduce carbon dioxide emissions by 80%-90%. The disadvantage is that the process is energy-intensive, and the carbon capture equipment reduces the efficiency of the power plant nor is long-term underground or ocean storage currently resolved. Modernization of power plants is a challenge in several states, such as Poland, where implementation is long overdue. In Germany and the Netherlands, public opposition to underground storage of carbon dioxide [17].

In the United States, half of greenhouse gas emissions come from energy production and industrial activities [5]. According to the International Energy Agency estimates that carbon dioxide emissions from energy production and industrial activities could be reduced by 20% using carbon capture and storage technology [18]. The three strands of CCS technology are currently being developed: post-combustion separation, pre-combustion separation by coal gasification and oxyfuel combustion. The closest technology to implementation and application is post-combustion separation. Several methods have been developed for the separation of carbon dioxide from the flue gas, for example, chemical method, physical membrane, or cryogenic method. Which technology is used is largely determined by the composition of the flue gas to be treated, which depends fundamentally on the quality of the fuel and the design of the combustion. The advantage of capturing carbon dioxide after combustion is that it can be retrofitted to existing power plants; according to current knowledge, carbon capture reduces the efficiency of a power plant by 6-10%. The gross efficiency of coal-fired power plants varies between 27-45% [19-20].

Oxyfuel combustion is one of the most developed technologies for carbon capture and storage. Oxyfuel combustion refers to fuel being burned in a mixture of oxygen and recycled flue gas [21]. Idea is that after combustion the fuel apart from pollutants consists only of carbon dioxide and water vapor. Therefore, it is not necessary to remove the carbon dioxide, only to remove the water vapor from the mixture and the remaining product is (almost) pure carbon dioxide [22]. According to research by the Argonne National Laboratory, the formation of nitrogen oxides can be reduced by 50% using oxyfuel technology [23]. The deployment of CCS technologies in the case of existing power plants, in the absence of support, can increase the price of electricity by 50-90% [24]. Nor can it be overlooked that according to the U.S. Environmental Protection Agency (EPA) not all countries have sufficient carbon storage capacity. Furthermore, according to surveys, no one wants to set up carbon storage facilities near them.

4.2. European renewable energy directive (RED)

Renewable energy sources (wind, solar, hydropower, biomass and biofuels) are alternatives to fossil fuels that help reduce greenhouse gas emissions and diversify the energy mix and also reduce the dependence of fossil fuels on an unreliable volatile market. In the Renewable Energy Directive, the EU regulatory framework has undergone significant development in recent years. EU leaders set a target in 2009 for 20% of EU energy consumption to come from renewable energy by 2020, which has been achieved and in 2018 a target has been set to increase this by a further 12% by end of 2030 [25-26].

4.3. Hungarian National Energy and Climate plan (NEKT)

The most important goal in international and domestic climate plans is the decarbonisation of energy production and everyday life, which is only possible with the combined use of nuclear and renewable energy, writes in NEKT. In addition to the decarbonisation of energy production, the main objective of the NEKT is to strengthen energy sovereignty and energy security while maintaining low prices [27].

- Carbon-neutral nuclear energy accounts for almost half of Hungary’s electricity production.

As mentioned earlier, the European Union expects member states to have an overall climate-neutral economy by 2050, which means that natural gas consumption must be fully replaced, and transport must be put on an electric basis. Hungary attaches great importance to the implementation of the “polluter pays” principle, according to which the costs of decarbonisation should be borne by the countries and companies that are most responsible for the current situation [27].

4.4. Decarbonisation of domestic energy production

According to NEKT, one of the most important domestic decarbonisation tasks in the transformation of the lignite-fired Mátra power plant is based on low-carbon technologies, thus removing coal and lignite from domestic electricity production by 2030. At the same time, the Mátra power plant's strategically important base power plant is also the largest carbon dioxide emitter in Hungary, accounting for almost 50% of the carbon dioxide emissions of the entire energy sector, thus accounting for 14% of the total domestic greenhouse gas emissions. The transformation of the Mátra power plant is the construction of a gas turbine power plant and construction of a new photovoltaic power plant and an industrial energy storage unit, as well as the energy utilization of non-recyclable waste. Furthermore, by 2030, two new 120 MW nuclear power plant units will be built in Paks in Hungary [27].

4.5. Domestic renewable energy

The share of renewable energy in the heating and cooling sector – by additional measures – can reach 30% in 2030. Efficient utilization of biomass in heating systems, both in district heating and in the use of ambient heat through heat pumps. The implementation of the Green District Heating Program (Zöld Távhő Program) and the placement of as many of the individually heated buildings as possible on a renewable basis will play a key role in replacing natural gas and increasing their use of renewable energy sources in the heat market. In addition to domestic natural gas, the use of alternative gas sources (biogas, biomethane, hydrogen in the future). According to their estimates, biogas can realistically replace about 1% of the natural gas demand. In the area of convergence, Hungary sets a renewable energy share of at least 14% by 2030. To achieve this goal, the share of first-generation biofuels produced from food and feed crops will increase to almost 7% and the share of second-generation (or advanced) biofuels and biogas produced from waste will increase to 3.5% in Hungary’s transport final energy consumption [27].

5. WITHOUT COAL-BASED ENERGY PRODUCTION

Table 2. Distribution of world electricity generation [28]

Source	World (2020)	Europe (2019)	Hungary (2020)
Coal	33.79%	17.49%	10.63%
Natural gas	22.79%	19.23%	26.17%
Hydro	16.85%	15.84%	0.8%
Nuclear	10.12%	23.25%	47.52%
Wind	6.15%	11.56%	1.94%
Oil	4.37%	1.3%	1.03%
Solar	3.27%	3.87%	4.79%
Other renewables	2.72%	5.52%	7.12%

Tab. 2 shows the distribution of world electricity generation. Currently, a significant portion of electricity comes from coal-fired power plants. However, Europe differs significantly from the world average. Much

of Europe's electricity production comes from nuclear power plants, followed closely by gas, coal and water, followed by wind and then by other renewables, solar and oil-based energy in the smallest proportion. In total, renewable energies account for 36.79% of Europe's total electricity, so if we add them up, renewables account for the largest share of electricity generation within Europe, which is 3-4% ahead of the world average. Almost half of the electricity generation in Hungary comes from the Paks Nuclear power plant, renewables (in total) account for 14.65% of electricity generation. Coal-fired electricity generation is 10.63% in Hungary and almost 70% in Poland. In Hungary, coal-fired electricity means a 10.63% outage, which must be made up by 2050 [29-30].

5.1. What are the possibilities?

- CCS-technologies
- Renewable energy sources
- Nuclear energy
- Import

CSS technologies have already been discussed above, can be costly to implement and have a negative social impact, as the share of coal-fired energy production is less significant in Hungary, so other solutions may be more cost-effective, but in Poland where almost 70% of energy production is based on coal, the development of CCS technologies may be more cost-effective.

To replace it with renewable energy, let's look at domestic numbers.

Table 3. Domestic energy production [28]

Source	Quantity [TWh]
Nuclear	16.06
Natural gas	8.85
Coal	3.59
Other renewables	2.41
Solar	1.62
Wind	0.66
Oil	0.35
Water	0.27
Altogether	33.81

The current amount of renewable energy production is 4.96 TWh, an additional 3.59 TWh is needed to replace coal-based production, of course without considering the growing electricity demand as switching from transmission to electricity is likely to significantly increase electricity demand. Since in Hungary the 277/2016. (IX. 15.) on the construction of wind turbines [31], therefore, the most obvious solution from the renewable energy sources is the establishment of solar parks, which would mean increasing the current solar energy production by 2.5 times, which would involve a significant financial investment and the involvement of large areas of land that had been prepared.

Nuclear energy is playing a prominent role in the NEKT [27], it is no coincidence, the nuclear energy accounts for almost half of Hungary's electricity generation. In France, nuclear power plants account for 67% of electricity generation and the remaining 33% is 23% renewables and 10% fossil fuels (6.5% gas, 2% oil and less than 1% coal). 90% of French electricity production comes from climate-neutral energy sources. It can be observed that in countries where natural factors are not favourable for the use of renewable energies, nuclear energy or import is the most appropriate way to placing electricity production on a climate-neutral basis.

Table 4. Distribution of world electricity production [28]

Source	France (2020)	Germany (2020)	Belgium (2020)
Coal	0.81%	23.66%	0.11%
Natural gas	6.48%	16.15%	30.32%
Water	11.74%	3.3%	0.32%
Nuclear	67.21%	11.33%	39.33%
Wind	7.42%	23.71%	14.42%
Oil	2.18%	3.97%	4.13%
Solar	2.5%	8.99%	5.37%
Other renewables	1.66%	8.9%	6.02%

As already mentioned, the European Union expects its member states to have an overall climate-neutral economy by 2050. For Hungary to have climate-neutral electricity production, the full replacement of natural gas consumption, the full relocation of transport to electricity, will cost about 50,000 billion Hungarian Forint [27].

6. SUMMARY, DIRECTION OF DEVELOPMENT

There are currently several debates about which direction would be appropriate. Some scientists and some members of the public support systems based on completely renewable energy sources with batteries, hydro storages, or other forms of energy storage. Another direction suggests the combined use of nuclear and renewable energy sources, as both directions have challenges (of course, not only these two directions exist), which can be assured that reducing fossil-based energy production is common in these directions.

6.1. The direction of development I propose

The development direction I propose would focus on energy production from nuclear and renewable energy sources, similar to France's energy production and proposed by NEKT. Energy production based solely on renewable energy sources carries several problems, so for the time being, this trend must be avoided in my opinion. It is important to note that the essence of carbon neutrality is the total value of emissions zero, which means that it is not necessary to completely exclude emitting technologies, but only to reduce them to an extent that can be neutralized by "sinks" (e.g., forests) in the country. I consider it important to develop an energy mix based on a full life cycle analysis, for example, the production of solar panels and the processing of waste has a significant environmental impact. Another important aspect is that currently a significant proportion (about 50%) of household waste is landfilled. Much of the waste that ends up in landfills has a high calorific value. Waste co-incineration with fossil fuels or incineration itself is not a negligible factor as waste is not included in greenhouse gas emissions. The European Union's goal is to reduce the landfill rate to less than 10% by 2035. Energy recovery of waste is a much better solution than landfilling if recycling in its material is not possible. The waste incinerator in Budapest incinerates 400,000 tons of waste annually, of which more than 1 million GJ of energy is sold, which covers the annual electricity needs of 140,000 residents and provides district heating to 25,000 homes [32]. These solutions have negative social repercussions. In my opinion because of the lack of knowledge and information. To change this, it is necessary to educate and enlighten people properly. It is important to highlight that the waste cannot be incinerated in households' fireplaces and boilers, when we incinerate waste at home it releases highly toxic gases because of the lack of burning temperature and flue gas treatment.

6.2. European Green Deal important aspects

According to Green Deal, it is necessary to achieve carbon neutrality by 2050, which is a very ambitious goal. Here several aspects are essential to consider, as we can easily cause a bigger problem. Above all, it is important to ensure a reliable energy supply and to continuously meet the ever-increasing energy demand for development.

6.3. Other ways to reduce environmental impacts

When we talk about climate protection and energy, we must talk about the importance of waste as well. Minimizing waste, avoiding the production of unnecessary things, buying from local producers, selective waste collection, all help to save energy and protect the climate. The shorter the transport distance, the lower the CO₂ emissions. If there is more recycled waste in its material, there is less needed to coat new raw material, which saves energy. For example, recycling metals saves 70% of energy compared to mining, by recycling 1 ton of paper, we protect 17 trees also if we are recycling plastic, there is less chance that plastics will end up in the ocean. We can save a lot of energy with prevention and with proper waste management, so this is an important aspect. During the Proof-of-Concept innovation tender announced by the University of Miskolc in 2020, the development of an application that helps people to follow more environmentally friendly behaviour in everyday life has started by GW Tech [33]. The application will help everyone in selective waste collection and provide us with important and interesting facts, as above.

REFERENCES

- [1] Houghton, J. (2005). Global warming. Reports on Progress in Physics, 68(6), 1343–1403. <https://doi.org/10.1088/0034-4885/68/6/r02>
- [2] Archer, D. (2016). The long thaw: How humans are changing the next 100,000 years of Earth's climate. Princeton University Press. ISBN: 9780691169064
- [3] Saklani, N., & Khurana, A. (2019). Global warming: Effect on living organisms, causes and its solutions. International Journal of Engineering and Management Research, 09(05), 24–26. <https://doi.org/10.31033/ijemr.9.5.4>
- [4] Boeker, E., & Grondelle, R. van. (2012). Environmental physics: Sustainable energy and climate change. John Wiley & Sons.
- [5] “Overview of Greenhouse Gases,” EPA, 14-Apr-2021. [Online]. Available: <https://www.epa.gov/ghgemissions/overview-greenhouse-gases>. [Accessed: 26-May-2021].
- [6] H. Ritchie, “Energy mix,” Our World in Data, 2019. [Online]. Available: <https://ourworldindata.org/energy-mix>. [Accessed: 26-May-2021].
- [7] Martins, F., Felgueiras, C., & Smitková, M. (2018). Fossil fuel energy consumption in European countries. Energy Procedia, 153, 107–111. <https://doi.org/10.1016/j.egypro.2018.10.050>
- [8] Á. S. Woperáné and I. Szűcs, Levegőtisztítás, 1st ed., vol. 280, 280 vols. Miskolc: Miskolci Egyetemi kiadó, 2001.
- [9] W. K. H. Kft., “4/2011. (I. 14.) VM rendelet a levegőterheltségi szint határértékeiről és a helyhez kötött légszennyező pontforrások kibocsátási határértékeiről - Hatályos Jogszabályok Gyűjteménye,” Wolters Kluwer. [Online]. Available: <https://net.jogtar.hu/jogszabaly?docid=a1100004.vm>. [Accessed: 26-May-2021].
- [10] Eurostat, “Greenhouse gas emission statistics - air emissions accounts,” Gas Emission Statistics - Air Emissions Accounts, vol. 8, pp. 1–8, 2021.
- [11] Shindell, D., & Faluvegi, G. (2010). The net climate impact of coal-fired power plant emissions. Atmospheric Chemistry and Physics, 10(7), 3247–3260. <https://doi.org/10.5194/acp-10-3247-2010>

- [12] Dominković, D. F., Bačeković, I., Čosić, B., Krajačić, G., Pukšec, T., Duić, N., & Markovska, N. (2016). Zero carbon energy system of South East Europe in 2050. *Applied Energy*, 184, 1517–1528. <https://doi.org/10.1016/j.apenergy.2016.03.046>
- [13] E. Council, “Lex Access to European Union law,” EUR, 2019. [Online]. Available: <https://eur-lex.europa.eu/legal-content/EN/TXT/?uri=COM%3A2019%3A640%3AFIN>. [Accessed: 26-May-2021].
- [14] E. Council, “Lex Access to European Union law,” EUR, 2020. [Online]. Available: <https://eur-lex.europa.eu/legal-content/EN/TXT/?uri=CELEX%3A52020PC0563>. [Accessed: 26-May-2021].
- [15] E. Parliament, “Lex Access to European Union law,” EUR, 2009. [Online]. Available: https://eur-lex.europa.eu/legal-content/EN/TXT/?uri=uriserv%3AOJ.L_2009.140.01.0016.01.ENG. [Accessed: 26-May-2021].
- [16] E. Parliament, “Lex Access to European Union law,” EUR, 2017. [Online]. Available: <https://eur-lex.europa.eu/legal-content/HU/TXT/?uri=CELEX%3A52017DC0048&qid=1620389622499>. [Accessed: 26-May-2021].
- [17] Eikeland, P. O., & Skjærseth, J. B. (2020). The politics OF Low-Carbon INNOVATION. <https://doi.org/10.1007/978-3-030-17913-7>
- [18] Iea, “The Role of CO2 Storage – Analysis,” IEA, 2019. [Online]. Available: <https://www.iea.org/reports/the-role-of-co2-storage>. [Accessed: 26-May-2021].
- [19] Leung, D. Y. C., Caramanna, G., & Maroto-Valer, M. M. (2014). An overview of current status of carbon dioxide capture and storage technologies. *Renewable and Sustainable Energy Reviews*, 39, 426–443. <https://doi.org/10.1016/j.rser.2014.07.093>
- [20] I. Gács, “Energetika II.,” *Digitális Tankönyvtár*, 2012. [Online]. Available: https://regi.tankonyvtar.hu/hu/tartalom/tamop412A/2010-0017_34_energetika_2/ch03s05.html [Accessed: 26-May-2021].
- [21] Boot-Handford, M. E., Abanades, J. C., Anthony, E. J., Blunt, M. J., Brandani, S., Mac Dowell, N., Fernández, J. R., Ferrari, M.-C., Gross, R., Hallett, J. P., Haszeldine, R. S., Heptonstall, P., Lyngfelt, A., Makuch, Z., Mangano, E., Porter, R. T., Pourkashanian, M., Rochelle, G. T., Shah, N., ... Fennell, P. S. (2014). Carbon capture and storage update. *Energy Environ. Sci.*, 7(1), 130–189. <https://doi.org/10.1039/c3ee42350f>
- [22] Buhre, B. J. P., Elliott, L. K., Sheng, C. D., Gupta, R. P., & Wall, T. F. (2005). Oxy-fuel combustion technology for coal-fired power generation. *Progress in Energy and Combustion Science*, 31(4), 283–307. <https://doi.org/10.1016/j.pecs.2005.07.001>
- [23] Davies, L. L., Uchitel, K., & Ruple, J. (2013). Understanding barriers TO commercial-scale carbon capture and sequestration in the United States: An empirical assessment. *Energy Policy*, 59, 745–761. <https://doi.org/10.1016/j.enpol.2013.04.033>
- [24] Dooley, J. J. (n.d.). Carbon Dioxide Capture and Geologic Storage: a Core Element of a Global Energy Technology Strategy to Address Climate Change. The Global Energy Technology Strategy Program. http://www.globalchange.umd.edu/data/gtsp/workshops/2006/ccs_report.pdf
- [25] Eikeland, P. O., & Skjærseth, J. B. (2020). The politics OF Low-Carbon INNOVATION. <https://doi.org/10.1007/978-3-030-17913-7>
- [26] Oberthür Sebastian, Pallemarts, M., & Kelly, C. R. (2010). The new climate policies of the European Union: Internal Legislation and Climate Diplomacy. VUB Press, Brussels University Press.
- [27] Innovációs és Technológiai Minisztérium. (2021). Nemzeti Energia- és Klímaterv. https://ec.europa.eu/energy/sites/ener/files/documents/hu_final_necp_main_hu.pdf

- [28] H. Ritchie, "Electricity Mix," Our World in Data, 2020. [Online]. Available: <https://ourworldindata.org/electricity-mix>. [Accessed: 26-May-2021].
- [29] Hong, S., Bradshaw, C. J. A., & Brook, B. W. (2015). Global zero-carbon energy pathways using viable mixes of nuclear and renewables. *Applied Energy*, 143, 451–459. <https://doi.org/10.1016/j.apenergy.2015.01.006>
- [30] International Atomic Energy Agency. (2019). Adapting the Energy Sector to Climate Change. https://www-pub.iaea.org/MTCD/Publications/PDF/P1847_web.pdf
- [31] W. K. H. Kft., "277/2016. (IX. 15.) Korm. rendelet a szélérőművekre vonatkozó szabályok módosításáról - Hatályos Jogszabályok Gyűjteménye," Wolters Kluwer, 2016. [Online]. Available: <https://net.jogtar.hu/jogszabaly?docid=A1600277.KORxhft=20160923&txtreferer=00000001.txt> [Accessed: 26-May-2021].
- [32] FKF Nonprofit Zrt. (2018). A fővárosi hulladékhasznosító mű. Budapest, Hungary; FKF Nonprofit Zrt. <https://www.fkf.hu/storage/app/media/Kiadvanyok/2018-FHHM%20-%20MAGYAR.pdf>
- [33] Miskolci Egyetem. (2020, October 22). Lezárult AZ ELSŐ „proof of CONCEPT” innovációs pályázat. Hallgatói - Technológia és Tudástranszfer Igazgatóság. Retrieved September 12, 2021, from <https://techtransfer.uni-miskolc.hu/Hallgatoi/Lezarult-az-első-PROOF-OF-CONCEPT-innovacios-palyazat>.

DETECTION OF EFFICIENCY OF MICROWAVE-ENHANCED SLUDGE TREATMENTS BY DIELECTRIC MEASUREMENTS

Laura Haranghy, Zoltán Jákói, Cecília Hodúr, Sándor Beszédes

University of Szeged Faculty of Engineering, Department of Biosystems Engineering, Moszkvai krt. 9, H-6725 Szeged, Hungary.
e-mail: beszedes@mk.u-szeged.hu

ABSTRACT

Microwave irradiation is a promising pre-treatment method for sludge stabilisation, but there are few studies focusing its effect on organic matter solubility and biodegradability of wastewater and sludge originated from the food industry. In our research, microwave irradiation was applied standalone and in combination with alkaline treatment to enhance the solubilisation and biodegradation of organic matter content of meat industry wastewater and municipal sludge, respectively. The energy efficiency was investigated, as well. Dielectric measurement is a suitable method to detect physicochemical changes; therefore our research work covered the determination of dielectric properties of the investigated materials. Our experimental results have revealed that the lower power and energy intensity microwave-alkaline treatments were the most efficient pre-treatment process from energetically aspects to increase the organic matter solubility and biodegradability of wastewater and sludge. Furthermore, a strong linear correlation was found between the dielectric constant and the indicators of the solubility of organic matter (SCOD/TCOD) and aerobic biodegradability (BOD/COD) in both treated materials, respectively. Our results show that the dielectric measurements can be applied for detection of physicochemical changes, predict the improvement of biodegradability, and considered as a promising method to estimate the efficiency of sludge pre-treatment methods.

Keywords: wastewater, sludge, microwave, dielectric measurements, biodegradability

1. INTRODUCTION

Due to the urbanization, the increased water consumption of population and industry generate a significant amount of wastewater and sludge. Because of the high cost of operating and treatment processes, it should be taken into consideration to utilize the arising amount of sludge. Instead of deposition and incineration, the application of biological utilisation methods (e.g. composting or anaerobic digestion) are preferred to reduce the organic matter content of sludge. For economic reasons the application of different pre-treatment technologies are required to enhance the efficiency of the utilisation processes.

Microwave irradiation (MW) is proven to be a promising pre-treatment method in different food technologies and biomass utilisation based on previous studies [1, 2, 3, 4]. As a result of its unique heating mechanism provides a fast and selective heating ability [5], the applicability of microwave treatments in sludge stabilisation processes need to be investigated thoroughly. Due to its thermal effect it can enhance the disposal of sludge with the disruption of microbial cell wall. The released cytoplasm increases the soluble organic matter content of the sludge, since proteins, carbohydrates, lipids become more available for the microorganisms [6]. Alkaline dosage is a suitable chemical treatment method the increase disintegration of bacterial cell wall however, many studies pointed out that in combination with physical pre-treatments, the efficiency could be enhanced [7, 8]. The characteristics of microwave treatment of municipal sludge is vigorously investigated [5, 6, 9], but there is few studies available related to wastewater and sludge originated from the food industry.

Dielectric materials, like wastewater and sludge can absorb the microwave interval of the electromagnetic spectrum, and its extent depends on the material properties, structure, temperature and frequency. The dielectric behaviour of a material can be described with certain dielectric properties.

Complex relative permittivity (ϵ) includes the characteristics that affect the reflection of electromagnetic waves from the material interface, as well the energy loss that occurs with the absorption of the electromagnetic wave [10]. The dielectric constant (ϵ') represents the electrical energy absorption capacity

of the dielectric material, the dielectric loss factor (ϵ'') describes the dissipation ability of the dielectric material and j is the imaginary factor:

$$\epsilon = \epsilon' - j \cdot \epsilon'' \quad (1)$$

The product of free space permittivity (ϵ_0) and the relative permittivity (ϵ_r') gives the dielectric constant:

$$\epsilon' = \epsilon_0 \cdot \epsilon_r' \quad (2)$$

Measuring dielectric properties is a rapid, non-destructive way of determine structural and/or molecular changes in the raw material matrix, and such, it is a suitable method to detect the organic matter removal efficiency of wastewater treatment processes [11, 12].

The main aim of our research work was to investigate correlation between the dielectric parameters and the mentioned conventional analytical indicators (COD, BOD).

2. MATERIALS AND METHODS

In our experiments, 100-100 cm³ of meat processing wastewater and municipal sludge were used for the treatments and dielectric measurement.

The samples were pre-treated by microwave irradiation with a total energy intensity of 300, 450 and 600 J/mL at two different power levels (250 and 500 W), with the corresponding the irradiation time of 1-4 minutes. For the microwave treatments laboratory scale microwave equipment (Labotron 500) was used.

In combination with the MW treatment - as an alkaline treatment- 2 cm³ 40 m/m% NaOH solution was dosed.

To investigate the effects of each treatment on solubility the total chemical oxygen demand (TCOD) was determined. Based on previous studies focusing on the determination of soluble chemical oxygen demand (SCOD), we applied the organic matter fractionation method, i.e. sedimentation, centrifugation (RCF=6000 for 10 minutes) and filtration (0,45µm pore filter), which was followed by a colorimetric method (Hanna, COD cuvet test, after 2 hours thermomodigestion at 180 °C) to determine the exact values of SCOD. The SCOD/TCOD parameter describes the ratio between the amount of organic matter in the soluble phase and the total chemical oxygen demand of the observed sample.

For the characterisation of aerobic biodegradability, biochemical oxygen demand (BOD) was measured in respirometric BOD meter, and as an indicator, the ratio of BOD and COD (BOD/COD) was used. To investigate the efficiency of biogas production lab-scale batch mesophilic anaerobic digestion tests were carried out.

For the dielectric measurements a DAK 3.5 (SPEAG) open-ended coaxial dielectric probe was used, connected to a ZVL-3 vector network analyser (Rohde&Schwarz). The dielectric properties – the dielectric constant (ϵ') and the dielectric loss factor (ϵ'') - were measured in the frequency range of 200-2400 MHz, at the temperature of 28 °C.

3. RESULTS AND DISCUSSION

In our research work, we applied different power and energy intensity microwave treatments standalone and in combination with alkaline dosage in order to enhance the solubility and biodegradability of meat processing wastewater and municipal sludge. Our results show microwave-alkaline combined pre-treatments increased the most the indicators of organic matter solubility (SCOD/TCOD), since it affects the SCOD/TCOD parameter in a way which indicates that the solubility of the organic compounds of the treated material is enhanced in the soluble phase. When combined pre-treatment was applied the indicator of aerobic biodegradability (BOD/SCOD) also shows a larger growing tendency compared to the raw control and the standalone MW treatments, since the increased solubility causes better availability of the

organic matter for the microorganisms in the soluble phase. The MW-alkaline treatments enhanced the biogas yield of anaerobic digestion tests, as well. Furthermore, from energetically aspects those processes were the most efficient, when the NaOH treatment was intensified with MW irradiation, especially on lower (2.5 W/mL) power levels.

In our study, besides the investigation of energy efficiency of each treatment, we also focused on the determination of correlation between dielectric parameters, solubility and biodegradability indicators.

After the pre-treatments, each sample was cooled to the temperature of 28°C to carry out the dielectric measurements. The results of dielectric measurement show that the ratio of dielectric constant (300MHz/2400MHz) has a linear correlation with the SCOD/TCOD in both treated materials, respectively:

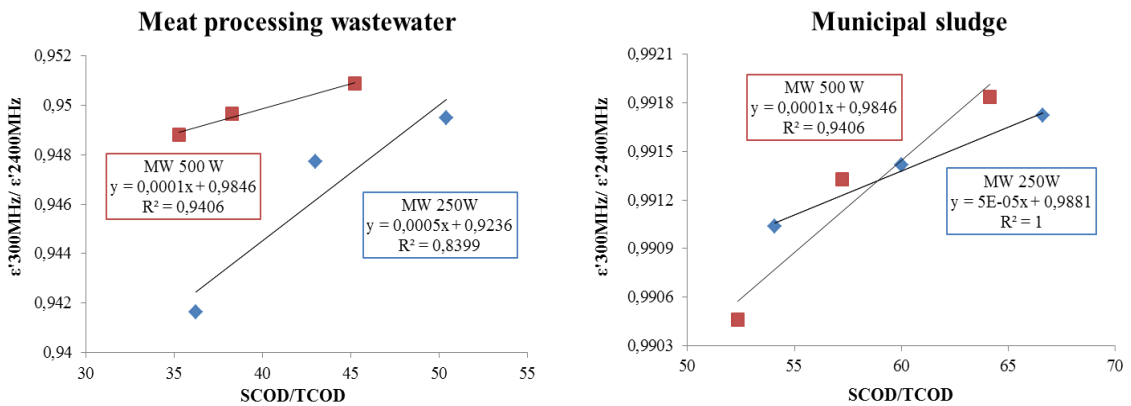


Figure 1. The correlation between SCOD/TCOD and ratio of dielectric constant (300MHz/2400MHz)

Figure 1. shows that the applied power intensity and the type of treated material affect the regression equations, but the presented correlation is independent from these factors. The higher organic matter solubility can be traced back to the degradation effect of the MW on the solid particles and the macromolecules of the sludge, causing deflocculation [12].

As the indicator of aerobic biodegradation, the ratio of BOD and COD were determined (Fig.2).

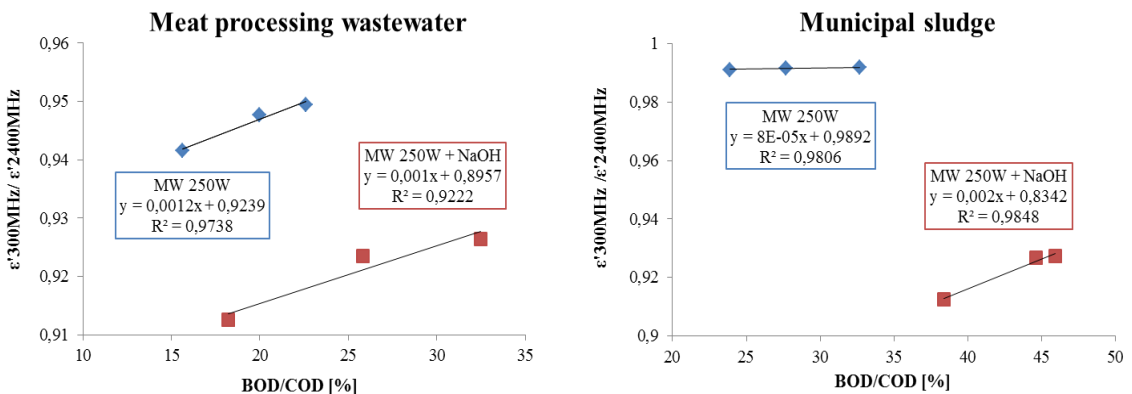


Figure 2. The correlation between BOD/COD and ratio of dielectric constant (300MHz/2400MHz)

Similarly to the solubility (Fig.1), the BOD/COD ratio also shows a strong linear correlation with the determined ratio of dielectric constant ($\epsilon'_{300\text{MHz}} / \epsilon'_{2400\text{MHz}}$) in meat processing wastewater and municipal sludge, respectively. This result verifies the connection with the increased organic matter solubility.

Based on the results of our research, dielectric measurement is an applicable method to investigate the changes of the organic matter content in food industry wastewater and municipal sludge. In order to get more accurate and detailed information about the dielectric behaviour of these materials, further investigation is needed and the range of measuring frequency should be extended. The determination of dielectric properties - in the presence of appropriate correlations – could be a faster, more precise, chemical free and non-destructive method for the characterisation treated sample. Thereby, dielectric measurement is concluded suitable for the estimation of the expected efficiency.

4. CONCLUSIONS

In this study we compared the efficiencies of different energy and power intensity standalone and alkaline-combined MW treatments on the solubility of organic matter in meat industry wastewater and municipal sludge samples. Based on our results, microwave irradiation, especially in combination with alkaline-dosage is proved to be an applicable wastewater and sludge pre-treatment method. The lower power level MW- alkaline treatments intensified the solubility and biodegradation of organic matter content, in aerobic (BOD/COD) and anaerobic (increase of biogas yield) ways, as well.

In order to gain a more detailed understanding of how microwave irradiation affects the other raw material matrix of different sludge samples originated from the food industry, further researches are recommended. Our study also focused on to investigate the correlation between the dielectric constant (ϵ'), solubility and aerobic biodegradability indicators (SCOD/TCOD, BOD/COD). With the application of dielectric measurement the change in the solubility and biodegradability of organic matter can be detected, since these parameters and the change of dielectric constant and shows a linear correlation between each other. The results show that dielectric measurement is proved to be a promising detection method to estimate the efficiency of various sludge pre-treatments.

ACKNOWLEDGEMENTS

The research is supported by the UNKP-21-2-SZTE-317 (Haranghy L.) and UNKP-21-5-SZTE-556 (Beszédes S.) New National Excellence Program of the Ministry for Innovation and Technology from the source of the National Research Development and Innovation Fund. The authors thank the support of the János Bolyai Research Scholarship of the Hungarian Academy of Sciences (BO/00161/21/4- Beszédes S.).

REFERENCES

- [1] Korzenszky, P.; Géczi, G.; Kaszab, T.: Comparing microwave and convective heat treatment methods by applying colour parameters of wine. *Progress In Agricultural Engineering Sciences*, 16 : S1 pp. 105-113. , 9 p. (2020) <https://doi.org/10.1556/446.2020.10011>
- [2] Kapcsándi, V. ; Neményi, M. ; Lakatos, Erika: Microwave steam explosion and enzymatic hydrolysis of vine-branch, *Acta Alimentaria: An International Journal Of Food Science*, 47: 4 pp. 443-452., 10 p. (2018) <https://doi.org/10.1556/066.2018.47.4.7>
- [3] Korzenszky, P.; Sembery, P.; Géczi, G.: Microwave Milk Pasteurization without Food Safety Risk. *Potravinarstvo*, 7 : 1 pp. 45-48. , 4 p. (2013) <https://doi.org/10.5219/260>
- [4] Kapcsándi, V.; Cserpán, M.; Hanczné, Lakatos E.: Impact assessment of microwave treatment of raw cow's milk on its microbiological properties. *Analecta Technica Szegedinensia*, 14 : 2 pp. 69-76. , 8 p. (2020) <https://doi.org/10.14232/analecta.2020.2.69-76>

- [5] Appels L., Houtmeyers S., Degrève J., Impe J.V., Dewil R: Influence of microwave pre-treatment on sludge solubilization and pilot scale semi-continuous anaerobic digestion. *Bioresource Technology*, 2013, 128, 598-603. <https://doi.org/10.1016/j.biortech.2012.11.007>
- [6] Ahn, J.H., Shin, S.G., Hwang S.: Effect of microwave irradiation on the disintegration and acidogenesis of municipal secondary sludge. *Chemical Engineering Journal*, 2009, 153, 145-150. <https://doi.org/10.1016/j.cej.2009.06.032>
- [7] Doğan I., Sanin F.D. (2009): Alkaline solubilization and microwave irradiation as a combined sludge disintegration and minimization method. *Water Research*, 43, 2139–2148. <https://doi.org/10.1016/j.watres.2009.02.023>
- [8] Alqaralleh R.M., Kennedy K., Delatolla R. (2019): Microwave vs. alkaline microwave pretreatment for enhancing thickened waste activated sludge and fat, oil, and grease solubilization, degradation and biogas production. *Journal of Environmental Management*, 233, 378-392. <https://doi.org/10.1016/j.jenvman.2018.12.046>
- [9] Wang H., Sun J., Xu Y., Feng H., Duan L., Xin H. (2019): Investigation on characteristics of microwave treatment of organic matter in municipal dewatered sludge. *Applied Sciences*, 9 (6), 1175. <https://doi.org/10.3390/app9061175>
- [10] S. Chandrasekaran, S. Ramanathan, T. Basak: Microwave Material Processing—A Review. *AIChE Journal*, 2012, 58, 2, 330-363.
- [11] Jákó Z., Hodúr C., László Z., Beszédes S.: Detection of the efficiency of microwave–oxidation process for meat industry wastewater by dielectric measurement, *Water Science & Technology*, 2018, 78, 10, 2141-2148. <https://doi.org/10.2166/wst.2018.491>
- [12] Kovács V.P., Lemmer B., Keszthelyi-Szabó G., Hodúr C., Beszédes S.: Application of dielectric constant measurement in microwave sludge disintegration and wastewater purification processes, *Water Science & Technology*, 2018, 77, (9), 2284-2291. <https://doi.org/10.2166/wst.2018.144>

GASOLINE LIKE FUEL FROM PLASTIC WASTE PYROLYSIS AND HYDROTREATMENT

Balázs Hegedüs, Zsolt Dobó

Institute of Energy and Quality, University of Miskolc, Miskolc, Hungary
hege.balazs94@gmail.com

ABSTRACT

Recycling of plastic waste is desirable to lower environmental pollution and fulfil the requirements of circular economy. Energetic utilization is another possibility, however, municipal solid waste containing plastics is usually combusted to generate heat and electricity. An attractive way of dealing with plastic waste is pyrolysis, which has the potential of producing liquid hydrocarbons suitable as a transportation fuel. The pyrolysis results of three plastics produced in the largest amount globally, namely polyethylene, polypropylene and polystyrene as well as their mixtures are presented. The experiments were performed in a laboratory scale batch reactor. The pyrolysis oils were further processed by distillation to provide gasoline and diesel like (distillation cuts at 210 and 350 °C) hydrocarbons. The gasoline fractions were analysed by GC-MS and the composition was compared with the EU gasoline standard. It was found that the oils from PE, PP and PS contain compounds present in standard gasoline. Mixing PS with PE and PP before the pyrolysis, or the oils afterward produces much closer results to standard requirements as PS pyrolysis generates mostly aromatic content. As standard maximizes the olefin content of gasoline to 18 Vol%, hydrogenation was also performed using Pd based catalyst. The hydrogenation process significantly reduced the number of double bonds resulting in low olefin content. Results show that the pyrolysis of plastic waste mixtures containing PE, PP and PS is a viable method to produce pyrolysis oil suitable for gasoline-like fuel extraction and further hydrogenation of the product can provide gasoline fuels with low olefin content.

Keywords: plastic waste, pyrolysis, hydrotreatment, gasoline

1. INTRODUCTION

According to global statistics, since the beginning of industrial plastic production in 1950, approximately 7,5 billion tonnes of plastic have been produced until 2015, and the amount produced grows each year [1]. From the vast amount of plastic generated so far, only ~10% was recycled, and ~15% was utilized by incineration, which means that more than 5 billion tonnes are discarded or landfilled [2]. Considering these facts, new technologies are being developed and applied for the efficient and economical treatment of plastic waste including pyrolysis. This method not only offers a way to dispose of used plastic products, but it can also produce value-added raw materials or even transportation fuels in the form of pyrolytic oil.

From literature and statistics, it is determined that three plastics produced in the largest amount globally, namely high- and low-density polyethylene (HDPE, LDPE), polypropylene (PP) and polystyrene (PS). PE and PP mainly degrade into various hydrocarbons with diverse molecular mass, while the product from PS is usually made of aromatic compounds [3]. However, for these oils to be applied as fuel, more precisely as gasoline, they must meet various parameters stated in regulations [4]. Usually, the biggest difference is the concentration of olefins in the oils, which is maximized at 18 Vol% in the EN 228 standard. The olefins are hydrocarbon molecules containing at least one carbon double bond. Basically, olefins can improve the performance of internal combustion engines; however, it also causes deposition inside the engine shortening its lifespan. Adding PS into the solid waste blend can also lessen the olefin ratio, however, it is not enough to produce standard quality gasoline.

Hydrotreatment is a possible method to decrease the concentration of olefins. This technology is widely used in the petrochemical industry. During the hydrogenation process catalyst and hydrogen are used to saturate the molecules. There are two types of this method. One of them is hydrotreatment at mild temperatures when the saturation of molecules can be achieved without significantly changing the boiling temperature of the components in oil, as no cracking occurs. The other type is destructive hydrotreatment

or hydrocracking. This process combines the cracking and the saturation into one step. It is mainly used in crude oil refinement.

This paper investigates the fuel properties of plastic waste gasoline obtained from the distillation of various pyrolysis oils, utilizing LDPE, HDPE, PP and PS waste materials. Additionally, catalytic hydrogenation was performed in case of one fuel to investigate the possibility of lowering the olefin content.

2. MATERIALS AND METHODS

The experiments were carried out in a laboratory-scale batch reactor (Fig. 1). An air-cooled reflux is connected to the reactor, and after that a water-cooled heat-exchanger. The primary role of the reflux is regulating the pyrolysis gas temperature, therefore changing the molecular weight distribution of the liquid product, while the heat-exchanger ensures the condensation of hydrocarbon vapours. The non-condensable gases in the case of experiments without continuous hydrogen flow were separately collected and analysed. During the experiment where hydrogen stream was applied, the gases were flared. A hydrogen pre-heater unit was also used in the case of continuous hydrogen flow to avoid cold gas inlet into the reactor. Typically, the hydrogen temperature was set to 300 °C, while the flow rate to 15 l/h (standard conditions).

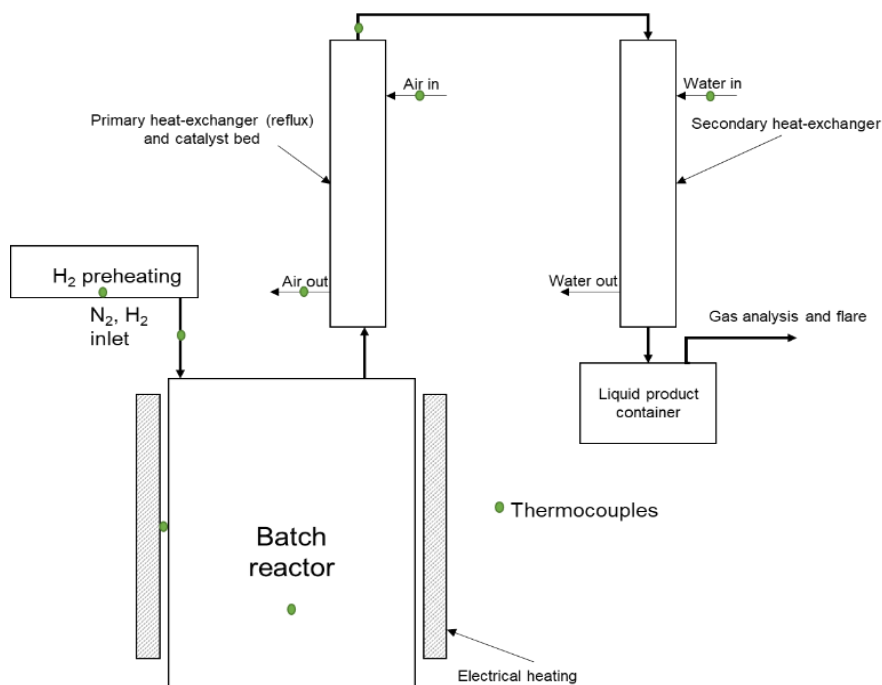


Figure 1. Schematic illustration of the experimental setup.

HDPE, LDPE, PP and PS plastic wastes were used with ratios summarized in Table 1. Seven experiments were performed with various feed compositions. Samples I-IV. were the individual plastic materials, while sample V. and sample VI. were mixtures, with and without PS, respectively. The composition of the mixtures was determined by plastic production statistics [5]. Another pyrolysis run was performed to reduce the ratio of olefins in the liquid product (sample VII.), where 15 g Pd-based catalyst was applied, placed into the reflux.

In each case, 150 g of plastic waste materials were prepared. The endpoint of the pyrolysis experiments was indicated by the inner temperature of the reactor reaching 530 °C, as all the plastic materials used are degraded by reaching that temperature [6].

The pyrolytic oils were separated by atmospheric distillation into three fractions, “gasoline” fraction at the 210 °C cut, “diesel” fraction at the 350 °C cut, and the residue containing heavy hydrocarbons with higher boiling temperatures. The gasoline fractions were analyzed by GC-MS to investigate the molecular distribution of such distillates. It is worth noting that during the distillation process, there was a certain amount of material loss in each case. This loss is attributed to the light hydrocarbons with low boiling temperatures, which were not able to condense. The “gasoline” fraction of sample VI. was hydrogenated separately using the same type of Pd catalyst as it was during the pyrolysis experiment. The process was performed in a hydrogenation reactor at 300 °C and with 15 g catalyst.

Table 1. Composition of the batches prepared for pyrolysis.

Sample ID	HDPE wt%	LDPE wt%	PP wt%	PS wt%	Note
I.	100	0	0	0	-
II.	0	100	0	0	-
III.	0	0	100	0	-
IV.	0	0	0	100	-
V.	14	20,5	45,5	20	-
VI.	17.5	25.62	56.88	0	-
VII.	17.5	25.62	56.88	0	Hydrogen + Pd catalyst

3. RESULTS

The summary of the oil yields from the pyrolysis experiments and the distillation is summarized in Table 2. PS pyrolysis provided the highest oil yield of 84,6 wt%, while LDPE pyrolysis resulted in the lowest oil yield of 62,07 wt%. A decrease can be observed in the oil yield in the case of sample VII. and also there is a significant change in different distillation cuts, compared to sample VI. This can be explained by the additional hydrogen stream, which physically “pushed” the pyrolysis gas through the reflux, therefore it could not efficiently regulate the molecular weight distribution. It is also shown in the table, that the material loss during the distillation is non-negligible. This loss can mainly affect the distillation step parameters of the EN 228 standard.

Table 2. Pyrolysis oil and the different distillation cut yields.

Sample	Oil yield, wt%	20-210 °C		210-350 °C		Above 350°C		Loss	
		wt%	g/kg _{plastic}	wt%	g/kg _{plastic}	wt%	g/kg _{plastic}	wt%	g/kg _{plastic}
I.	70.47	50.4	355.1	37.56	264.67	8.08	56.95	3.96	41.88
II.	62.07	53.01	311.68	37.78	222.16	4.51	26.53	4.70	41.5
III.	79.60	63.73	507.30	31.17	248.12	3.71	29.52	1.39	16.6
IV.	84.60	90.36	764.42	1.92	12.83	6.72	56.83	1.41	17.87
V.	76.00	63.58	483.22	37.63	250.86	3.05	23.14	0.37	4.17
VI.	75.20	58.59	440.58	38.48	256.56	4.12	30.96	3.18	35.83
VII.	66.00	36.61	241.61	32.5	328.00	16.7	196.82	1.07	10.61

The 20-210 °C fractions were compared to EN 228 European gasoline standard, the results are summarized in Table 3. The properties in grey coloured cells were not measured, green indicates the value meets the parameters stated in the standard, while red means that the parameter is out of range. As expected, the samples from normal thermal degradation have high olefin content excluding the oil from polystyrene which is made of aromatic compounds entirely. Regarding density, all the 20-210 °C distillates originating from the mixtures meets the standard parameters, while from the individual plastic pyrolysis, sample III. and IV. are out of range. In the case of sample VII. the olefin content, while still higher than 18 Vol%, was significantly decreased. The best outcome, respective to the olefin content, was achieved with sample VI.H, the separately hydrogenated distillate of sample VI. In this case, the olefin content almost entirely disappeared, however during the hydrogenation process the same material loss was observed as during the distillation, therefore the 100 °C distillation step is not met.

Table 3. Comparison of the EN 228 standard and the pyrolysis oil distillates.

Parameter	Units	Limits		Properties of the „gasoline” fractions											
		Min.	Max.	I.	II.	III.	IV.	V.	VI.	VII.	VI.H	VI.He	VI.Htb		
Research octane number		95	-	-	-	-	-	-	-	-	-	-	-	-	-
Motor octane number		85	-	-	-	-	-	-	-	-	-	-	-	-	-
Vapour pressure, summer period	kPa	45	60	-	-	-	-	-	-	-	-	-	-	-	-
Density (15°C)	mg/cm ³	720	775	724	721	716	887	765	721	736	723	731	729		
Distillation															
Percentage evaporated at 70 °C	% (V/V)	20	48	50.77	52.04	35.03	0.00	27.28	41.00	24.75	24.42	21.98	23.27		
Percentage evaporated at 100 °C	% (V/V)	46	71	63.61	62.34	37.7	0.00	30.38	45.56	31.75	33.92	41.38	44.1		
Percentage evaporated at 150 °C	% (V/V)	75	-	91.88	91.31	99.01	100	95.38	96.14	96.35	80.18	82.16	83.15		
Residue above 210 °C	% (V/V)	-	2	0.38	0.54	0.24	0	0.24	0.7	0.34	0.57	0.51	0.49		
Hydrocarbon analysis															
Olefins	% (V/V)	-	18	70.51	70.65	75.28	0	46.06	63.85	48.6	0.62	0.59	0.53		
Aromatics	% (V/V)	-	35	1.13	1.5	0.29	100	31.21	0.73	0.97	3.67	0.87	0.82		
Benzene	% (V/V)	-	1	0.15	0.17	0.06	0	0.18	0.08	0.18	0.17	0.14	0.14		
Oxygen content	% (m/m)	-	3.7	-	-	-	-	-	-	-	-	3.33	3.23		
Oxygenates:															
Methanol	% (V/V)	-	3	<3	<3	<3	<3	<3	<3	<3	<3	<3	<3		
Ethanol	% (V/V)	-	10	<10	<10	<10	<10	<10	<10	<10	<10	10	<10		
Iso-propyl-alcohol	% (V/V)	-	12	<12	<12	<12	<12	<12	<12	<12	<12	<12	<12		
Tert-butyl-alcohol	% (V/V)	-	15	<15	<15	<15	<15	<15	<15	<15	<15	<15	15		
Iso-butyl-alcohol	% (V/V)	-	15	<15	<15	<15	<15	<15	<15	<15	<15	<15	<15		
Ethers containing five or more carbon atoms per molecule	% (V/V)	-	22	<22	<22	<22	<22	<22	<22	<22	<22	<22	<22		
Other oxygenates	% (V/V)	-	15	<15	<15	<15	<15	<15	<15	<15	<15	<15	<15		
Sulphur content	mg/kg	-	10	-	-	-	-	-	-	-	-	-	-		
Lead content	g/l	-	0.005	-	-	-	-	-	-	-	-	-	-		

The difference between the distillation curves of sample VI. and VI.H can be seen in Fig. 2. Additional distillation scenarios are also depicted as adding various alcohols to the gasoline in limited concentrations is enabled by the EN228 standard. For this reason, ethanol and tert-Butyl alcohol addition were investigated regarding the distillation properties of plastic waste fuel. Usually, these oxygenates are added to gasoline to increase the octane rating, but the oxygen content in the fuel provides more complete combustion as well, improving the emission properties of the engine [7].

In this case, adding alcohol to plastic fuel also helps to achieve the distillation requirements. As seen in Table 3, by adding ethanol to VI.H sample the percentage of evaporation till 100 °C increased to 41.4 Vol%, while the same in case of adding tert-Butyl alcohol is 44.1 Vol%. It is worth noting, that although these numbers do not fulfil the distillation properties, they are close enough to presumably reach the requirement by fine-tuning the operational parameters of pyrolysis and distillation steps.

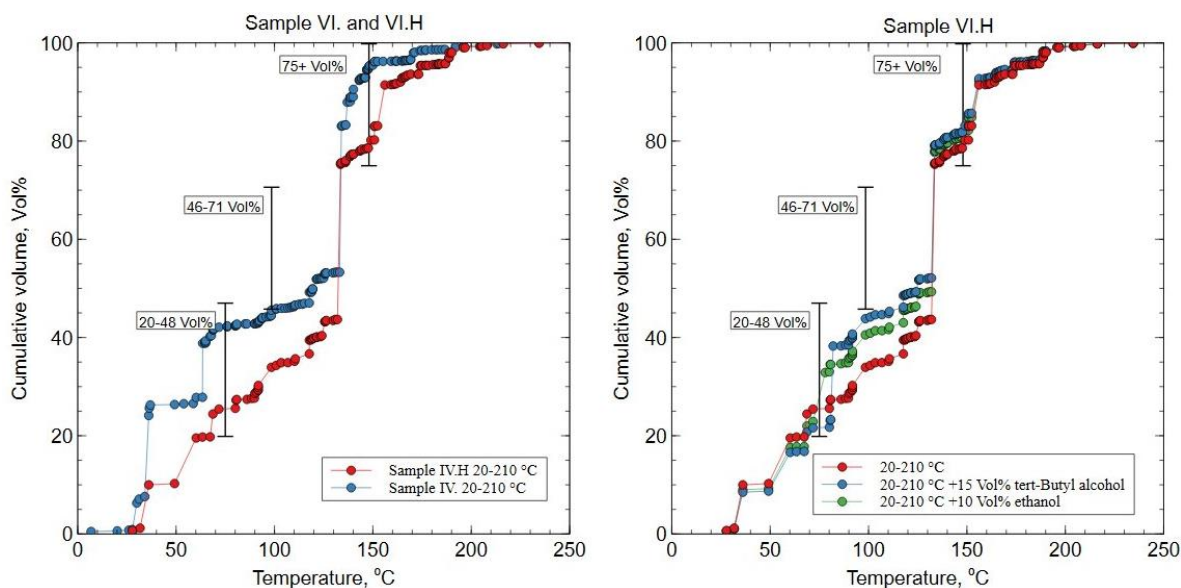


Figure 2. Distillation curves of sample VI., VI.H, and VI.H with ethanol and tert-Butyl alcohol additives.

4. CONCLUSIONS

The thermal degradation of high-density polyethylene (HDPE), low-density polyethylene (LDPE), polypropylene (PP), and their mixtures resulted in oils with high olefin content. In the case of pure polystyrene (PS) being pyrolyzed, the GC-MS analysis showed only aromatic compounds. Adding 20 wt% PS into the mixture, significant decrease could be observed in the olefin content. The experiments performed with Pd-based catalyst placed into the reflux and continuous hydrogen flow also showed a decrease in the olefin content, however in this case the oil yield, and especially the gasoline range hydrocarbon yield decreased as well. The olefin content disappeared almost entirely in the case of the separately hydrogenated gasoline fraction of sample VI. as it was converted to saturated hydrocarbons. Adding oxygenates, such as ethanol or tert-Butyl alcohol to gasoline fraction obtained from pyrolysis oils further improves the quality of plastic gasoline. These results suggest, that hydrotreatment and mixing alcohol to the gasoline is a potential pathway to improve the quality of gasoline fractions.

REFERENCES

- [1] E. Beckman, „THE CONVERSATION,” 03 12 2020. [Online]. Available: <https://theconversation.com/the-world-of-plastics-in-numbers-100291>.
- [2] H. Ritchie, „Our World in Data,” 02 09 2018. [Online]. Available: <https://ourworldindata.org/faq-on-plastics#what-are-the-environmental-impacts-of-landfills>. [07 12 2020].
- [3] R. Miandad, M. Barakat, M. Rehan, A. Aburizaiza, I. Ismail és A. Nizami, „Plastic waste to liquid oil

through catalytic pyrolysis using natural and synthetic zeolite catalysts,” *Waste Management*, 2017 .
<https://doi.org/10.1016/j.wasman.2017.08.032>

[4] „European Parliament Directive 2009/30/EC,” 2009.

[5] „Manufacturers, PlasticsEurope - Association of Plastics,” 2019. [Online]. Available:
https://www.plasticseurope.org/application/files/9715/7129/9584/FINAL_web_version_Plastics_the_facts2019_14102019.pdf. [03 12 2020].

[6] Z. Dobó, Z. Jakab, G. Nagy, T. Koós, K. Szemmelveisz és G. Muránszky, „Transportation fuel from plastic wastes: Production, purification and SI engine tests,” *Energy*, 2019.
<https://doi.org/10.1016/j.energy.2019.116353>

[7] F. Nadim, P. Zack, G. E. Hoag és S. Liu, „United States experience with gasoline additives,” *Energy Policy*, 29(1) 2001, 1-5. [https://doi.org/10.1016/S0301-4215\(00\)00099-9](https://doi.org/10.1016/S0301-4215(00)00099-9)

DEVELOPMENT OF IRON ORESSINTERING MACHINE FOR BLAST FURNACE PROCESS.

¹John Femi Akinfolarin, ²Buliaminu Kareem and ³Oladunni Oyetola Alabi

^{1,2} Department of Mechanical Engineering, Federal University of Technology Akure, PMB 704, Ondo State, Nigeria.

³ Department of Metallurgical and Materials Engineering, Federal University of Technology Akure, PMB 704, Ondo State, Nigeria, e-mail: jfakinfolarin@futa.edu.ng

ABSTRACT

There must be proper means to sinter and, agglomerated iron ore concentrate before it can be further processed in the blast furnace. A Sintering machine of 5kg capacity of agglomerated ore was designed and fabricated using mild steel material, which was locally sourced. The machine was fabricated with a combustion chamber of 30 by 30 cm and with 15cm depth. It was also lined with refractory material to reduce the chamber to the volume of 3375 cm³. However, the sintering chamber was designed to have a truncated square pyramid shape to the volume of 2150 cm³ after lining with refractory material. The design was made to utilize coke and palm kernel shell char as fuel which will be ignited to produce heat into the sintered material by suction of the heat into the agglomerated sintered ore. Tests such as tumbler index, abrasion, and porosity test were carried out on the sintered products in agreement with ASTM E276 and E389 standards. The results from the test gave a tumbler index of 70.2% and 65.7% for coke and palm kernel shells respectively. Also, abrasion index of 5.1% and 4.6% for coke and palm kernel char, and porosity of 6.8% and 6.5% for coke and palm kernel char respectively. The results from the experimental test were in agreement with other research work. Therefore, the developed iron ore sintering machine has a better efficiency of producing sinter for blast furnace operation.

Keywords: sintering system, coke, palm kernel char, test for quality of the sinters.

1. INTRODUCTION

A large number of iron ore fines was processed to supply high-quality sinters for the smooth running of blast furnaces for the production of steel. Since iron ore fine cannot be charged directly into the blast furnace, there is a need for further processing known as the agglomeration process and this process was classified into briquette, nodulization, sintering, pelleting, and vacuum extrusion process [1]. Among the listed processes for agglomeration of iron ores, a sintering technique will be required for this process, which is the process iron ore fines were agglomerated into a porous and lumpy mass by the introduction of heat produced from solid fuel known as coke [2]. More so, a lot of research had been done on this work with different modes of operation, the size of the machine, and the fuelling of the machine.

The Sintering process was invented as far back 1887 to sinter sulphide ores placed in a cylindrical container (pot sintering method) with the sintering bed being fired with dried wood and with firing operation which is from up with the aids of the burner from the top of the sintering machine and also blown with air from the bottom upwards (3). A Stationary sintering pot machine was invented with the application of pressure in the sinter pot test flow sheet and the material in the pot was ignited using liquefied petroleum gas (LPG) (4). Dwight-Lloyd system has a sintering grate which is the continuous chain of large length and width formed by the union of a series of pallet cars that make the sinter strand [7].

Machine design is the art of creating and developing a brand new or improving on an existing machine for meeting human needs or purposes [6, 8]. Also, design is an innovative, decision making and problem-solving process involving scientific knowledge. Designers generate concepts and decide dimensions for devices or products from little or little information [8].

Manufacturing is derived from the Latin word manufactures means made by hand. It involves bringing or making products out from raw material by using a different method of manufacturing processes that involve, making use of hand tools, machinery, or even computers. Therefore, it is the study of the processes required to make parts and to assemble them in machines. However, manufacturing in the area of application to engineering industries, shows how solutions can be provided to different problems related to the development of various machines produced by studying the physical, chemical, and other laws governing the manufacturing process (9).

Therefore, manufacturing technology techniques are very important in modern-day industries where machines, tools, and equipment are produced from raw or basic materials with the use of manufacturing technique process (10). Manufacturing processes can be classified into the following methods such as machining processes, casting processes powder processes, joining processes, deformation processes, heat treatment, and surface treatment processes, assembly processes, inspection and certification, packaging, warehousing, and forwarding processing (10).

However, the conceptualization and the design of iron ores sintering machine for the production of sinters for small-scale iron ore sinters producer for the smooth running of blast furnace using locally sourced materials for the production of sintering machine. More so, the machine will be designed in such a way that will accommodate any form of fuel for sintering operations and the performance of the design machine was then compared with other works.

2. MATERIALS AND METHODS

Development of sintering machine using a suction mechanism

The system was developed to produce sinters for Blast furnace processing from their deposit, using locally sourced materials for the fabrication. Design conditions were considered in the development of the Iron ores sintering system this includes:

1. The weight, melting temperature, Density, chemical composition, capacity, and quantity of the iron ore and coke in the sintering chamber for effective sintering.
2. For easy assembling and dismantling of the machine with the use of locally sourced material to enhance the possibility of replacing damaged parts with less expensive ones but equivalently satisfactory available spare – parts.
3. The strength, durability, and corrosion resistance of the selected materials. Also, the safety of the operator, production cost, and reliability of the machine without compromising for efficiency was considered.

2.1. Material Selection

The knowledge of materials selection, properties, and availability of the materials selected play a key role in the choice of different fabricated machine components or parts. The selected materials satisfy the design requirement and operation conductions of the machine. The table below shows the materials selection, criteria, and reason for the selection.

S/N	Components	Suitable Engineering Materials	Criteria for Material Selection	Material Selected	Remarks
1	Hoppers (Combustion and sintering chamber)	Mild steel, galvanized steel, high speed steel, cast iron, stainless steel sheet	Strength, workability, lightness, cost	Mild steel	Strength and Workability.
2	Screen/Sieve	Mild steel, galvanized steel, high speed steel, stainless steel sheet	Strength, ductility, corrosion resistance, workability, lightness, cost	Stainless steel	Strength, ductility and corrosion resistance.
3.	Bolt and nut	Mild steel, galvanized steel, high speed steel, cast iron, stainless steel	Strength, corrosion resistance, workability, lightness, and cost	Mild steel	Strength, rigidity.
4	Screw	Mild steel, galvanized steel, steel, cast iron, stainless steel	Strength, corrosion resistance, workability, lightness, and cost	Mild steel	Strength, rigidity.
5	Suction fan	Aluminum, Cast iron, stainless steel.	Strength, corrosion resistance, workability, lightness, and cost	Aluminum	Strength, corrosion resistance, Lightness, Heat resistance
6	Switch	Stainless steel button and plastic button	Strength, corrosion resistance and light.	Plastics button switch	Corrosion resistance.
7	Refractories	Clay, silica sand with additives	Heat resistance, light.	Clay	Heat resistance.

2.2. Equations for designing the Machine

Machine Description

The fabricated sintering system consists of four major units which are combustion chamber, sintering chamber, suction fan compartment, and chimney (Air Duct).

1. Combustion chamber

The combustion chamber which was placed on the sintering chamber is made of mild steel, the combustion chamber accommodates the fuel (coke) which was the source of heat for sintering of Iron ore and the chamber was lagged with locally sourced refractory clay to prevent heat loss from the chamber. The volume of the combustion chamber was calculated using the equation below:

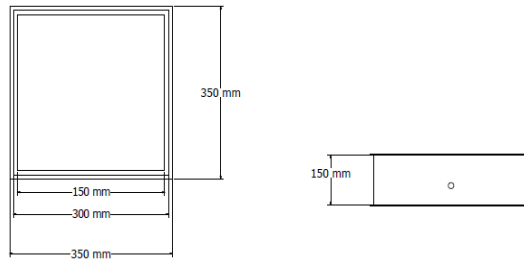


Figure 1: Combustion Chamber

$$AB = AC = BD = CD$$

Where AB = CD represents the whole sides of the cubic respectively.

$$\begin{aligned} V_{cc} &= (L \times W \times H) \\ &= (150 \times 150 \times 150) \\ &= 3375000 \text{ mm}^3 \text{ or } 3375 \text{ cm}^3 \end{aligned} \tag{1}$$

Where V_{cc} is the volume of the combustion chamber, L is the length of the combustion chamber, W is the width of the combustion chamber, H is the height of the combustion.

The combustion and sintering chamber has a cubic shape and truncated square pyramid. Therefore, the volume calculated as follows;

The thickness of the lining of the shell was 75 mm was considered in the calculation. The mass of coke used, and the density of coke was essential to be known as the quantities of coke required for iron ore sintering. The coke density is 0.9g/cm^3 , and the calculated volume of the chamber is 3375 cm^3 .

$$\begin{aligned} M_c &= D_c \times V_{cc} \\ &= 0.9 \times 3375 \\ &= 3037.5 \text{ g or } 3.0375 \text{ Kg} \end{aligned} \tag{2}$$

Hence, 3 kg of coke used to sinter Iron ore

Where M_c is the mass of coke, D_c is the density of coke, V_{cc} is the volume of the combustion chamber.

2. Sintering Chamber

The sintering chamber is under the combustion chamber that accommodates the Iron ore for sintering. The sintering chamber is lagged to prevent heat loss from chamber because heat is needed for the sintering of Iron ore. The volume of the sintering chamber was calculated.

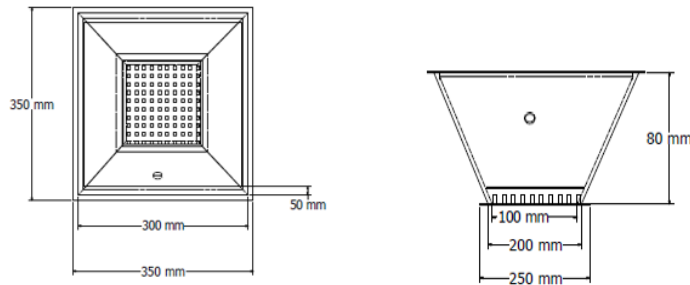


Figure 2: Sintering Chamber

$$\begin{aligned}
 V_s &= \frac{1}{3} (A^2 + AB + B^2)H & (3) \\
 &= \frac{1}{3} ((20)^2 + ((20)(10) + (10)^2)8 \\
 &= 1866700 \text{ mm}^3 \text{ or } 1866.7 \text{ Cm}^3
 \end{aligned}$$

The mass of iron ore needed also calculated using the density of iron ore which is 2.5g/cm³, and the volume of the sintering chamber calculated was 1866.7 Cm³

$$\begin{aligned}
 M_f &= (D_f \times V_s) & (4) \\
 &= 2.5 \times 1866.7 \\
 &= 4666.75 \text{ g or } 4.66675\text{kg}
 \end{aligned}$$

Calculation of Efficiency of the Sintering Machine produced

According to the Bureau of Energy Efficiency (2005), the efficiency of coke used for sintering machine can be judged by measuring the amount of fuel needed.

$$Z = \frac{Q}{D} \quad (5)$$

Z = Thermal Efficiency of sintering

Q = Heat Output

D = Heat in the fuel consumed for sintering the iron ore (Heat input)

Quantity of heat imparted (Q) (heat output) on the Iron ore can be found from

$$Q = M \times C_p (t_1 - t_2) \text{ where}$$

Q = Quantity of heat of Iron ore in k Cal.

M = Weight of Iron ore in kg

C_p = Mean specific heat of Iron ore in k Cal/kg °C

t₁ = Final temperature of Iron ore desired, °C

t₂ = Initial temperature of the Iron ore before it enters the furnace, °C

Mean specific heat of Iron ore = 0.108k Cal/kg °C

Total mass of the Iron ore (Sintering Machine) = 5kg

Total mass of coke fuel for sintering 5kg of iron ore =3kg

$t_1 = 1350^{\circ}\text{C}$

$t_2 = 35^{\circ}\text{C}$

Density of coke = $0.9\text{g}/\text{Cm}^3$

Gross calorific value (GCV) of coke = 7481.72 KCal/kg

Heat output = $MC_p(t_1 - t_2) = 3 \times 0.108 \times (1350 - 35) = 427.68 \text{ KCal}$

To calculate the Efficiency of the sintering machine by using equation 3.5 above

$$Z = \frac{Q}{D} \times 100$$

Heat in the fuel consumed for sintering the iron ore (heat input) = $3 \times 7481.72 = 22445.16$

Total of fuel needed.

$$Z = \frac{427.68 \times 100}{22445.16} = 1.91\%$$

The efficiency of 1.91% of the heat generated by the coke fuel was able to sinter the iron ore in the sintering chamber.

The Engineering drawings for Iron ore Sintering Machine

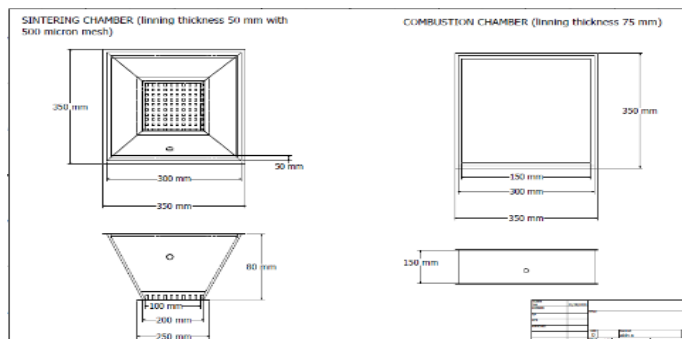


Figure 3: The Front and Plan View of the Sintering and Combustion Chamber.

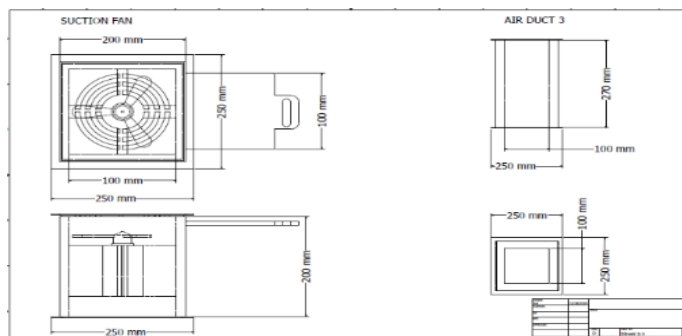


Figure 4: The Front and Plan View of the Suction Fan Compartment.

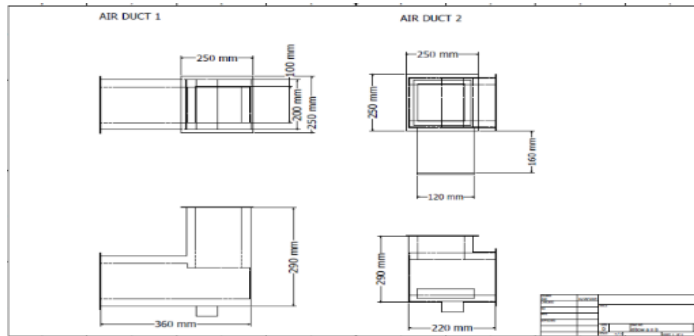


Figure 5: The Front and Plan View of the Air duct (Chimney).

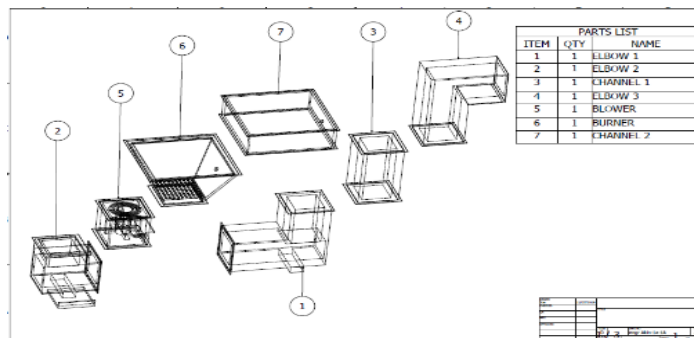


Figure 6: The Exploded Diagrams.

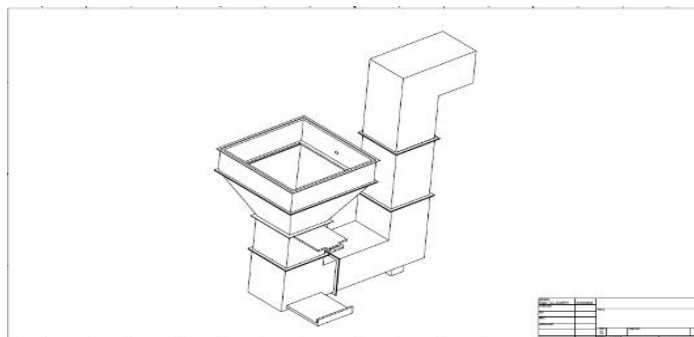







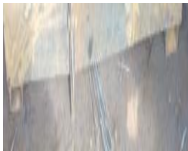
Figure 7: The Isometric Drawing of Sintering

Fabrication Processes and Assembling System

The fabrication of the Iron ore sintering system was carried out using the engineering drawing, various manufacturing processes and tools available that was suitable for each component of the machine.

The fabricated machine parts were joined together with the aid of an electric arc welding machine and assembly using suitable bolts and nuts.

Table 2: Manufacturing Processes and Tool Used.

S/N	Components	Material Used	Manufacturing Process	Tools Used
1	Combustion Chamber 	Mild Steel	Cutting, Welding and Grinding	Electric Arc Welding Machine, Hack Saw And Grinding Machine.
2	Sintering Chamber 	Mild Steel	Cutting, Welding and Grinding	Electric Arc Welding Machine, Hack Saw And Grinding Machine.
3	Suction Compartment Fan 	Mild Steel	Cutting, Welding and Grinding	Electric Arc Welding Machine, Hack Saw And Grinding Machine.
4	Chimney 	Mild Steel	Cutting, Welding and Grinding	Electric Arc Welding Machine, Hack Saw And Grinding Machine.
5	Flange 	Mild Steel (Angle Bar)	Cutting, Welding and Grinding	Electric Arc Welding Machine, Hack Saw And Grinding Machine.
6	Machine Base 	Mild Steel (Square Pipe)	Cutting, Welding and Grinding	Electric Arc Welding Machine, Hack Saw And Grinding Machine.



7	<p>Lining Material</p> 	Refractory Clay	Ramming Process	Shovel, Rammer and Hand Trowel
8	<p>Assembled Machine</p> 	Mild Steel	Bolts and Nuts, Electric Arc Welding	Electric Arc Welding, Set of Spanner, Paint and Brush.



Figure 8: Fabrication of the Iron Ore Sintering System.

The principle of Operation of the Iron Ore Sintering System

The design concept of the Iron Ore Sintering System is on the principle of heat transfer by conduction. The heat was transferred from one medium to another, and the heat transferred was used to sinter the Iron ore by suction mechanism with the aid of suction fan and the lining of the system only minimize the rate of heat loss to the environment.

Recommended Maintenance practice

The system should be properly used as specified by the designer, routine maintenance should be carried out on the system, the bolts and nuts should be lubricated to prevent rusting, the electrical part of the suction fan should be checked from time to time and the lining refractory lining should be checked after been used for sometimes.

Performance Evaluation

The Iron ore sintering system has the capacity of 5Kg with two compartments which are the combustion chamber and sintering chamber. Mesh of 500 micron size aperture was placed at the base of the sintering chamber, thereafter 5Kg of iron ores of 75 micron size with $\frac{1}{4}$ of limestone (fluxing agent) of 75 micron size added to the Iron ore and mixed together thoroughly with the addition of 6 – 8% of water (as binder) and loaded into the sintering machine and 3Kg of coke was also arranged on the iron ores and the coke was

ignited with fire and the suction fan of 1 horse power (HP) with 1350 revolution per minute (RPM) was switched on to suck in air and the fire from combustion zone was progressing downward to the iron ores due to air flow through permeable bed, while thermocouple attached to sintering chamber read temperature of 1350°C which is the melting point of iron ore. The entire mass of the material was converted to porous and strong sinter. The produced sinter was allowed to cool down, crushed and screened to the recommended particle size. The undersize sinter was also recycled back to the sintering machine.

3. RESULTS AND DISCUSSION

1. Tumbler Index

Table 3:1 The result of the Tumbler Index Test using coke as source of heat.

Weight of sinter product			
	A	B	C
Initial weight of sinter	1000	1000	1000
Retained weight of sinter at +6.3mm	673	700	733
% Tumbler Index	67.3%	70%	73.3%

$$\text{Average Tumbler Index} = \frac{67.3 + 70 + 73.3}{3} = 70.2\% \quad (6)$$

Table 3:2 The result of the Tumbler Index Test using palm kernel char as source of heat

Weight of sinter product			
	A	B	C
Initial weight of sinter	1000	1000	1000
Retained weight of sinter at +6.3mm	653	657	660
% Tumbler Index	65.3%	65.7%	66.0%

$$\text{Average Tumbler Index} = \frac{63.3 + 65.7 + 66.0}{3} = 65.7\% \quad (7)$$

2. Abrasion Index

Table 3:3 The result of the Abrasion Index Test using coke as source of heat.

Weight of sinter product			
	A	B	C
Initial weight of sinter	1000	1000	1000
Retained weight of sinter at - 0.5mm	47	52	55
% Abrasion Index	4.7%	5.2%	5.5%

$$\text{Average Abrasion Index} = \frac{4.7 + 5.2 + 5.5}{3} = 5.1\% \quad (8)$$

Table 3:4 The result of the Abrasion Index Test using palm kernel char as source of heat.

Weight of sinter product			
	A	B	C
Initial weight of sinter	1000	1000	1000
Retained weight of sinter at -0.5mm	40	47	52
% Abrasion Index	4.0%	4.7%	5.2%

$$\text{Average Abrasion Index} = \frac{4.0+4.7+5.2}{3} = 4.6\% \tag{9}$$

3. Porosity

Table 3:5 The result of the porosity Test using coke as source of heat.

Weight of sinter product			
	A	B	C
Initial weight of sinter	112	110	115
Soaked weight of sinter	120	116	124
Different in weight	8	6	9
% porosity	7.1%	5.4%	7.8%

$$\text{Average Porosity} = \frac{7.1+5.4+7.8}{3} = 6.77\% \tag{10}$$

Table 3:6 The result of the porosity Test using palm kernel char as source of heat.

Weight of sinter product			
	A	B	C
Initial weight of sinter	90	112	110
Soaked weight of sinter	96	118	118
Different in weight	6	6	8
% porosity	6.7%	5.4%	7.3%

$$\text{Average Porosity} = \frac{6.7+5.4+7.3}{3} = 6.5\% \tag{11}$$

The tumbler index range percentage of 88wt% -93wt% was significantly higher than the stipulated between 60-70 wt.%. For the use of coke and palm kernel char to sinter, the result obtained for the tumbler test was at the rate of 70.2% and 65.7%, were by stipulated results. As the abrasion index of sinter fall between the range of 0.54 - 3.41wt% term to be lower than the acceptable abrasion limit (5wt%), the abrasion index test result has 5.1% and 4.6% using the same fuel as a source of heat respectively, (2). The porosity test was in the range of 5.1% to 9.82% exhibits quality sinter. Therefore, the result from the sintering process using coke and palm kernel char as a fuel shows the results of porosity 6.77% and 6.5%(9). With these results gathered, the sinter can be handled, loaded, and transported without disintegration to a small particle. However, the developed iron ores sintering machine has better efficiency of producing sinter for blast furnace operation.

4. CONCLUSIONS

In this study, development of iron ores sintering system for blast furnace process was successfully achieved. However, the possibility of producing sinters for blast furnace feeding was attained by designing, fabricating and tested to determine the performance evaluation of the machine and its effectiveness. In this work, coke and palm kernel char were used as a source of fuel in the sintering process, as tumbler index, abrasion index, and porosity test of the sinters product were evaluated. The result of Tumbler Index using coke and palm kernel char as a source of fuel were 70.2% and 65.7% respectively. Moreover, the abrasion index test result using the same source of fuel for the sintering process was achieved at a rate of 5.1% and 4.6% respectively. The best significance porosity result test was also attained at the level of 6.77% and 6.5% respectively. However, the performance evaluation results obtained from this research work were compared with other similar work done by other researchers. The comparison of the result showed that the sinters product were of good quality. The machine was developed and fabricated from locally sourced materials which make it cheaper and affordable for both small and medium scale for miners in local areas. However, the developed iron ore sintering machine is about 99% cheaper in price as compared to imported iron ore sintering machine. Finally, this machine requires little or no expertise or training for its operation and maintenance.

The machine for sintering Iron ore was successfully developed to produce quality sinters with the use of coke and palm kernel char as source of heat for the sintering of the iron ore with a reduced cost. However, the further research work can also be carried out in the area of using charcoal and other Agro-waste materials as source of heat, instead of making use of Liquefied Petroleum Gas (LPG), Diesel Burner and Blower.

REFERENCES

- [1]. Abhishek. M., (2015): "Sintering of Iron Ore". Project and Seminar Pp 5 – 6.
- [2]. Abraham. J.B.M., Andrey. V.K., Joseph. K.B., and Par. G.J., (2012): "Characterisation of the physical and metallurgical properties of Natural Iron Ore for Production", ISRN Material Science, Vol 2012, Pp 1 – 2.
- [3]. Ajaka. E. O., Adesina. A. E., and Lawal A. I., (2015): "Determination of the Optimum Conditions for Beneficiation of Selected Nigerian Iron Ores using Shaking Table". Annals of Faculty Engineering Hundoara, International Journal of Engineering, Pp 207.
- [4]. Arikata. Y., Yamamoto. K., and Sassa. Y., (2013): "Effect of Coke Breeze Addition Timing on Sintering Operation." ISIJ International, 53, Pp. 1523–1528
- [5]. Cores. A., Verdeja. I. F., Ferreira. S., Ruiz-Bustinza. I., and Mochón. J., (2013): "Iron Ore Sintering. Part I. Theory and Practice of the Sintering Process." DYNA Colombia, 80, Pp. 152–171.
- [6]. De la Torre. L., (2011): Natural Resources Sustainability: Iron Ore Mining. DYNA, Vol. 78, Pp. 227-234,
- [7]. Fernandez-Gonzalez. D.R, Ruiz- Bustinza. I, Mochon. J, Gonzalez-Casca. C, and Verdeja, L.F., (2017): "Iron Ore Sintering: Raw Materials and Granulation". Mineral Processing and Extractive Metallurgy Review 38, Pp. 36 – 46.
- [8]. Legemza. J., Fröhlichová. M., Findorák. R., Bakaj. F., (2010): The thermovision measurement of temperature in the iron-oresintering process with the biomass, Acta Metallurgica Slovaca1, 70-75.
- [9]. Ma. X., Bruckard. W. J., Holmes. R. J., (2009): Effect of collector,pH and ionic strength on the cationic flotation of kaolinite, International Journal of Mineral Processing 93, 54-58.

INVESTIGATION OF LAYER HEIGHT INFLUENCING THE IMPACT STRENGTH OF POLYLACTIC ACID (PLA)

József Richárd Lennert, József Sárosi

Faculty of Engineering, University of Szeged, Mars tér 7. 6724, Szeged, Hungary
e-mail: sarosi@mk.u-szeged.hu

ABSTRACT

The aim of this study is to investigate the effect of layer height used during 3D printing on the impact strength, their standard deviations, and the printing time by using UNI EN ISO 180 unnotched specimens manufactured by FDM 3D printing technology. Every specimen is made of PLA, which is the most basic material of the FDM printing technology by using the same 3D printer. In this study it plays a key role to find out whether the layer height can be used to optimize the researched mechanical property within an economical framework or not. What is more, the possibly observable tendencies and crucial influential parameters will be analysed as well.

Keywords: PLA, 3D printing, layer height, additive manufacturing, impact strength

1. INTRODUCTION

The additive manufacturing, which is often mentioned as 3D printing, is one of the most dynamic and intensive developing manufacturing technologies. 3D printing has many different types just like FDM (Fused Deposition Modelling), SLS (Selective Laser Sintering), and SLA (Stereolithography) [1], [2]. Besides, the 3D printers used to print different types of plastics. However, nowadays there are printers which are suitable to print different types of materials such as metals, ceramics, composites, concretes, and even biomaterials can be printed [2]. It must be mentioned that 3D printers using materials different from plastic are used mostly for industrial and scientific purpose hence both the 3D printers and the 3D printing provided by the companies are too expensive for the average consumers. Among the 3D printers, which are appropriate to print different types of plastics, the 3D printers using FDM technology are one of the most common and the cheapest ones [3]. Out of the many advantages of 3D printing, the most important one is that almost any kind of complex shapes can be created by using this technology hence it creates the object layer by layer. Therefore, zero or almost zero waste is produced during the process making this technology extraordinarily favourable from the point of view of a waste management. There are a lot of factors affecting 3D printing, but their effect on the mechanical properties is often not properly known for us. This will not cause any problems if the product is a prototype or is produced for a purpose in which it is not exposed to any kind of mechanical impacts.

However, the effects of the printing parameters on the mechanical properties become a key factor if the 3D printed product is any kind of replacement part.

Thanks to the industrial spread of this technology, more and more scientific articles are published in connection with the effect of printing parameters on the mechanical properties during the last few years. Most of these scientific articles investigate their effects on tensile strength or yield strength [3], [4], [5]. Nevertheless, there are articles examining the printing parameters' effects on the impact strength [6], [7]. These articles concerning the impact strength are mainly related to notched specimens due to the drastic impact strength reduction caused by the stress collector place on the object. In several studies, the effect of infill pattern, infill density, printing temperature, printing direction, layer height, print speed or other parameters on the impact strength was analysed [8], [9]. In every study it was proven that the examined mechanical properties were influenced by the parameters used during the printing, but the degree of influence was different relating to every single parameter [10].

2. MATERIALS AND METHODS

The Polylactic acid or PLA is a biodegradable, rigid thermoplastic produced mostly from different types of grains containing a huge amount of starch. In 3D printing, PLA is one of the most common materials especially for hobby hence it has not only a reasonable price, but it can be printed easily without a special printing area. For this reason, it is very easy to work with it without any experience in 3D printing. This material is used especially for producing disposable products over and above in 3D printing, to create prototypes and a huge variety of hobby products. Due to its biodegradability, PLA is extremely advantageous in terms of waste management. It is important to mention that the research made in different scientific areas pointed out that 3D printed PLA could be often a better choice than traditional technical plastics such as ABS [11].

Thanks to the development of 3D printing technology, more and more special PLA is available on the market meaning that there can be a huge difference among the mechanical properties of the PLA filaments produced by different companies. Even ABS-like and flexible PLA can be found.

For the measurements, a Galdabini Impact 25 impact testing machine (Figure 1) was used. This precision measuring instrument makes it possible to measure to two decimal places and it gives the impact strength immediately in kJ/m^2 if a standard specimen known by the machine is used preventing the faults caused by the calculation and reading errors and saving time.

This measuring instrument has only a 5 J hammer making it impossible to measure plastics specimen with higher impact strength. Despite the incorrect values caused by the low measuring limit, it is ideal to measure plastics like PLA. For the proper measurement of technical plastics like ABS, a bigger hammer would be necessary.



Figure 1. Galdabini Impact 25 impact testing machine

For the measurement UNI EN ISO 180 standard unnotched specimens were used (Figure 2), whose dimensions are $80 \times 10 \times 4$ mm. This type of specimens was chosen, because it is known by the Galdabini Impact 25 impact testing machine making the work more precise and faster. The unnotched type was chosen because the manufacturers test their material by using notched specimens. Nevertheless, in some cases, there is no stress collector on the product causing oversizing and unnecessary material usage if the impact strength measured on notched specimens is used for the designing. The proper impact strength value is especially important in cases when it is the key sizing aspect of the product. In most scientific articles about impact strength, notched specimens were used giving another reason to use unnotched specimens for this research.

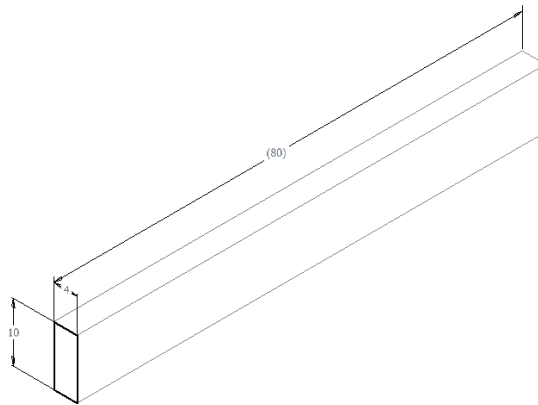


Figure 2. The model of specimen used for the measurements

The measurements were done in every case at room temperature to make possible comparisons of the results in the future. Before the measuring process every specimen was kept under such circumstances for a minimum time of 24 hours. During the measuring process, the specimen supported at both ends was hit in the middle by the hammer of the Charpy breaking the specimens and making it possible to determine the value of impact strength correctly.

The essential Gcodes for the printing were created by the software Ultimaker Cura 4.4 allowing the modification of a huge amount of 3D printing parameters. The Gcodes with different layer height were made by using this software.

The 3D printed PLA specimens were produced by using a Creality CR-10S Pro V2 3D printer. This printer provides a very reliable printing due to its built-in filament break detection module and self-levelling. Due to its excellent printing quality and favourable price, this 3D printer is one of the best middle class FDM printers on the market.

For the printing, 3DJake EcoPLA was used with a printing temperature of 200 °C, and a build plate temperature of 50 °C. The specimens were printed on their 10×80 mm side and an infill density of 100% was used.

3. RESULTS

3.1. Printing time

Printing time is one of the most crucial features of 3D printing, because in most cases it determines the price of printing and that is why the number of products could be produced with this technology economically. The printing time is affected by many factors just like the impact strength. One of these aspects is the layer height (Figure 3). It can be easily established, that the reduction of layer height increases the printing time drastically.

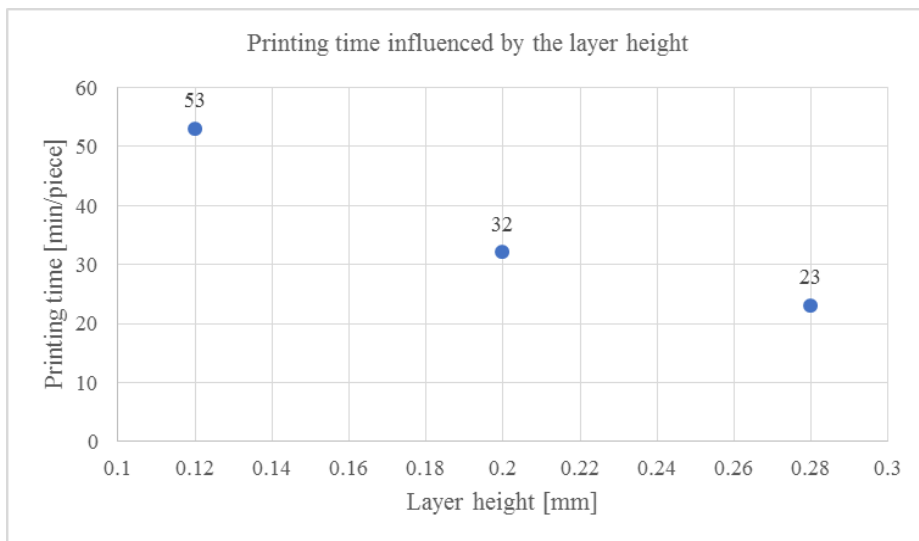


Figure 3. Printing time influenced by the layer height

3.2. The layer height's effect on the impact strength

The layer height used during the printing is one of the key parameters in FDM 3D printing technology. By using lower layer height, a finer surface can be reached, but it causes the increment of printing time thus the product will be made of more layers on the same speed that is why FDM technology is not economical under a certain layer height.

In this study 0,12 mm (Figure 4, Table 1), 0,2 mm (Figure 5, Table 2) and 0,28 mm (Figure 6, Table 3) layer heights were examined. The layer heights used during the study were chosen with the help of the Ultimaker Cura 4.4 slicer program. In this slicer program the default layer height is 0,2 mm, while the default steps to increase and reduce layer height is 0,08 mm.

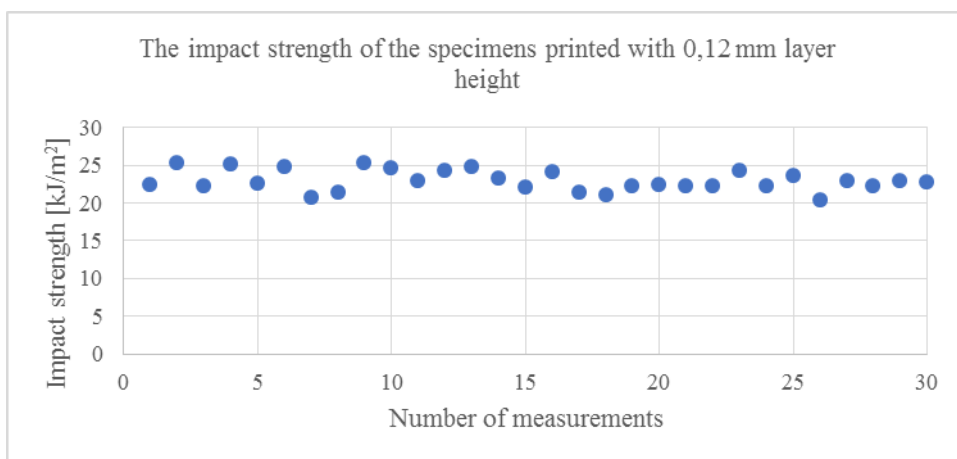


Figure 4. The impact strength of the specimens printed with 0,12 mm layer height

Table 1. The results of specimens printed with 0,12 mm layer height

The results of specimens printed with 0,12 mm layer height [kJ/m ²]					
PLA-L012-1	22,33	PLA-L012-11	22,94	PLA-L012-21	22,22
PLA-L012-2	25,21	PLA-L012-12	24,17	PLA-L012-22	22,22
PLA-L012-3	22,12	PLA-L012-13	24,69	PLA-L012-23	24,17
PLA-L012-4	25,1	PLA-L012-14	23,24	PLA-L012-24	22,22
PLA-L012-5	22,53	PLA-L012-15	22,02	PLA-L012-25	23,55
PLA-L012-6	24,69	PLA-L012-16	24,07	PLA-L012-26	20,32
PLA-L012-7	20,61	PLA-L012-17	21,32	PLA-L012-27	22,83
PLA-L012-8	21,32	PLA-L012-18	21,01	PLA-L012-28	22,12
PLA-L012-9	25,21	PLA-L012-19	22,22	PLA-L012-29	22,83
PLA-L012-10	24,58	PLA-L012-20	22,43	PLA-L012-30	22,73

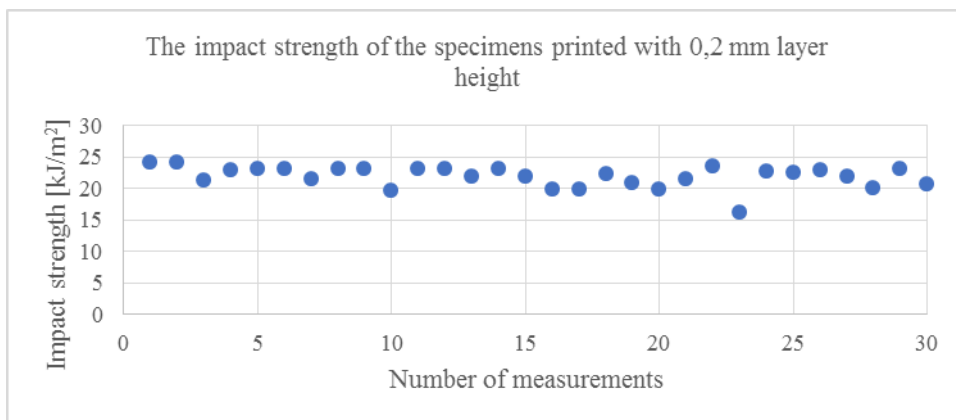


Figure 5. The impact strength of the specimens printed with 0,2 mm layer height

Table 2. The results of specimens printed with 0,2 mm layer height

The results of specimens printed with 0,2 mm layer height [kJ/m ²]					
PLA-S10×80-1	24,13	PLA-S10×80-11	23,14	PLA-S10×80-21	21,52
PLA-S10×80-2	24,17	PLA-S10×80-12	23,14	PLA-S10×80-22	23,45
PLA-S10×80-3	21,32	PLA-S10×80-13	21,92	PLA-S10×80-23	16,24
PLA-S10×80-4	22,83	PLA-S10×80-14	23,14	PLA-S10×80-24	22,63
PLA-S10×80-5	23,04	PLA-S10×80-15	21,81	PLA-S10×80-25	22,53
PLA-S10×80-6	23,14	PLA-S10×80-16	19,82	PLA-S10×80-26	22,94
PLA-S10×80-7	21,42	PLA-S10×80-17	19,82	PLA-S10×80-27	21,82
PLA-S10×80-8	23,14	PLA-S10×80-18	22,22	PLA-S10×80-28	20,12
PLA-S10×80-9	23,14	PLA-S10×80-19	20,81	PLA-S10×80-29	23,14
PLA-S10×80-10	19,62	PLA-S10×80-20	19,72	PLA-S10×80-30	20,71

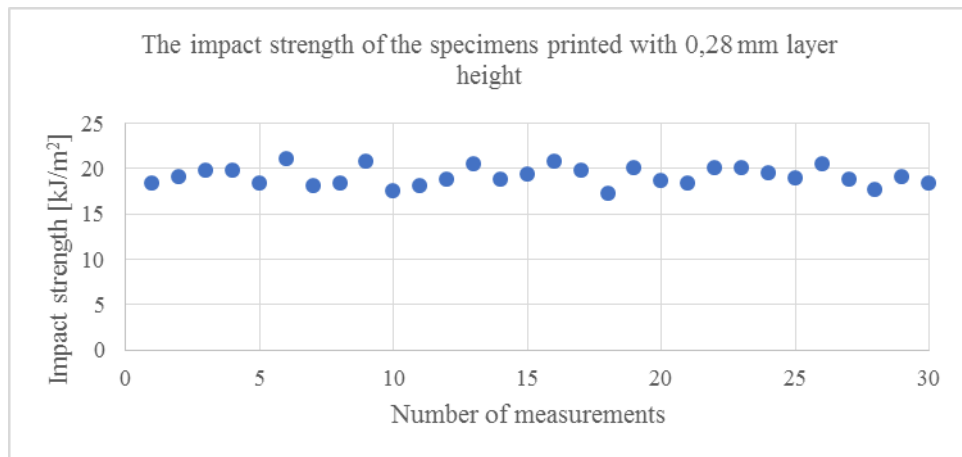


Figure 6. The impact strength of the specimens printed with 0,28 mm layer height

Table 3. The results of specimens printed with 0,28 mm layer height

The results of specimens printed with 0,28 mm layer height [kJ/m ²]					
PLA-L028-1	24,13	PLA-L028-11	23,14	PLA-L028-21	21,52
PLA-L028-2	24,17	PLA-L028-12	23,14	PLA-L028-22	23,45
PLA-L028-3	21,32	PLA-L028-13	21,92	PLA-L028-23	16,24
PLA-L028-4	22,83	PLA-L028-14	23,14	PLA-L028-24	22,63
PLA-L028-5	23,04	PLA-L028-15	21,81	PLA-L028-25	22,53
PLA-L028-6	23,14	PLA-L028-16	19,82	PLA-L028-26	22,94
PLA-L028-7	21,42	PLA-L028-17	19,82	PLA-L028-27	21,82
PLA-L028-8	23,14	PLA-L028-18	22,22	PLA-L028-28	20,12
PLA-L028-9	23,14	PLA-L028-19	20,81	PLA-L028-29	23,14
PLA-L028-10	19,62	PLA-L028-20	19,72	PLA-L028-30	20,71

Based on the previous results, it can be easily noticed that the layer height used during the printing process influences the impact strength of the product (Figure 7). The lower the layer height was, the higher impact strength was measured. However, as it was shown before in this study, at the printing time the reduction of layer height increases the printing time drastically. That is why it is important to decide whether it is worth increasing the impact strength a little bit this way, while the printing time increases dramatically.

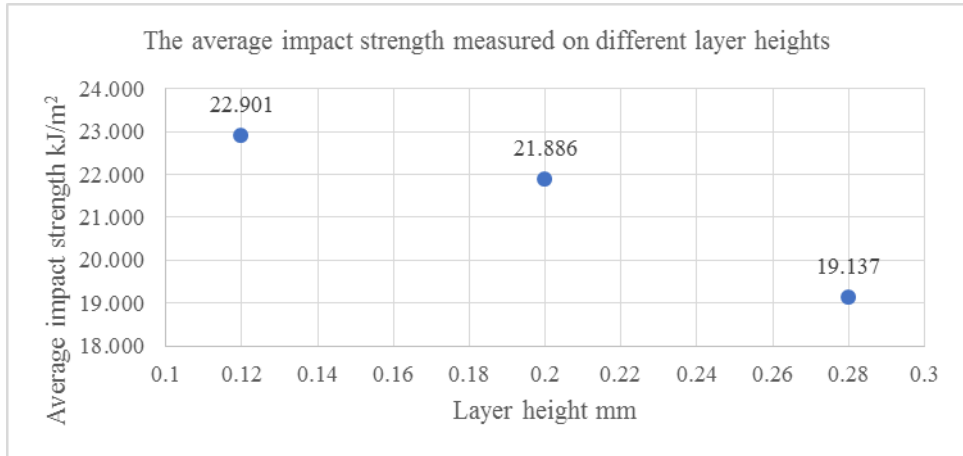


Figure 7. The average impact strength measured on different layer heights

The layer height used during printing processes influences the standard deviation of the impact strength just a little bit, which can be seen on Figure 8.

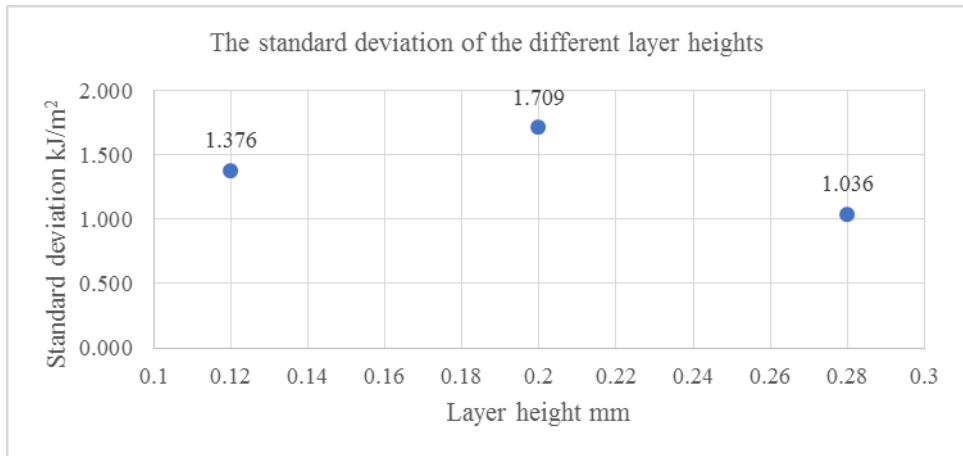


Figure 8. The standard deviation of the different layer heights

4. CONCLUSIONS

Based on the measurement results, it can be determined that the layer height influences the impact strength and a tendency can be noticed showing that the increment of layer height decreases both the impact strength and the printing time. However, it must be mentioned that the layer height effects the printing time much better than the impact strength therefore this parameter is not suitable to increase the impact strength economically. In the case of standard deviation, no tendency can be noticed, but it must be mentioned that the default layer height has the highest and the 0,28 mm layer height has the lowest standard deviation, which can mean that a possible tendency can be found via investigating more layer heights.

REFERENCES

- [1] J. R. C. Dizon, A. H. Espera Jr., Q. Chena, R. C. Advincula, Mechanical Characterization of 3D-printed Polymers, *Additive Manufacturing*, Vol. 20, 2018, pp. 44-67
<https://doi.org/10.1016/j.addma.2017.12.002>
- [2] N. Shahrubudin, T. C. Lee, R. Ramlan, An Overview on 3D Printing Technology: Technological, Materials, and Applications, *Procedia Manufacturing*, Vol. 35, 2019, pp. 1286-1296
<https://doi.org/10.1016/j.promfg.2019.06.089>
- [3] G. Ćwikła, C. Grabowik, K. Kalinowski, I. Paprocka, P. Ociepka, The Influence of Printing Parameters on Selected Mechanical properties of FDM/FFF 3D-printed Parts, *IOP Conference Series: Materials Science and Engineering*, Vol. 227, 2017, pp. 1-10
<https://doi.org/10.1088/1757-899X/227/1/012033>
- [4] A. J Qureshi, S. Mahmood, W. L .E Wong, D. Talamona, Design for Scalability and Strength Optimisation for Components Created Through FDM Process, *Proceedings of the 20th International Conference on Engineering Design (ICED 15, Milan, Italy, 27-30 July, 2015)*, pp. 255-266
- [5] K. G. J. Christiyani, U. Chandrasekhar, K. Venkateswarlu, A Study on the Influence of Process Parameters on the Mechanical Properties of 3D Printed ABS Composite, *IOP Conference Series: Materials Science and Engineering*, Vol. 114, 2016, pp. 1-8
<https://doi.org/10.1088/1757-899X/114/1/012109>
- [6] A. K. Sood, R. K. Ohdar, S. S. Mahapatra, Parametric Appraisal of Mechanical Property of Fused Deposition Modelling Processed Parts, *Materials and Design*, Vol. 31, 2010, pp. 287-295
<https://doi.org/10.1016/j.matdes.2009.06.016>
- [7] L. Wang, D. J. Gardner, Effect of Fused Layer Modeling (FLM) Processing Parameters on Impact Strength of Cellular Polypropylene, *Polymer*, Vol. 113, 2017, pp. 74-80
<https://doi.org/10.1016/j.polymer.2017.02.055>
- [8] M. Samykan, S. K. Selvamani, K. Kadirgama, W. K. Ngui, G. Kanagaraj, K. Sudhakar, Mechanical Property of FDM Printed ABS: Influence of Printing Parameters, *The International Journal of Advanced Manufacturing Technology*, Vol. 102, 2019, pp. 2779-2796
<https://doi.org/10.1007/s00170-019-03313-0>
- [9] S. Wang, Y. Ma, Z. Deng, S. Zhang, J. Cai, Effects of Fused Deposition Modeling Process Parameters on Tensile, Dynamic Mechanical Properties of 3D Printed Polylactic Acid Materials, *Polymer Testing*, Vol. 86, 2020
<https://doi.org/10.1016/j.polymertesting.2020.106483>
- [10] D. Popescu, A. Zapciu, C. Amza, F. Baci, R. Marinescu, FDM Process Parameters Influence over the Mechanical Properties of Polymer Specimens: A review, *Polymer Testing*, Vol. 69, 2018, pp. 157-166
<https://doi.org/10.1016/j.polymertesting.2018.05.020>
- [11] N. Yanar, M. Son, E. Yang, Y. Kim, H. Park, S-E. Nam, H. Choi, Investigation of the Performance Behavior of a Forward Osmosis Membrane System Using Various Feed Spacer Materials Fabricated by 3D Printing Technique, *Chemosphere*, Vo. 202, 2018, pp. 708-715
<https://doi.org/10.1016/j.chemosphere.2018.03.147>
- [12] Y. Song, Y. Li, W. Song, K. Yee, K.-Y. Lee, V. L. Tagarielli, Measurements of the Mechanical Response of Unidirectional 3D-printed PLA, *Materials and Design*, Vol. 123, 2017, pp. 154-164
<https://doi.org/10.1016/j.matdes.2017.03.051>

ANALOG AND DIGITAL MODELING OF SOUND AND IMPAIRED PERIODONTAL SUPPORTING TISSUES DURING MECHANICAL TESTING

¹Veronika T. Szabó, ²Balázs Szabó, ³Tamás Tarjányi, ⁴Eszter Szőke-Trenyik³,
⁴Balázs Szabó P³, ¹Márk Fráter

¹University of Szeged, Faculty of Dentistry, Department of Operative and Aesthetic Dentistry, Tisza Lajos krt. 64., 6726, Szeged, Hungary

²University of Szeged, Faculty of Dentistry, Department of Periodontology, Tisza Lajos krt. 64., 6726, Szeged, Hungary

³University of Szeged, Faculty of Dentistry, Department of Oral Biology and Experimental Dental Research, Tisza Lajos krt. 64., 6726, Szeged, Hungary

⁴University of Szeged, Faculty of Engineering, Department of Food Engineering, Moszkvai krt. 9., 6725, Szeged, Hungary

E-mail: tszaboveronika@gmail.com, szabobalazs77@gmail.hu, tarjanyi.tamas@stoma.szote.u-szeged.hu, szpb@mk.u-szeged.hu, meddentist.fm@gmail.com,

ABSTRACT

Periodontitis is one of the most common conditions affecting oral health among adults, posing a great challenge for both patients and also for dentists aiming to treat this disease. In severe stages such deterioration of the supporting tissues, namely the periodontal ligaments and the bone, can occur, which will affect the biomechanical behavior and therefore the longevity and survival of the affected teeth. In order to be able to plan both periodontal and subsequent restorative treatment properly, valid modelling of the current clinical situation is advised. The aim of the present article is to comprehensively discuss possible analog and digital modeling methods of periodontally affected teeth and the periodontal structures surrounding them. Modelling possibilities can serve later as the basis of mechanical load, digital finite element studies, and also aid clinical treatment planning.

Keywords: analog and digital modelling, periodontally compromised teeth, molar tooth, furcation involvement, finite element analysis

1. INTRODUCTION

Periodontitis is one of the most common conditions affecting oral health among adults, accounting for severe social and health problems [1]. Although individual differences can occur, similar results are available worldwide on disease incidence from epidemiological surveys [2].

Types of periodontal disease involving the supporting tissues usually result in irreversible destruction of the alveolar bone. In parallel with bone degradation, the periodontal ligaments that anchor the teeth are also damaged, resulting in attachment loss that –if left untreated– can lead to consequential tooth loss [3]. Deterioration of the attachment apparatus is usually a slow process and over time may show individual differences in extent and clinical appearance [4]. In case of multi-rooted teeth, this can create a special situation, so-called furcation involvement [5], the treatment of which is one of the greatest challenges among periodontal therapies.

In the treatment of periodontal diseases conservative and surgical therapeutic solutions are available. In general, we might state that the more extensive defects should be rather treated surgically [6]. Resective surgery seeks to create a stable, sustainable state by further reducing the remaining tissues, while regenerative surgery aims to restore the original structures in form and function. One type of resective procedure is root amputation, in which one or more roots are surgically removed. Restoration and maintenance therapy of teeth that have undergone root amputation poses a serious challenge in most cases to the periodontist, dentist, and patient alike.

The aim of the present article is to comprehensively discuss possible analog and digital modeling methods of periodontally affected teeth and the periodontal structures surrounding them that can serve later as the basis of mechanical load or digital finite element studies. It should be emphasized that the model created should mimic a realistic clinical situation.

1.1. Preliminary data acquisition

Anatomical, clinical, and radiological knowledge regarding teeth and periodontal tissues is essential in this topic. Although dental and periodontal anatomy has been extensively circumscribed in the literature, the present clinical state of the tooth-periodontal unit in function is more difficult to examine and evaluate, especially in the case of multi-rooted teeth.

This can be aided by the rapidly evolving CBCT technique, which is able to reveal the given clinical situation in three dimensions. This is also important in research planning as clinically relevant situations are worth examining. The majority of softwares that we use to evaluate scans, are also capable of 3D rendering of the mapped area (volume rendering), but often their quality and handling are unsatisfactory (Figure 1) [7]. Of course, the imaging technology itself is also evolving by leaps and bounds (volume ray casting, texture-based volume rendering, etc.), but has not gained in everyday dental practice as much importance as using and analyzing dental CBCTs.

In modeling, however, CBCT images can play an important role in creating a three-dimensional (3D) model based on a so-called segmentation technique. Segmentation allows different structures to be embodied in the form of different models (Figure 2) [8]. In addition, their relationship to each other and their three-dimensional position can be well observed, which is of utmost importance from the practical point of view. Without doubt, 3D visualization provides better understanding of many clinical situations, for instance the position of an inflammatory lesion in relation to a tooth (Figure 3), or periodontal and other anatomical structures, compared to two-dimensional images. However, the current state of technology has not yet allowed us to create virtual bodies of the same size and shape as real structures based on CT scans. (Figure 4, 5)

If required, the created bodies can also be printed out as scale models serving for additional source of research or mere information gathering. Printed teeth can also aid educational process, namely practicing of certain procedures (Figure 6).

It should be mentioned that certainly the two-dimensional, traditional X-rays are also used for data collection currently as well, however, they provide less and often insufficient information.

Intraorally scanned images occur predominantly in clinical usage, but can also facilitate research and educational purposes, which in several cases might be of great help in a given issue. In addition, CBCT imaging, when used in conjunction with intraoral scans, allows for special dental planning, especially in navigated treatments of implantology or endodontics.

The methods presented in a non-exhaustive way above, can help us to examine clinical situations more thoroughly and accordingly, to have realistic modeling.

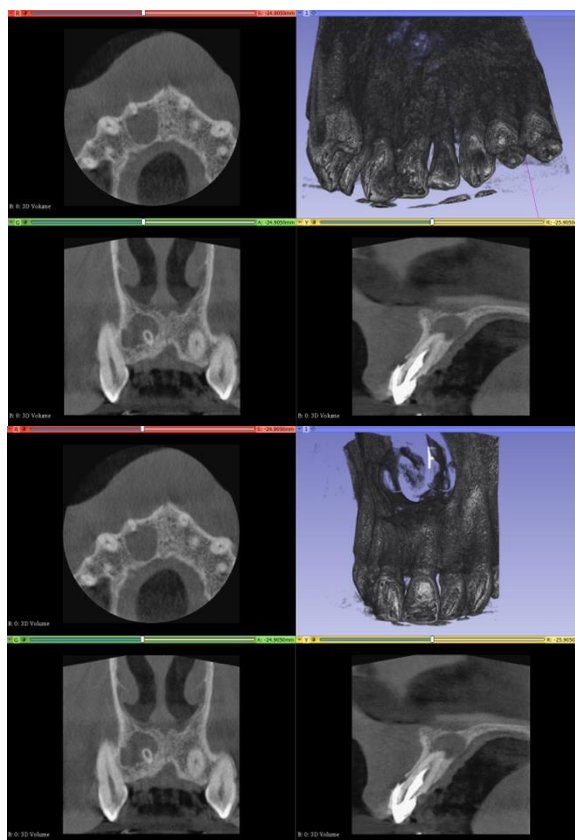
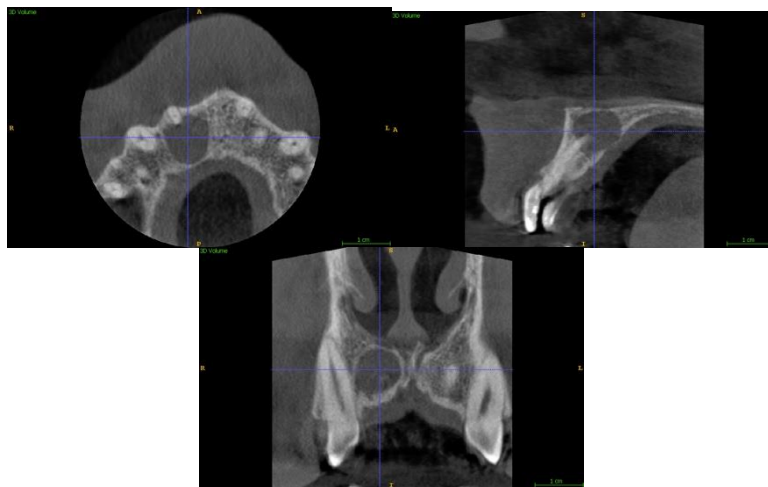


Figure 1. CBCT image and volumetric rendering

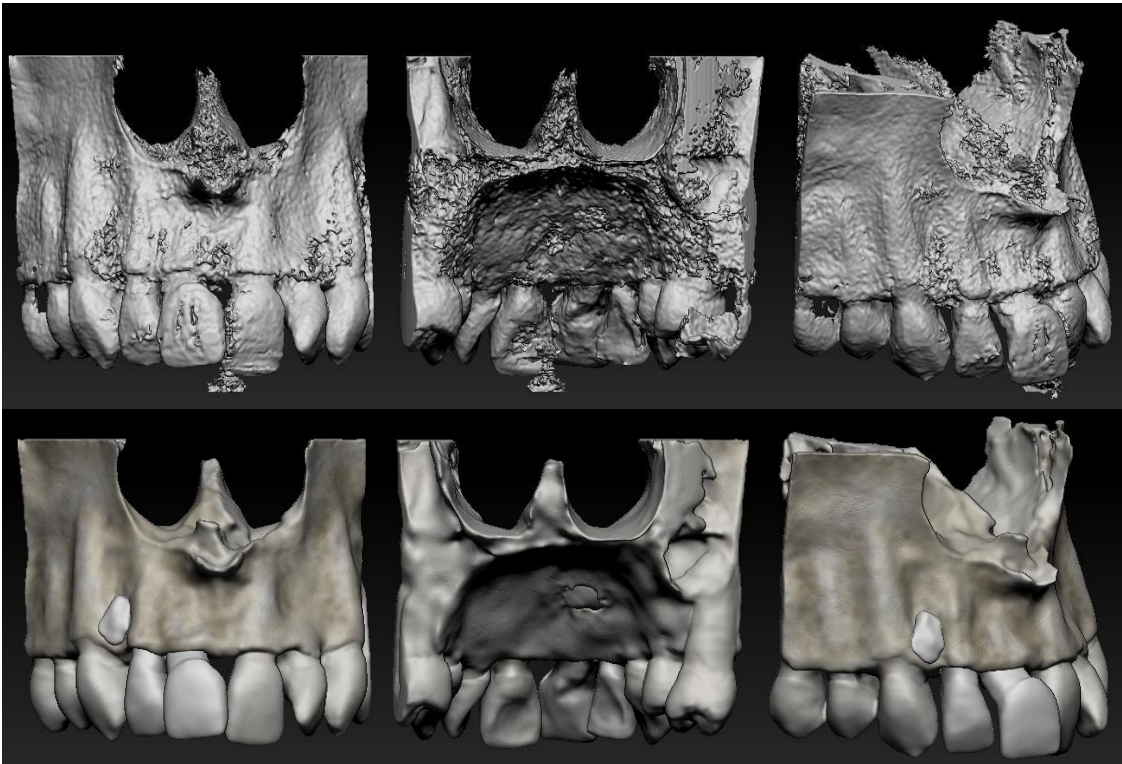


Figure 2. Noise reduction of the CBCT image shown in the Figure 1. by segmentation technique

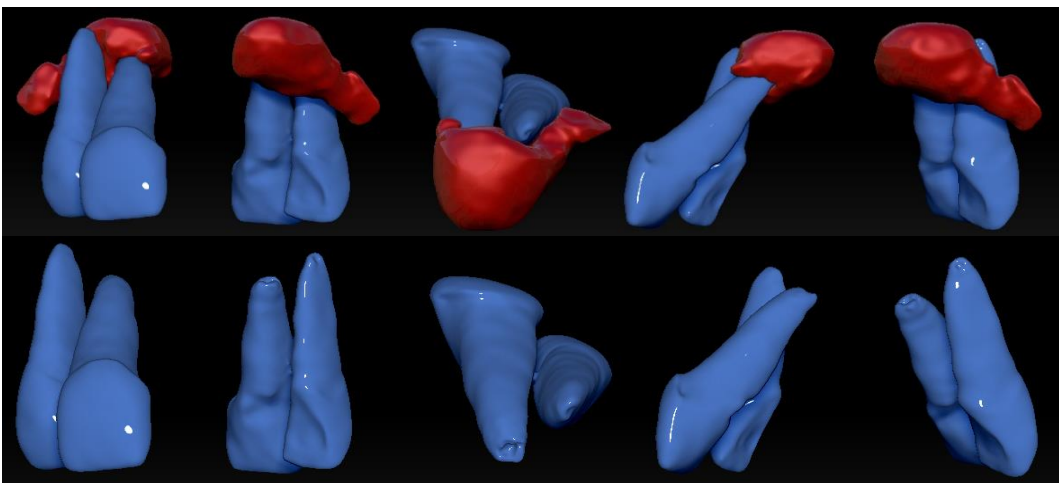


Figure 3. 3D visualization of the periapical inflammation of the upper right central incisor created by segmentation based on the CBCT image of Figure.1

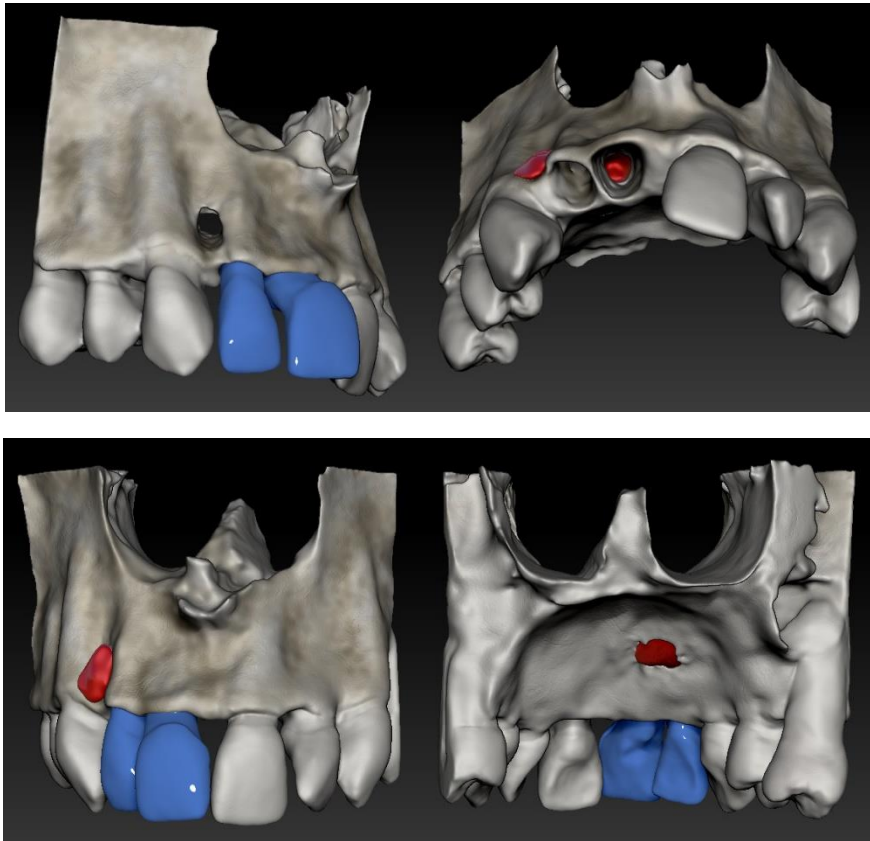


Figure 4. 3D model of the case presented above

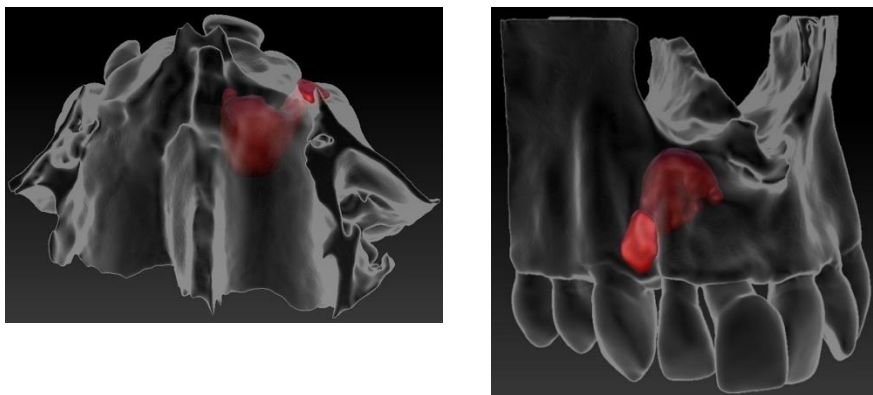


Figure 5. 3D model of the case presented above



Figure 6. Teeth printed with different materials and techniques

2. ANALOG MODELING

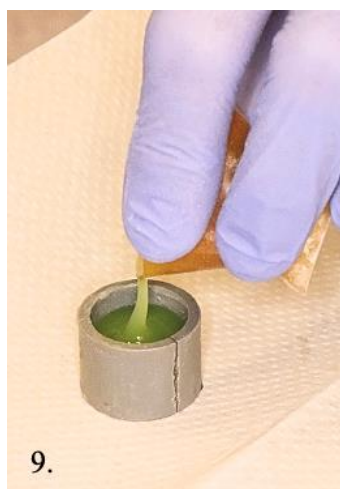
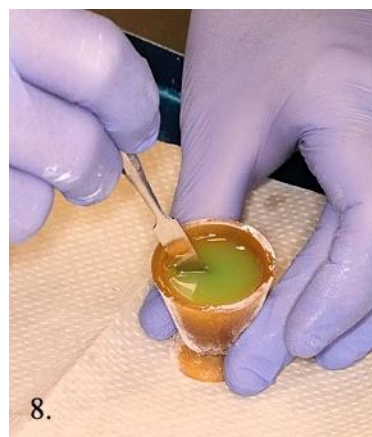
2.1. Embedding teeth

By embedding the samples, the bony support is mimicked. In normal conditions the physiological bone level is located 2 mm apically from the cemento-enamel junction (CEJ) of teeth. If we want to simulate reduced periodontal support, the level of the embedding material must be positioned even more apically from the above mentioned normal level. The simulation of furcation involvement in multi-rooted teeth, when the level of bone is withdrawn until the level of root distribution, is of particular clinical significance. As furcation-involvement can develop in varying extent and severity, only those conditions worth modeling in studies that still fall into the sustainable category. The presence of furcation involvement also depends on the anatomical parameters of the tooth, such as the apico-coronal dimension of the root trunk, which would influence the distance between the embedding material and the CEJ in any study. In case of Class I and II furcation involvement, the level of bony support is approximately 4-6 mm apically from the CEJ. During embedding of molar teeth, the occlusal surface is positioned parallel to the tabletop and is retained in this position. Accordingly, the most coronal part of the embedding material will also create a parallel surface. With this setting, we can simulate horizontal bone loss, which characterizes the clinical appearance of chronic periodontitis.

Based on the available literature, the embedding material is mainly acrylate resin in in vitro studies. For instance, Technovit 4004 (Heraeus-Kulzer) acrylate resin was used in the studies of the Biomechanical Research Group in Szeged [9-14]. The material is available in powder-liquid form. After mixing, it is poured into plastic cylinders and the teeth are embedded to the appropriate levels. Because the embedding material easily creeps on the inserted object, areas that are not intended to be embedded and are exposed to the former phenomenon should be blocked out with modelling wax. This is a particularly important step when modeling teeth with furcation-involvement (Figure 7-10).

We would like to emphasize that realistic modeling also requires the simulation of periodontal ligaments. Periodontal ligaments establish a functional connection between the alveolar bone and the cementum covering the root surface. They play crucial role in force transmission, enabling the teeth to move physiologically approximately 0.05 mm in the alveolus. In their absence, the physiological mobility of teeth, the force transmission, the local remodeling of the alveolar bone and the thickness of the cementum would change. Moreover, a model without ligaments would simulate a clinically rare, so-called ankylotic condition, which is more relevant when examining implants. In our studies, the surfaces of the roots are coated with a rubber separating agent (Rubber-Sep, Kerr, Orange, CA) according to the degree of embedding [15-17]. The separating material is applied in a single thin layer to the root surface. This can be

done with a factory-packaged nail polish brush in a single layer, thus standardizing the thickness of the separator as much as possible. There are also other material options to simulate periodontal ligaments, e.g., polyether impression material, polysulfide impression material, latex, or polyurethane. In case of the latter materials, the root is dipped into liquid, but due to the flow of the material, towards the apex of the root the separating medium will not appear evenly, but rather in excess, which makes these techniques less standard and the model less realistic.



*Figure 7. Application of the separator
Figure 8-9. Mixing and molding of embedding material
Figure 10. The finished sample*

Embedding is followed by mechanical testing of the samples. In our previous article we have already thoroughly overviewed the advantages, disadvantages, objectives, and rationale of the static fracture test [15].

If our equipment enables us, it is always worth performing dynamic loading tests on analog samples to analyze fatigue performance. The classical dynamic loading test represents one of the most valid mechanical loading methods, as it enables us to reproduce the oral conditions during chewing almost

perfectly. This means teeth are loaded with relatively small, repetitive forces through endless cycles, simulating chewing periods and time spent in oral function up to several years. When the samples are loaded in liquid (fluid chamber), we get the currently most valid mechanical testing method possible. However, from a practical point of view it must be mentioned that the classical dynamic loading is extremely time-consuming (loading 1 sample can last up to 1 week in 0-24), so it does not only make it almost impossible to perform tests and comparisons with larger sample size and group numbers, but also requires shift work from the staff.

While static load-to-fracture tests mimic a sudden, greater force, traumatic injury, the dynamic loading is more intended to illustrate the mechanical consequences of the forces occurring during ordinary chewing. An accelerated dynamic loading test represents a realistic compromise between the two extremes. In this test, although cyclic loading occurs, the magnitude of the force is not constant (only within a given cycle) but increases after a given number of cycles for the duration of the next cycle. In this specific testing it is recommended to increase the applied force until reaching the maximum chewing force of the given tooth group or oral region. As the samples are subjected to dynamic loading, we will not be able to obtain their fracture resistance values, but rather their fatigue and survival rates, which are clinically more informative data. In addition, the great advantage of this test is that the samples can be tested within a reasonable time (hours), so in terms of time consumption, it takes place in between the static load-to-fracture test and the classical dynamic loading test [18,19].

In case of periodontally affected teeth, it is of paramount importance that a dynamic loading test (classical or accelerated) should be performed first, and after that the survived samples should undergo static load-to-fracture test also. Even if dynamic is always the best, static load-to-fracture test should also be carried out in this special situation, because clinically more mobile teeth –due to either the reduced periodontal support (furcation involvement, etc.) or root amputation– are more prone to sudden fracture compared to their sound, periodontally not compromised counterparts [15,17].

3. DIGITAL MODELING

3.1. Finite element method (FEM)

Independent of which way (analog or digital) we approach the topic, preliminary information gathering is required. In the analog approach, we create real models –first a prototype in general– that allows us to perform the steps of the planned test and if it succeeds, we proceed the test with a larger sample size. Usually, creating a model/sample consumes a lot of time and energy, so the question arises, whether this time-consuming step could be replaced by a method that can substitute it or not.

The digital, finite element method (FEM) does not require the production of real models, the tests can be performed on virtually created digital models using a special software such as Comsol or Ansys, which is widely used in engineering. The FEM is a numerical method. Its operational concept is to break down the created geometries into finite number of smaller elements – hence the name 'finite element'– thus simplifying it. This means that the dimensions of spatial elements are discretized, and the equations describing the problem can be solved algebraically by specifying the geometries and meshing, then specifying the boundary conditions (for example, load, support surfaces, etc.). Analysis performed by FEM methods is called Finite Element Analysis (FEA).

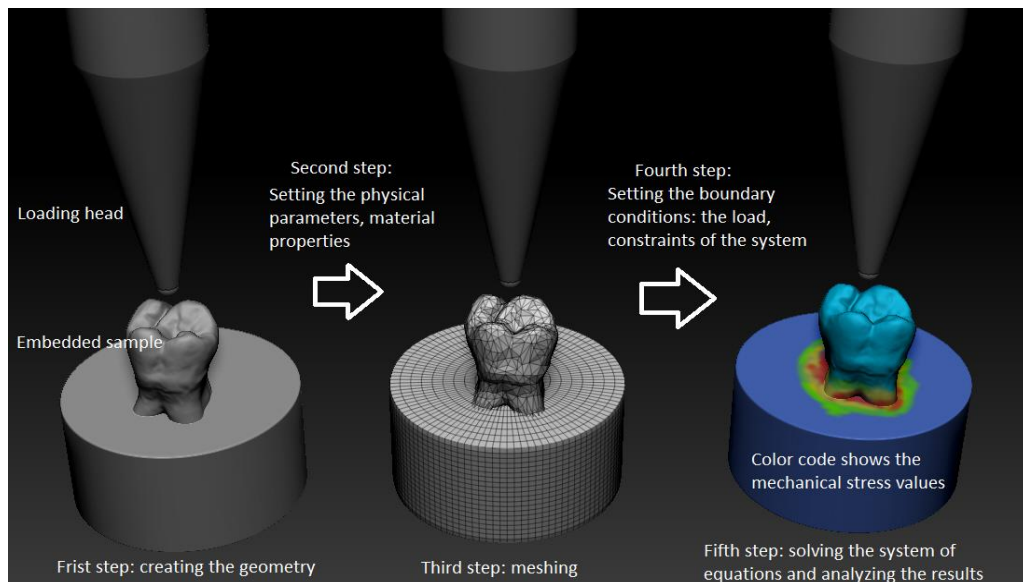


Figure 11. Steps of FEM in our field of interest

Its application is diverse and widespread: extremely popular in mechanical engineering but can be found in many fields of science as well. The method can even solve complex dental problems, such as deformation of a body under load or heat conduction in certain materials. It is also possible to utilize FEM in our research topic with a suitable software.

The first step in this process is to create the 3D object we want to work with, in our case it will be a 3D scanned tooth that we can import into the finite element calculation software.



Figure 12. The created 3D object that we will work with

During the experimental measurements, the teeth are embedded in Technovit poured in cylindrical holders. The level of embedding – or other parameters – can be adopted to the situation we want to reconstruct. This can also be done in the software by creating an appropriately sized cylindrical geometry of around the tooth (Figure 13).

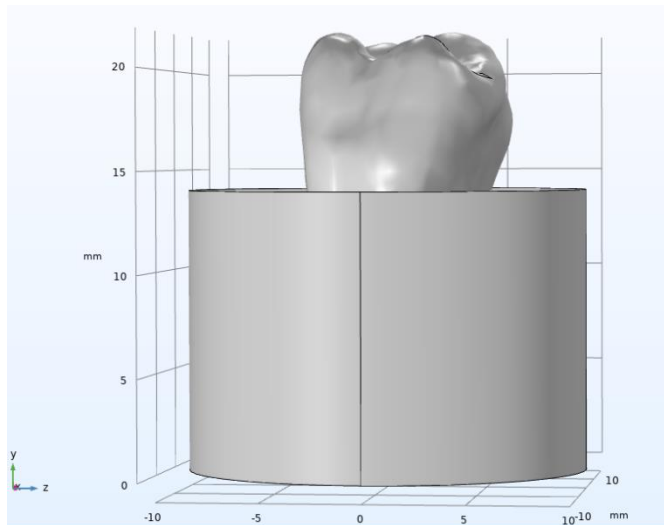


Figure 13. The imported tooth is surrounded by the cylindrical geometry

For subsequent calculations, it is necessary to determine what material the created geometries are made of. There is a built-in library in the programs, in which we can find the one that suits our purposes, or we can create any material constant for the program. For example, if the mechanical parameters of the tooth have been found in the literature (such as Young's modulus, density, and Poisson's ratio) (Figure 14) and parameters of Technovit from the manufacturer's site, we can enter all data using the latter method.

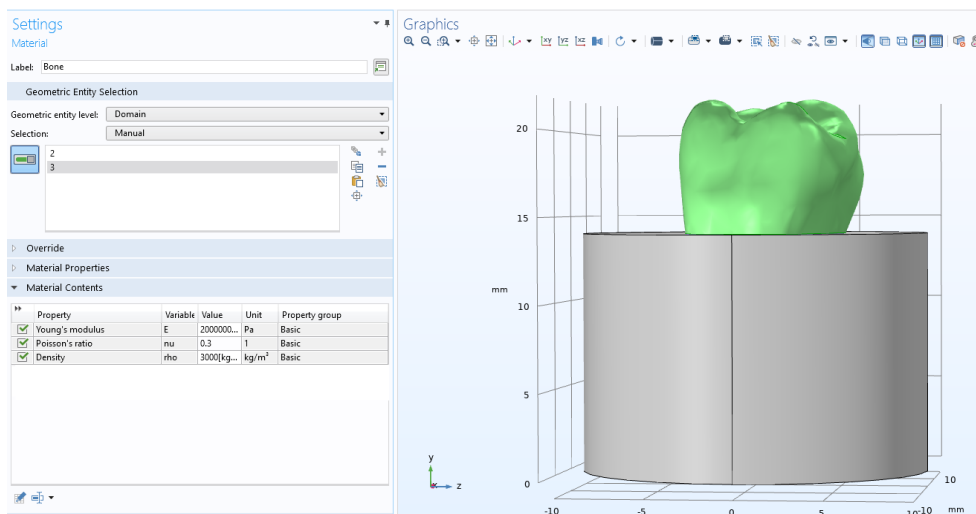


Figure 14. The material parameters of the created geometries must be determined

In the next steps, the boundary conditions must be determined, where the constraints of the system are given and the surfaces are selected, where the forces will be applied (Figure 15). In order to do this, you need to select the associated surfaces.

In our case, the bottom of the cylindrical embedding material will be the support surface. On the surface of the tooth, we can adjust how much load we want to exert (e.g., during mastication or during the experiment).

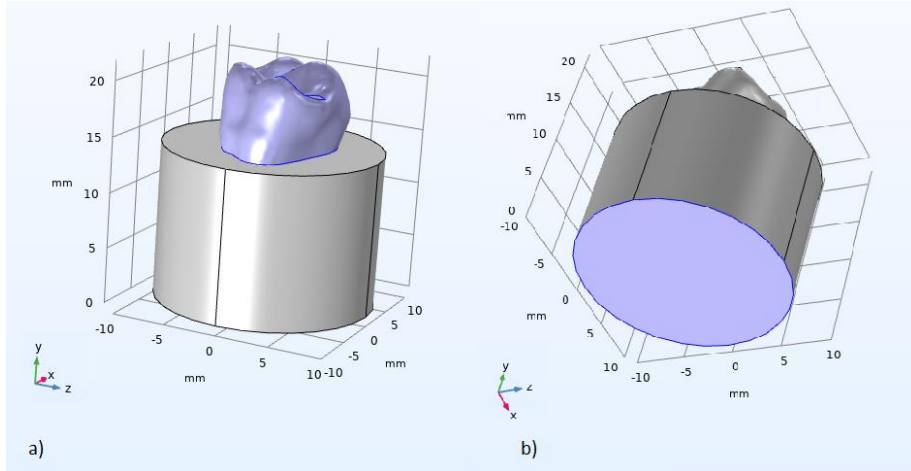


Figure 15. In the software settings we can select the loading and support surfaces. The loaded surface is on the left and the support surface is on the right.

In the case of FEM, we discretize the system and only have to solve the given problem for small surface elements. The next step, then, is to divide the surface into these smaller elements, called the mesh of the body (Figure 16).

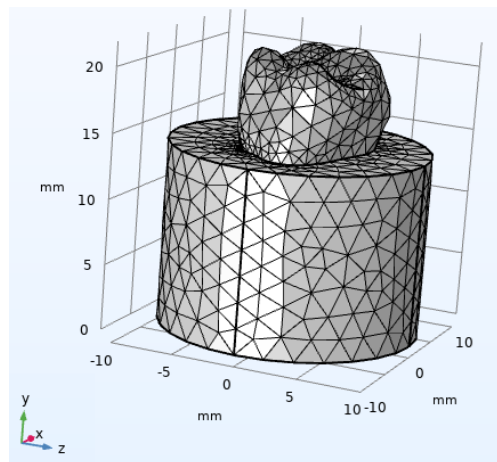


Figure 16. Mesh geometry.

Finally, we perform the calculations, in this case, we work in the mechanical module of the software. As a result, we can visualize the mechanical deformations in the material, as well as the different mechanical stress values represented by color coding. If we switch to transparent mode, we can see through the material, and the changes can be seen (Figure 17).

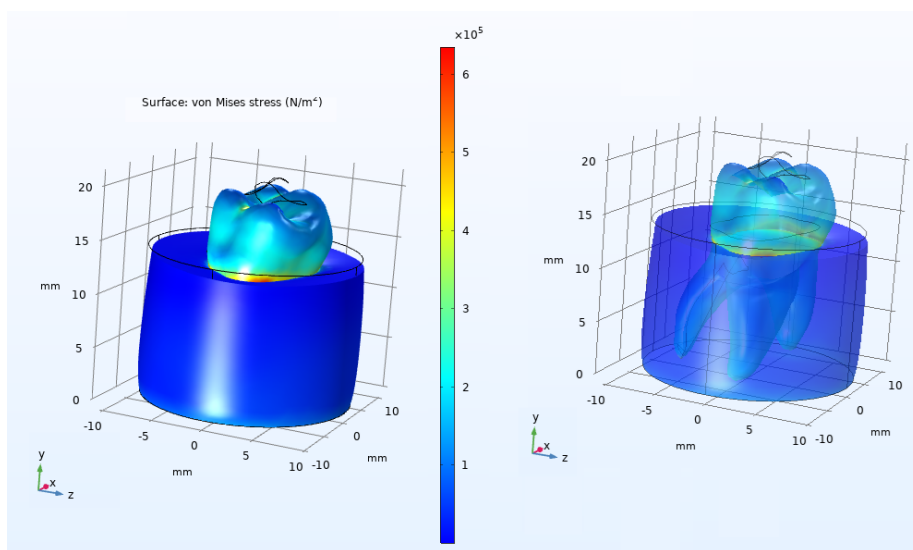


Figure 17. Distribution of mechanical stress in the material is visualized by color coding. The mechanical stress values and the deformation of the sample is shown on the left and in transparent mode on the right.

4. SUMMARY

In our article, we have generally presented our experiences in connection with the modeling of mechanical tests performed on periodontally compromised teeth. In addition, we dealt with preliminary data acquisition, which is essential for the establishment of an appropriate research plan. A significant part of dental studies is in vitro, and with the rapid development of technology we have better and better opportunities to implement them. The continuous improvements of new, up-to-date materials, techniques, equipment, and devices are available on both the analog and digital palettes. Accordingly, better and better real physical study models can be prepared, but the same can be observed in the digital world. It is extremely promising that with the help of more complex software and faster computers, real physical experiments can be simulated, but they cannot be replaced yet, maybe they never will be. We will see what the future holds, until it is essential to pay attention to the advances of both approaches and benefit from their present advantages, if possible.

ACKNOWLEDGMENT

This study was supported by the Bolyai János Research Scholarship (BO/701/20/5) and by the ÚNKP-21-2-SZTE, ÚNKP-21-5-SZTE New National Excellence Program of The Ministry for Innovation and Technology from the Source of National Research, Development and Innovation Fund, Hungary.

REFERENCES

- [1.] Eke P. I., Wei L., Borgnakke W. S., Thornton-Evans G., Zhang X., Lu H., McGuire L. C., Genco R. J. (2016): Periodontitis prevalence in adults ≥ 65 years of age, in the USA. *Periodontol* 2000. 2016 Oct;72(1):76-95. doi: 10.1111/prd.12145.

- [2.] Eke P. I., Dye B. A., Wei L., Slade G. D., Thornton-Evans G. O., Borgnakke W. S., Taylor G. W., Page R. C., Beck J. D., Genco R. J. (2015): Update on Prevalence of Periodontitis in Adults in the United States: NHANES 2009 to 2012. *J Periodontol.* 2015 May;86(5):611-22. doi: 10.1902/jop.2015.140520.
- [3.] Albandar J. M. (1990): A 6-year study on the pattern of periodontal disease progression. *J Clin Periodontol.* 1990 Aug;17(7 Pt 1):467-71. doi: 10.1111/j.1600-051x.1990.tb02346.x.
- [4.] Albandar J. M., Rise J., Gjermo P., Johansen J. R. (1986): Radiographic quantification of alveolar bone level changes. A 2-year longitudinal study in man. *J Clin Periodontol.* 1986 Mar;13(3):195-200. doi: 10.1111/j.1600-051x.1986.tb01459.x.
- [5.] American Academy of Periodontology. Glossary of Periodontal Terms. 4th ed. American Academy of Periodontology; Chicago, LA, USA: 2001. [(accessed on 2 November 2017)].
- [6.] Lindhe J., Socransky S. S., Nyman S., Haffajee A., Westfelt E. (1982): "Critical probing depths" in periodontal therapy. *J Clin Periodontol.* 1982 Jul;9(4):323-36. doi: 10.1111/j.1600-051x.1982.tb02099.x.
- [7.] Palkovics D., Mangano F. G., Nagy K., Windisch P. (2020): Digital three-dimensional visualization of intrabony periodontal defects for regenerative surgical treatment planning. *BMC Oral Health.* 2020 Dec 1;20(1):351. doi: 10.1186/s12903-020-01342-w.
- [8.] Palkovics D., Solyom E., Molnar B., Pinter C., Windisch P. (2021): Digital Hybrid Model Preparation for Virtual Planning of Reconstructive Dentoalveolar Surgical Procedures. *J Vis Exp.* 2021 Aug 5;(174). doi: 10.3791/62743.
- [9.] Fráter M, Forster A, Keresztúri M, Braunitzer G, Nagy K. In vitro fracture resistance of molar teeth restored with a short fibre-reinforced composite material. *J Dent.* 2014 Sep;42(9):1143-50. doi: 10.1016/j.jdent.2014.05.004.
- [10.] Forster A, Braunitzer G, Tóth M, Szabó BP, Fráter M. In Vitro Fracture Resistance of Adhesively Restored Molar Teeth with Different MOD Cavity Dimensions. *J Prosthodont.* 2019 Jan;28(1):e325-e331. doi: 10.1111/jopr.12777.
- [11.] Sály T, Garoushi S, Braunitzer G, Alleman D, Volom A, Fráter M. Fracture behaviour of MOD restorations reinforced by various fibre-reinforced techniques - An in vitro study. *J Mech Behav Biomed Mater.* 2019 Oct;98:348-356. doi:10.1016/j.jmbbm.2019.07.006. Epub 2019 Jul 9. Erratum in: *J Mech Behav Biomed Mater.* 2020 Feb;102:103505.
- [12.] Fráter M, Sály T, Vincze-Bandi E, Volom A, Braunitzer G, Szabó P B, Garoushi S, Forster A. Fracture Behavior of Short Fiber-Reinforced Direct Restorations in Large MOD Cavities. *Polymers (Basel).* 2021 Jun 23;13(13):2040. doi:10.3390/polym13132040.
- [13.] Fráter M, Lassila L, Braunitzer G, Vallittu PK, Garoushi S. Fracture resistance and marginal gap formation of post-core restorations: influence of different fiber-reinforced composites. *Clin Oral Investig.* 2020 Jan;24(1):265-276. doi: 10.1007/s00784-019-02902-3. Epub 2019 May 16. Erratum in: *Clin Oral Investig.* 2021 May;25(5):3339-3340.
- [14.] Fráter M, Sály T, Jókai B, Braunitzer G, Säilynoja E, Vallittu PK, Lassila L, Garoushi S. Fatigue behavior of endodontically treated premolars restored with different fiber-reinforced designs. *Dent Mater.* 2021 Mar;37(3):391-402. doi:10.1016/j.dental.2020.11.026.
- [15.] Szabó P. B., Sály T., Szabó B. (2019). The key elements of conducting load-to-fracture mechanical testing on restoration-tooth units in restorative dentistry. *Analecta Technica Szegedinensia.* 13. 59-64. 10.14232/analecta.2019.2.59-64.
-

- [16.] Szabó B, Eördegh G, Szabó PB, Fráter M. In vitro fracture resistance of root amputated molar teeth restored with overlay: a pilot study. *Fogorv Szle.* 2017:111-116.
- [17.] Szabó B, Garoushi S, Braunitzer G, Szabó P B, Baráth Z, Fráter M. Fracture behavior of root-amputated teeth at different amount of periodontal support – a preliminary in vitro study. *BMC Oral Health.* 2019 Nov 27;19(1):261. doi:10.1186/s12903-019-0958-3.
- [18.] Fráter M, Sály T, Néma V, Braunitzer G, Vallittu P, Lassila L, Garoushi S. Fatigue failure load of immature anterior teeth: influence of different fiber post-core systems. *Odontology.* 2021 Jan;109(1):222-230. doi:10.1007/s10266-020-00522-y.
- [19.] Fráter M, Sály T, Braunitzer G, Balázs Szabó P, Lassila L, Vallittu PK, Garoushi S. Fatigue failure of anterior teeth without ferrule restored with individualized fiber-reinforced post-core foundations. *J Mech Behav Biomed Mater.* 2021 Jun;118:104440. doi: 10.1016/j.jmbbm.2021.104440.